



長崎大学  
NAGASAKI UNIVERSITY

**Chemical Study on the Bioactive Constituents from Red Sea  
Marine Organisms**

*A thesis*

**submitted as a partial fulfillment of the requirements for the  
degree of doctor of philosophy**

**By**

**REDA FOUAD AHMED ABDELHAMEED**

**2016, NAGASAKI UNIVERSITY  
GRADUATE SCHOOL OF BIOMEDICAL SCIENCES  
DEPARTMENT OF PHARMACEUTICAL SCIENCES  
DIVISION OF MEDECINAL NATURAL PRODUCT  
CHEMISTRY**



# Nagasaki University

## Graduate School of Biomedical Sciences

1-12-4 Sakamoto Nagasaki 852-8523, Japan  
Tel +81-95-819-7010, Fax +81-95-819-7168,  
<http://www.mdp.nagasaki-u.ac.jp/>

September 14, 2016

To Whom It May Concern:

We hereby certify that this is a typical copy of the original Doctor Thesis of Mr. **REDA FOUAD AHMED ABDELHAMEED**. This Doctor Thesis was successfully defended and officially accepted for the degree of Doctor of Philosophy in Pharmaceutical Science.

**Title of the Dissertation : Chemical Study on the Bioactive  
Constituents from Red Sea Marine Organisms**

Shil

Isao Shimokawa M.D., Ph.D.  
Dean, Graduate School of Biomedical Sciences  
Nagasaki University




Official stamp



يعتمد  
المستشار الثقافي باليابان  
رونيه مديع

٢٠١٦





**Chemical Study on the Bioactive Constituents from  
Red Sea Marine Organisms**

**A thesis  
submitted as a partial fulfillment of the requirements for the  
degree of doctor of philosophy**

**By**

**REDA FOUAD AHMED ABDELHAMEED**

*Under Supervision of*  
**Professor KOJI YAMADA**



**2016, NAGASAKI UNIVERSITY  
GRADUATE SCHOOL OF BIOMEDICAL SCIENCES  
DEPARTMENT OF PHARMACEUTICAL SCIENCES  
DIVISION OF MEDECINAL NATURAL PRODUCT  
CHEMISTRY**

# CONTENTS

|   |           |
|---|-----------|
| <b>1. General introduction</b> .....  | <b>1</b>  |
| <b>1.1.</b> Significance of the study.....  | 1         |
| <b>1.2.</b> The importance of natural products to the source organism.....  | 3         |
| <b>1.3.</b> The requirements and difficulties of the marine natural<br>products research.....                                     | 4         |
| <b>1.4.</b> Selected examples of some biologically active compounds<br>isolated from marine resources.....                        | 6         |
| <b>1.5.</b> Current status of natural products research.....  | 17        |
| <b>1.6.</b> Aim of the study.....   | 20        |
| <b>1.7.</b> General thesis contents.....  | 21        |
| <b>2. Results and discussion</b> .....  | <b>23</b> |
| <b>2.1.</b> Secondary metabolites isolated from <i>Thalassodendron ciliatum</i> ...   | 23        |
| <b>2.2.</b> Secondary metabolites isolated from <i>Mycale euplectellioides</i> .....  | 58        |
| <b>2.3.</b> Secondary metabolites isolated from <i>Stylissa carteri</i> .....   | 84        |
| <b>3. Biological activity</b> .....   | <b>93</b> |
| <b>3.1.</b> Acetylcholine esterase inhibitory activity (AChEI-assay) of the<br>marine sponge <i>Mycale euplectellioides</i> ..... | 93        |
| <b>3.2.</b> Determination of potential inhibitory activity of MEC-1 against<br>AChE by molecular docking.....                     | 93        |
| <b>4. Experimental section</b> .....  | <b>99</b> |
| <b>4.1.</b> General experimental procedures.....  | 99        |
| <b>4.2.</b> Marine organism materials.....  | 100       |

|   |            |
|---|------------|
| 4.3. Marine organism, Extraction and isolation..... | 101        |
| 4.4. Biological activity.....                       | 106        |
| <b>5. Acknowledgement.....</b>                      | <b>108</b> |
| <b>6. References.....</b>                           | <b>110</b> |

| <b>No.</b>   | <b>List of Tables</b>  | <b>Page</b> |
|--------------|--|-------------|
| <b>1.1.</b>  | NP-derived drugs launched since 2008 by year with reference to their lead compound, classification and disease area.....   | 17          |
| <b>1.2.</b>  | NP-derived drugs in late stage clinical development (NDA or equivalent and phase III) on 31 December 2013.....   | 18          |
| <b>2.1.</b>  | <sup>13</sup> C-NMR (100 MHz) and <sup>1</sup> H-NMR (400 MHz) spectroscopic data of TCC-1 (C <sub>5</sub> D <sub>5</sub> N, δ in ppm, <i>J</i> in Hz).....          | 27          |
| <b>2.2.</b>  | <sup>13</sup> C-NMR (100 MHz) and <sup>1</sup> H-NMR (400 MHz) spectroscopic data of compound 10 (CDCl <sub>3</sub> , δ in ppm, <i>J</i> in Hz).....                 | 44          |
| <b>2.3.</b>  | <sup>13</sup> C-NMR (100 MHz) and <sup>1</sup> H-NMR (400 MHz) spectroscopic data of compound 11 (CDCl <sub>3</sub> , δ in ppm, <i>J</i> in Hz).....                 | 47          |
| <b>2.4.</b>  | <sup>13</sup> C-NMR (100 MHz) and <sup>1</sup> H-NMR (400 MHz) spectroscopic data of compound 12 (pyridine- <i>d</i> <sub>5</sub> , δ in ppm, <i>J</i> in Hz) .....  | 50          |
| <b>2.5.</b>  | <sup>13</sup> C-NMR (100 MHz) and <sup>1</sup> H-NMR (400 MHz) spectroscopic data of compound 13 (pyridine- <i>d</i> <sub>5</sub> , δ in ppm, <i>J</i> in Hz) .....  | 53          |
| <b>2.6.</b>  | <sup>13</sup> C-NMR (100 MHz) and <sup>1</sup> H-NMR (400 MHz) spectroscopic data of compound 14 (CD <sub>3</sub> OD, δ in ppm, <i>J</i> in Hz).....                 | 56          |
| <b>2.7.</b>  | <sup>13</sup> C -NMR (100 MHz) and <sup>1</sup> H-NMR (400 MHz) spectroscopic data of MEC-1 (C <sub>5</sub> D <sub>5</sub> N, δ in ppm, <i>J</i> in Hz).....         | 65          |
| <b>2.8.</b>  | <sup>13</sup> C -NMR (100 MHz) and <sup>1</sup> H-NMR (400 MHz) spectroscopic data of compound 18 (CDCl <sub>3</sub> , δ in ppm, <i>J</i> in Hz).....                | 71          |
| <b>2.9.</b>  | <sup>13</sup> C -NMR (100 MHz) and <sup>1</sup> H-NMR (400 MHz) spectroscopic data of compound 19 (CDCl <sub>3</sub> , δ in ppm, <i>J</i> in Hz).....                | 74          |
| <b>2.10.</b> | <sup>13</sup> C -NMR (100 MHz) and <sup>1</sup> H-NMR (400 MHz) spectroscopic data of compound 20 (pyridine – <i>d</i> <sub>5</sub> , δ in ppm, <i>J</i> in Hz)..... | 76          |
| <b>2.11.</b> | <sup>13</sup> C -NMR (100 MHz) and <sup>1</sup> H-NMR (400 MHz) spectroscopic data of compound 21 (pyridine – <i>d</i> <sub>5</sub> , δ in ppm, <i>J</i> in Hz)..... | 78          |
| <b>2.12.</b> | <sup>13</sup> C -NMR (100 MHz) and <sup>1</sup> H-NMR (400 MHz) spectroscopic data of compound 22 (pyridine – <i>d</i> <sub>5</sub> , δ in ppm, <i>J</i> in Hz)..... | 80          |

|              |   |    |
|--------------|---|----|
| <b>2.13.</b> | $^{13}\text{C}$ -NMR (100 MHz) and $^1\text{H}$ -NMR (400 MHz) spectroscopic data of compound 23 (pyridine – $d_5$ , $\delta$ in ppm, $J$ in Hz)..... | 83 |
| <b>2.14.</b> | $^{13}\text{C}$ -NMR (100 MHz) and $^1\text{H}$ -NMR (400 MHz) spectroscopic data of SCC-1 24 ((pyridine – $d_5$ , $\delta$ in ppm, $J$ in Hz).....   | 88 |
| <b>2.15.</b> | $^{13}\text{C}$ -NMR (100 MHz) and $^1\text{H}$ -NMR (400 MHz) spectroscopic data of compound 25 ( $\text{CDCl}_3$ , $\delta$ in ppm, $J$ in Hz)..... | 92 |
| <b>3.1.</b>  | <i>In vitro</i> microplate assay for AChE activity of the marine sponge <i>M. euplectellioides</i> .....  | 93 |

| <b>No.</b> | <b>List of Figures</b>  | <b>Page</b> |
|------------|---|-------------|
| 1.1.       | Structure of ecteinascidin-743.....   | 3           |
| 1.2.       | Structure of metabolites act as a chemical defence for their host organism.....                   | 4           |
| 1.3.       | A general view of the search for useful bioactive compounds.....                                  | 6           |
| 1.4.       | Selected metabolites with promising antiviral activity.....                                       | 7           |
| 1.5.       | Selected metabolites with promising neuronal cell protection and anti-Alzheimer activity.....     | 8           |
| 1.6.       | Selected metabolites with promising anti-cancer activity.....                                     | 10          |
| 1.7.       | Selected metabolites with promising anti- inflammatory activity....                               | 12          |
| 1.8.       | Selected metabolites with promising antibacterial and antifungal activity.....                    | 14          |
| 1.9.       | Selected metabolites with promising antiprotozoal activity.....                                   | 15          |
| 1.10.      | Selected metabolites with promising antituberculosis activity.....                                | 16          |
| 1.11.      | Selected metabolites with CNS activity.....   | 16          |
| 2.1.       | Extraction and isolation scheme of the Red Sea grass <i>T. ciliatum</i> .....                     | 24          |
| 2.2.       | <sup>1</sup> H-NMR spectrum of TCC-1 (400 MHz, C <sub>5</sub> D <sub>5</sub> N).....              | 25          |
| 2.3.       | <sup>13</sup> C-NMR spectra of TCC-1 (400 MHz, C <sub>5</sub> D <sub>5</sub> N).....              | 25          |
| 2.4.       | FAB-MS (positive ion mode) of TCC-1.....  | 26          |
| 2.5.       | <sup>1</sup> H-NMR spectrum of FAMES after hydrolysis of TCC-1 (400 MHz, CDCl <sub>3</sub> )..... | 26          |
| 2.6.       | EI-MS of FAMES after hydrolysis of TCC-1.....   | 27          |
| 2.7.       | Analytical HPLC chromatogram of TCC-1.....  | 28          |
| 2.8.       | <sup>1</sup> H-NMR spectrum of TCC-1-1 (400 MHz, C <sub>5</sub> D <sub>5</sub> N).....            | 28          |



|              |   |    |
|--------------|---|----|
| <b>2.9.</b>  | FAB-MS (positive ion mode) of TCC-1-1.....  | 29 |
| <b>2.10.</b> | <sup>1</sup> H-NMR spectrum of TCC-1-2 (400 MHz, C <sub>5</sub> D <sub>5</sub> N).....  | 29 |
| <b>2.11.</b> | FAB-MS (positive ion mode) of TCC-1-2.....  | 30 |
| <b>2.12.</b> | <sup>1</sup> H-NMR spectrum of TCC-1-3 (400 MHz, C <sub>5</sub> D <sub>5</sub> N).....  | 30 |
| <b>2.13.</b> | FAB-MS (positive ion mode) of TCC-1-3.....  | 31 |
| <b>2.14.</b> | <sup>1</sup> H-NMR spectrum of TCC-1-4 (400 MHz, C <sub>5</sub> D <sub>5</sub> N).....  | 31 |
| <b>2.15.</b> | FAB-MS (positive ion mode) of TCC-1-4.....  | 32 |
| <b>2.16.</b> | <sup>1</sup> H-NMR spectrum of TCC-1-5 (400 MHz, C <sub>5</sub> D <sub>5</sub> N).....  | 32 |
| <b>2.17.</b> | <sup>13</sup> C-NMR spectrum of TCC-1-5 (100 MHz, C <sub>5</sub> D <sub>5</sub> N)..... | 33 |
| <b>2.18.</b> | FAB-MS (positive ion mode) of TCC-1-5.....  | 33 |
| <b>2.19.</b> | EI-MS (positive ion mode) of TCC-1-5-FAME.....  | 34 |
| <b>2.20.</b> | <sup>1</sup> H-NMR spectrum of TCC-1-6 (400 MHz, C <sub>5</sub> D <sub>5</sub> N).....  | 34 |
| <b>2.21.</b> | <sup>13</sup> C-NMR spectrum of TCC-1-6 (100 MHz, C <sub>5</sub> D <sub>5</sub> N)..... | 35 |
| <b>2.22.</b> | FAB-MS (positive ion mode) of TCC-1-6.....  | 35 |
| <b>2.23.</b> | EI-MS (positive ion mode) of TCC-1-6-FAME.....  | 36 |
| <b>2.24.</b> | <sup>1</sup> H-NMR spectrum of TCC-1-7 (400 MHz, C <sub>5</sub> D <sub>5</sub> N).....  | 36 |
| <b>2.25.</b> | <sup>13</sup> C-NMR spectrum of TCC-1-7 (400 MHz, C <sub>5</sub> D <sub>5</sub> N)..... | 37 |
| <b>2.26.</b> | FAB-MS (positive ion mode) of TCC-1-7.....  | 37 |
| <b>2.27.</b> | EI-MS (positive ion mode) of TCC-1-7-FAME.....  | 38 |
| <b>2.28.</b> | <sup>1</sup> H-NMR spectrum of TCC-1-8 (400 MHz, C <sub>5</sub> D <sub>5</sub> N).....  | 38 |
| <b>2.29.</b> | FAB-MS (positive ion mode) of TCC-1-8.....  | 39 |
| <b>2.30.</b> | <sup>1</sup> H-NMR spectrum of TCC-1-9 (400 MHz, C <sub>5</sub> D <sub>5</sub> N).....  | 39 |
| <b>2.31.</b> | FAB-MS (positive ion mode) of TCC-1-9.....  | 40 |
| <b>2.32.</b> | Structure of TCC-1.....   | 41 |

|       |  |    |
|-------|--|----|
| 2.33. | Structure of the isolated phytoceramides from TCC-1.....   | 43 |
| 2.34. | <sup>1</sup> H-NMR Spectrum of compound 10 (400 MHz, CDCl <sub>3</sub> ).....                      | 43 |
| 2.35. | <sup>13</sup> C-NMR Spectrum of compound 10 (100 MHz, CDCl <sub>3</sub> ).....                     | 44 |
| 2.36. | Structure of 7β-hydroxy cholesterol.....   | 46 |
| 2.37. | <sup>1</sup> H-NMR Spectrum of compound 11 (400 MHz, CDCl <sub>3</sub> ).....                      | 46 |
| 2.38. | <sup>13</sup> C-NMR Spectrum of compound 11 (100 MHz, CDCl <sub>3</sub> ).....                     | 47 |
| 2.39. | Structure of 7β-hydroxy sitosterol.....  | 49 |
| 2.40. | <sup>1</sup> H-NMR spectrum of compound 12 (400 MHz, C <sub>5</sub> D <sub>5</sub> N).....         | 49 |
| 2.41. | <sup>13</sup> C-NMR spectrum of compound 12 (100 MHz, C <sub>5</sub> D <sub>5</sub> N).....        | 50 |
| 2.42. | Structure of stigmasterol glucoside.....   | 52 |
| 2.43. | <sup>1</sup> H-NMR spectrum of compound 13 (400 MHz, C <sub>5</sub> D <sub>5</sub> N).....         | 52 |
| 2.44. | <sup>13</sup> C-NMR spectrum of compound 13 (100 MHz, C <sub>5</sub> D <sub>5</sub> N).....        | 53 |
| 2.45. | Structure of β-sitosterol glucoside.....   | 55 |
| 2.46. | <sup>1</sup> H-NMR spectrum of compound 14 (400 MHz, CDCl <sub>3</sub> ).....                      | 55 |
| 2.47. | <sup>13</sup> C-NMR Spectrum of compound 14 (100 MHz, CDCl <sub>3</sub> ).....                     | 56 |
| 2.48. | Structure of Asebotin.....   | 57 |
| 2.49. | Extraction and isolation scheme from <i>Mycale euplectellioides</i> .....                          | 59 |
| 2.50. | <sup>1</sup> H-NMR spectrum of MEC-1 (400 MHz, C <sub>5</sub> D <sub>5</sub> N).....               | 60 |
| 2.51. | <sup>13</sup> C-NMR spectra of MEC-1 (400 MHz, C <sub>5</sub> D <sub>5</sub> N).....               | 61 |
| 2.52. | FAB-MS (positive ion mode) of MEC-1.....   | 61 |
| 2.53. | <sup>1</sup> H-NMR spectrum of FAMES after hydrolysis of MEC-1 (400 MHz, CDCl <sub>3</sub> ).....  | 62 |
| 2.54. | <sup>13</sup> C-NMR spectrum of FAMES after hydrolysis of MEC-1 (400 MHz, CDCl <sub>3</sub> )..... | 62 |

|              |  |    |
|--------------|--|----|
| <b>2.55.</b> | EI-MS of FAMES after hydrolysis of MEC-1.....  | 63 |
| <b>2.56.</b> | <sup>1</sup> H-NMR spectrum of LCB after hydrolysis of MEC-1 (400 MHz, CD <sub>3</sub> OD).....  | 63 |
| <b>2.57.</b> | <sup>13</sup> C-NMR spectrum of LCB after hydrolysis of MEC-1 (400 MHz, CD <sub>3</sub> OD)..... | 64 |
| <b>2.58.</b> | FAB-MS (positive ion mode) of LCB after hydrolysis of MEC-1.....                                 | 64 |
| <b>2.59.</b> | Analytical HPLC chromatogram of MEC-1.....   | 65 |
| <b>2.60.</b> | FAB-MS (positive ion mode) of MEC-1-4.....   | 66 |
| <b>2.61.</b> | FAB-MS (positive ion mode) of MEC-1-7.....   | 66 |
| <b>2.62.</b> | FAB-MS (positive ion mode) of MEC-1-8.....   | 67 |
| <b>2.63.</b> | Analytical HPLC chromatogram of MEC-1-4, MEC-1-7 and MEC-1-8.....                                | 67 |
| <b>2.64.</b> | Structure of MEC-1.....  | 69 |
| <b>2.65.</b> | Structure of MEC-1-4, MEC-1-7 and MEC-1-8.....   | 70 |
| <b>2.66.</b> | <sup>1</sup> H-NMR spectrum of compound 18 (400 MHz, CDCl <sub>3</sub> ).....                    | 70 |
| <b>2.67.</b> | <sup>13</sup> C-NMR spectrum of compound 18 (100 MHz, CDCl <sub>3</sub> ).....                   | 71 |
| <b>2.68.</b> | Structure of compound 18 (chimyl alcohol).....   | 72 |
| <b>2.69.</b> | <sup>1</sup> H-NMR spectrum of compound 19 (400 MHz, CDCl <sub>3</sub> ).....                    | 73 |
| <b>2.70.</b> | <sup>13</sup> C-NMR spectrum of compound 19 (100 MHz, CDCl <sub>3</sub> ).....                   | 73 |
| <b>2.71.</b> | Structure of compound 19 (batyl alcohol).....  | 74 |
| <b>2.72.</b> | <sup>1</sup> H-NMR spectrum of compound 20 (400 MHz, C <sub>5</sub> D <sub>5</sub> N).....       | 75 |
| <b>2.73.</b> | <sup>13</sup> C-NMR spectrum of compound 20 (100 MHz, C <sub>5</sub> D <sub>5</sub> N).....      | 75 |
| <b>2.74.</b> | Structure of compound 20 (thymine).....  | 77 |
| <b>2.75.</b> | <sup>1</sup> H-NMR Spectrum of compound 21 (400 MHz, C <sub>5</sub> D <sub>5</sub> N).....       | 77 |
| <b>2.76.</b> | <sup>13</sup> C-NMR Spectrum of compound 21 (100 MHz, C <sub>5</sub> D <sub>5</sub> N).....      | 78 |

|       |   |    |
|-------|---|----|
| 2.77. | Structure of compound 21 (uracil).....  | 79 |
| 2.78. | <sup>1</sup> H-NMR spectrum of compound 22 (400 MHz, C <sub>5</sub> D <sub>5</sub> N).....  | 79 |
| 2.79. | <sup>13</sup> C-NMR spectrum of compound 22 (100 MHz, C <sub>5</sub> D <sub>5</sub> N).....   | 80 |
| 2.80. | Structure of compound 22 (deoxy thymidine).....   | 81 |
| 2.81. | <sup>1</sup> H-NMR spectrum of compound 23 (400 MHz, C <sub>5</sub> D <sub>5</sub> N).....  | 82 |
| 2.82. | <sup>13</sup> C-NMR spectrum of compound 23 (100 MHz, C <sub>5</sub> D <sub>5</sub> N).....   | 82 |
| 2.83. | Structure of compound 23 (deoxy uridine).....   | 84 |
| 2.84. | Extraction and isolation scheme from <i>Stylissa carteri</i> .....  | 85 |
| 2.85. | <sup>1</sup> H-NMR spectrum of SCC-1 (400 MHz, C <sub>5</sub> D <sub>5</sub> N).....  | 86 |
| 2.86. | <sup>13</sup> C-NMR spectra of SCC-1 (400 MHz, C <sub>5</sub> D <sub>5</sub> N).....  | 86 |
| 2.87. | FAB-MS (positive ion mode) of SCC-1.....  | 87 |
| 2.88. | FAB-MS of FAMEs after hydrolysis of SCC-1.....  | 87 |
| 2.89. | Structure of SCC-1 and FAMEs.....   | 90 |
| 2.90. | Structure of SCC-1.....   | 90 |
| 2.91. | <sup>1</sup> H-NMR spectrum of compound 25 (400 MHz, CDCl <sub>3</sub> ).....   | 91 |
| 2.92. | <sup>13</sup> C-NMR spectrum of compound 25 (100 MHz, CDCl <sub>3</sub> ).....  | 91 |
| 2.93. | Structure of compound 25 (2-bromoaldisine).....   | 92 |
| 3.1.  | Glide XP docked structure of ceramide with active site of AChE highlighting the hydrophobic interaction of ceramide with PAS and deeply penetration to esterating site..... | 95 |
| 3.2.  | Superimposition of ceramides (green colour) and donepezil (red colour) with AChE (PDBID:1EVE) generated by glide docking.....   | 95 |
| 3.3.  | Hydrogen bond interaction between ceramide and AChE.....  | 97 |
| 3.4.  | Compounds with AChE inhibitory activity.....  | 98 |

## List of abbreviations

|                                 |   |
|---------------------------------|---|
| AChE                            | Acetyl choline esterase                             |
| AChEI                           | Acetyl choline esterase inhibitor                   |
| ACTI                            | Acetyl thiocholine iodide                           |
| AD                              | Alzheimer disease                                   |
| ADC                             | Anti-body drug conjugates                           |
| Ara-A                           | Arabinosyl adenine                                  |
| Ara-C                           | Arabinosyl cytosine                                 |
| br.s.                           | Broad singlet                                       |
| BSA                             | Bovine serum albumin                                |
| CA cavity                       | Chorioalantoic cavity                               |
| °C                              | Degree centigrade                                   |
| <sup>13</sup> C-NMR             | Carbon 13 magnetic resonance                        |
| C <sub>5</sub> D <sub>5</sub> N | Deuterated pyridine                                 |
| CD <sub>3</sub> OD              | Deuterated methanol                                 |
| CDCl <sub>3</sub>               | Deuterated chloroform                               |
| CNS                             | Central nervous system                              |
| COX                             | Cyclooxygenase                                      |
| D                               | Doublet   |
| Dd                              | Doublet of doublet                                  |
| DBHB                            | Di bromo hemi bastadin                              |
| DEPT                            | Distortionless enhancement by polarization transfer |
| DMSO                            | Dimethyl Sulfoxide                                  |
| DTNB                            | 5,5'-dithio bis-2- nitrobenzoic acid                |
| EI-MS                           | Electron impact- mass spectroscopy                  |
| EtOAc                           | Ethyl acetate                                       |
| FAB-MS                          | Fast atom bombardment –mass spectroscopy            |
| FAMEs                           | Fatty acid methyl esters                            |
| Fig.                            | Figure  |
| G                               | Gram  |
| HAPI-H5N1                       | Highly pathogenic avian influenza A virus           |
| <sup>1</sup> H-NMR              | Proton magnetic resonance                           |
| iNOS                            | Inducible nitric oxide synthase                     |
| IR                              | Infrared  |
| <i>J</i>                        | Coupling constant                                   |
| Kg                              | Kilogram  |
| L                               | litre   |
| LCB                             | Long chain base                                     |
| Q                               | Quartet   |
| m/z                             | Mass to charge ratio                                |
| M <sup>+</sup>                  | Molecular ion                                       |

|            |   |
|------------|---|
| M          | Multiplicity                                  |
| M          | Multiplet                                     |
| MDCK       | Madin-Darby canine kidney                     |
| MEM        | Minimum essential medium                      |
| Mg         | Milligram                                     |
| MHz        | Mega hertz                                    |
| MIC        | Minimum inhibition concentration              |
| mm         | Millimetre                                    |
| MPO        | Myeloperoxidase                               |
| <i>n</i>   | Normal  |
| ng         | nanogram                                      |
| nm         | Nanometre                                     |
| NMR        | Nuclear magnetic resonance                    |
| NP         | Natural product                               |
| NP-derived | Natural product derived                       |
| ODS        | Octa decyl silyl                              |
| PAS        | Peripheral anionic site                       |
| PBS        | Phosphate buffered solution                   |
| PFU        | Plaque forming unit                           |
| ppm        | Part per million                              |
| RP         | Reversed phase                                |
| s          | Singlet                                       |
| SCUBA      | Self-contained underwater breathing apparatus |
| SS-NP      | Semi synthetic – natural product              |
| t          | Triplet                                       |
| TCID50     | Tissue culture infective dose                 |
| TLC        | Thin layer chromatography                     |
| UV         | Ultra violet                                  |
| 5-HT2B     | 5-Hydroxytryptamine receptor 2B               |

## 1. General Introduction:

### 1.1. Significance of the study

Nature is capable of producing chemotherapeutic molecules with multiple chiral centers that are designed to interact with biological systems. Natural products have the potential to provide medicine with a source of novel structures that are unobtainable from sources such as combinatorial synthesis. Natural products have inspired many developments in organic chemistry,<sup>1-4)</sup> leading to advances in synthetic methodologies and to the possibility of making analogues of the original lead compound with improved pharmacological or pharmaceutical properties.<sup>5)</sup>

Drugs of natural origin have been classified as an unmodified natural product, a modified natural product, a synthetic compound showing competitive inhibition of the natural product substrate, a synthetic compound with a natural product pharmacophore showing competitive inhibition of the natural product substrate. 63% of the new chemical entities discovered from January 1981 to October 2008 were inspired or derived from natural products.<sup>6)</sup>

At some point, the amount of chemical diversity available through nature must begin to tail off. Perhaps the best manner to determine the amount of chemical diversity remaining is to examine the amount of biodiversity remaining. Because biodiversity is so important to the continued discovery of novel natural products, it is important to know how much biodiversity remains. The greater the amount of remaining biodiversity to be studied, the greater the potential amount of chemical diversity remains to be discovered.

Natural products sources are basically of two types. Firstly, the terrestrial source, which includes plants, animals, and microorganisms, and secondly, the marine source that includes the marine source which contains well over 200,000 invertebrate and algal species. There exist nearly 150,000 species of Algae (sea weed): green (Chlorophyta), red (Rhodophyta), and brown (Phaeophyta), and some groups of marine invertebrates in which new chemical structures or biological activities have been reported: sponges (Porifera), cnidarians or coelenterates [corals, octocorals (including sea fans), hydroids, and sea anemones], nemertean (worms), bryozoans, ascidians (tunicates including sea squirts), mollusks (sea snails and sea slugs), and echinoderms (brittle stars, sea urchins, starfish, and sea cucumbers).<sup>7)</sup>Oceans host

32 out of the discovered 35 phyla of life on earth, and appear to cover about 71% of earth surface and the diversity of species per unit area is as high as 1000 species per square meter in the Indo-pacific Ocean with the highest species diversity being in coral reefs.<sup>8)</sup> Therefore it is not surprising that oceans are considered as vast untapped reservoirs of highly diverse and unique natural products.. From the taxonomic consideration, marine organisms are significantly more diverse than terrestrial organisms. Furthermore, in contrast to animals from terrestrial habitats, invertebrates from marine environment are rich sources of complex natural products derived from numerous biosynthetic pathways.<sup>9)</sup>

Terrestrial plants have proven to be rich sources of natural drugs that are used for the treatment of fatal diseases such as cancer (taxol) and microbial infections (penicillin). However, due to the resurgence of pathogenic microorganisms and parasites that have developed resistance to traditional chemotherapies, natural products chemists are increasingly turning to new sources in the search for biologically active compounds, and specifically to marine realm.<sup>10-11)</sup>

For the last 30–40 years, marine invertebrates have been an attractive research topic for scientists all over the world. A relatively small number of marine plants, animals and microbes have yielded more than 15,000 natural products including numerous compounds with potential pharmaceutical potential.<sup>12)</sup>

Basic scientific research in chemistry and pharmacology of marine natural products, and directed efforts in drug development have finally become fruitful for marine-based drug discovery. The first newly admitted drug from the sea, Prialt® also known as ziconotide ( $\omega$ -conotoxin MVIIA) which is a peptide originally isolated from the marine cone snail - was approved in 2004 act as a potent analgesic for chronic pain in spinal cord injury. A second drug - the antitumor compound Yondelis® (known also as trabectedin or ecteinascidin-743/ET-743) obtained from the tropical sea-squirt for the treatment of soft-tissue sarcoma, was approved in 2007 by the European Union. Several other candidate compounds are presently in the pipeline, and marine natural products are being evaluated in Phase I–III clinical trials in the United States and in Europe for the treatment of various cancers.<sup>13)</sup>



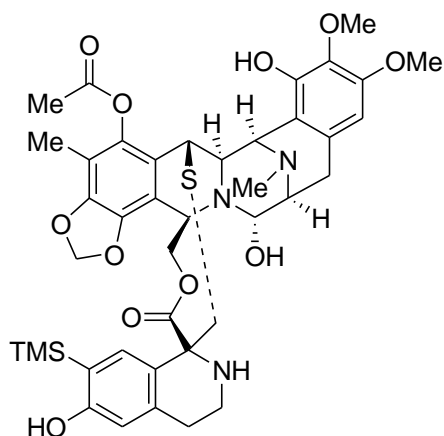


**Fig. 1.1. Structure of ecteinascidin-743**

## 1.2. The importance of natural products to the source organism

Many marine-living organisms are soft bodied and/or sessile. Consequently, they have developed toxic secondary metabolites or obtained them from microorganisms to defend themselves against predators or infection.<sup>12)</sup> So, some of the natural products are beneficial as chemical defense means including:

### 1.2.1. Chemical defense against predation

The sponge *Latrunculina magnifica* is well protected from predation by fishes due to its metabolites Latrunculins A and B<sup>14)</sup> (Fig. 1.2). Also, alkaloids of didemnin B and nor-didemnin obtained from the ascidian *Trididemnum solidum* have the ability to inhibit the reef fishes from feeding.<sup>15)</sup>

### 1.2.2. Chemical defense against fouling and spatial competition

The marine sponge *Aplysina aerophoba* has the ability to produce Aerophobin-2 and isofistularin-3 (Fig. 1.2). Those secondary metabolites were found to be enzymatically transformed into dienone and aeroplysinin-1, respectively, after injury. Dienone and aeroplysinin-1 have the potency to protect the *Aplysina aerophoba* from invasion of pathogenic microorganisms.<sup>16-17)</sup>

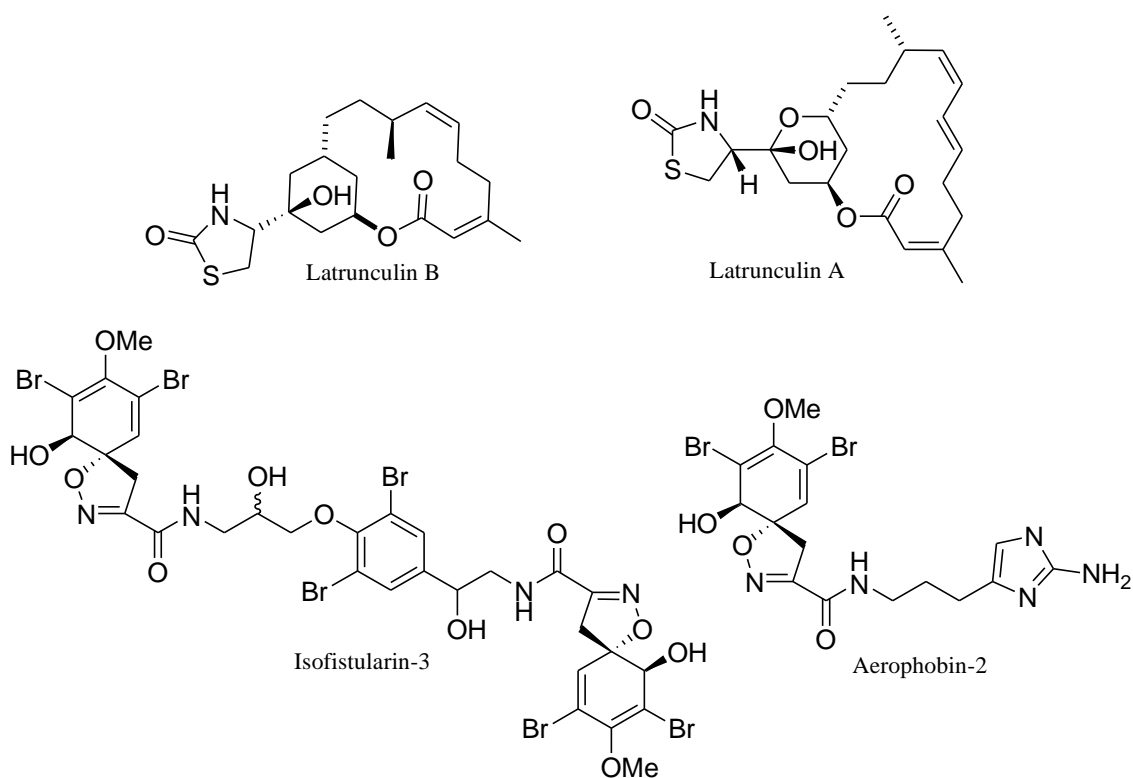


**Fig. 1.2. Structure of metabolites act as a chemical defense for their host organism**

### 1.3. The requirements and difficulties of the marine natural products research

Obviously, nature plays a vital role in the field of drug discovery, so that the mission of natural products chemists become important for work in isolation, structure elucidation, and synthesis of the leading isolated metabolites if possible. Natural products chemists must take in consideration the biological species which produce the bioactive metabolites, the elucidation of the isolated compounds, and the potency compared with the medicaments in the market. So the challenges of the natural products research are:

#### 1.3.1. Sample collection

The first step in these studies starts with sample collection and may be much more difficult in the marine environment than if compared with working on terrestrial organisms. This is not only due to the difficulties of collection in the marine environment but also due to problems associated with the taxonomy and the lack of sufficient biological material. The presence of symbionts (fungi, bacteria, microalgae) living on or inside the macro-organisms being studied introduces real uncertainty about the exact metabolic origin of the active

compounds isolated. This fact is further complicated by the difficulties encountered in the search for adequate condition for growth and cultivation of marine organisms, such as invertebrates (i.e. sponges, bryozoans) or microbe.<sup>18)</sup>

### **1.3.2. Number of samples screened**

The possibility to find potent bioactive metabolites is clearly dependent on the number of samples screened. Bulk collection is necessary and amounts of  $\geq 1$  kg of lyophilized material may be needed just to get the minimum amount of pure compound to check its activity and determine its structure.

### **1.3.3. Selection of the active sample**

Selection of the active sample is depending on fast, economic and representative primary tests. To achieve this step, selective extractions, separations and purification procedures are required. If the pure compound shows really interesting activity, further pharmacological assays (*in vitro*, *in vivo*, tolerated dose, and so on) and chemical work (structure modification, preparation of analog, structure-activity relationship, total synthesis, cultivation, etc.) should be carried out in order to enter the development step.<sup>19)</sup> A general view of the search for useful bioactive compounds is presented in Fig. 1.3.

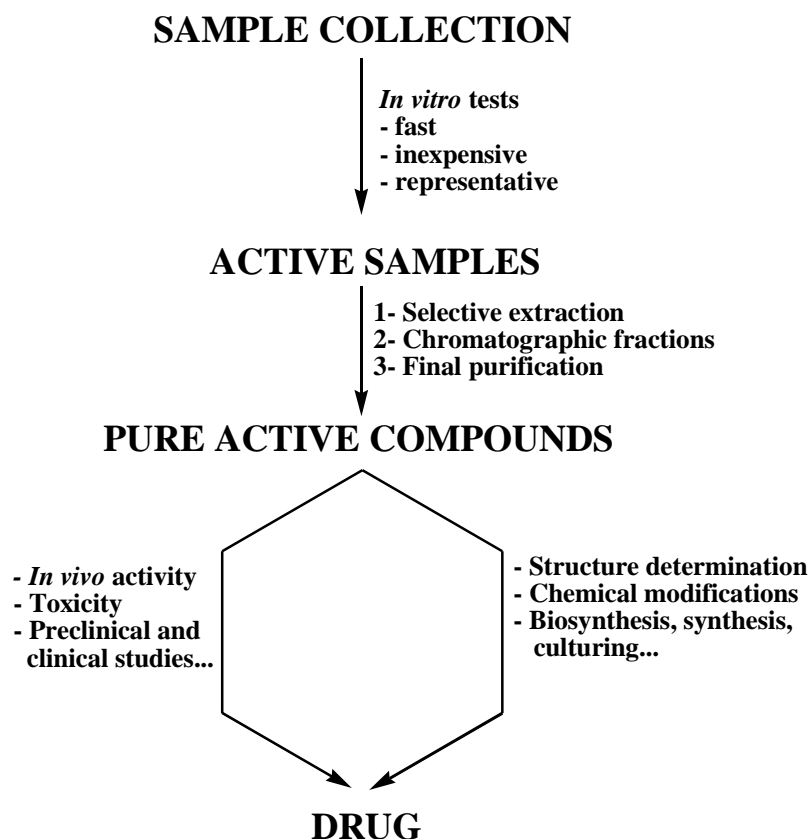


Fig. 1.3. A general view of the search for useful bioactive compounds

#### 1.4. Selected examples of some biologically active compounds isolated from marine resources

Bioactive metabolites from the marine environment have far-reaching past and present exploitation in the treatment of several diseases. They act as compounds of importance both in their natural form and as templates for synthetic modification. Several molecules isolated from various marine organisms (microorganisms, algae, fungi, invertebrates, and vertebrates) are currently under study at an advanced stage of clinical trials, some of them have already been marketed as drugs.<sup>20)</sup>

Screening through published literatures, based on types of disease-causing organisms, many categories of marine compounds can be classified into:

### 1.4.1. Antiviral compounds

The nucleoside Vidarabine (ara-A) is a semisynthetic compound based on the arabinosyl nucleosides purified from the sponge *Cryptotethia crypta* and its related derivatives (azidothymidine, ara-C, acyclovir) are all showing notable antiviral activity.<sup>21)</sup>

Mycalamide A, Mycalamide B are two antiviral compounds isolated from a New Zealand sponge of the genus *Mycale*. Mycalamide A also inhibited the Herpes simplex type I and Polio type I viruses at a concentration of 5 ng/disc. Mycalamide B was found to be more potent than mycalamide A, which was active at a concentration of 1–2 ng/disc.<sup>22-23)</sup>

A bromoindole alkaloid, named dragmacidin F was isolated from a marine sponge of the genus *Halicortex*. Dragmacidin F exhibited interesting antiviral properties. It was tested for anti HSV-1 and anti HIV-1 activities; the concentration achieving 50% protection of virus infected cells from HSV-induced destruction was 95.8  $\mu$ M. Furthermore, the concentration achieving 50% delay in formation of syncytia in HIV-1 virus infected cells was 0.91  $\mu$ M.<sup>24-25)</sup>

Avarol, a sesquiterpenoid hydroquinone with a rearranged drimane skeleton, was first isolated from the marine sponge *Disidea avara* in 1974.<sup>26)</sup> Avarol and avarone can inhibit human immunodeficiency virus at dose 0.1-1 $\mu$ g/ml in vitro and thus are of potential use in the treatment of AIDS.<sup>27)</sup>

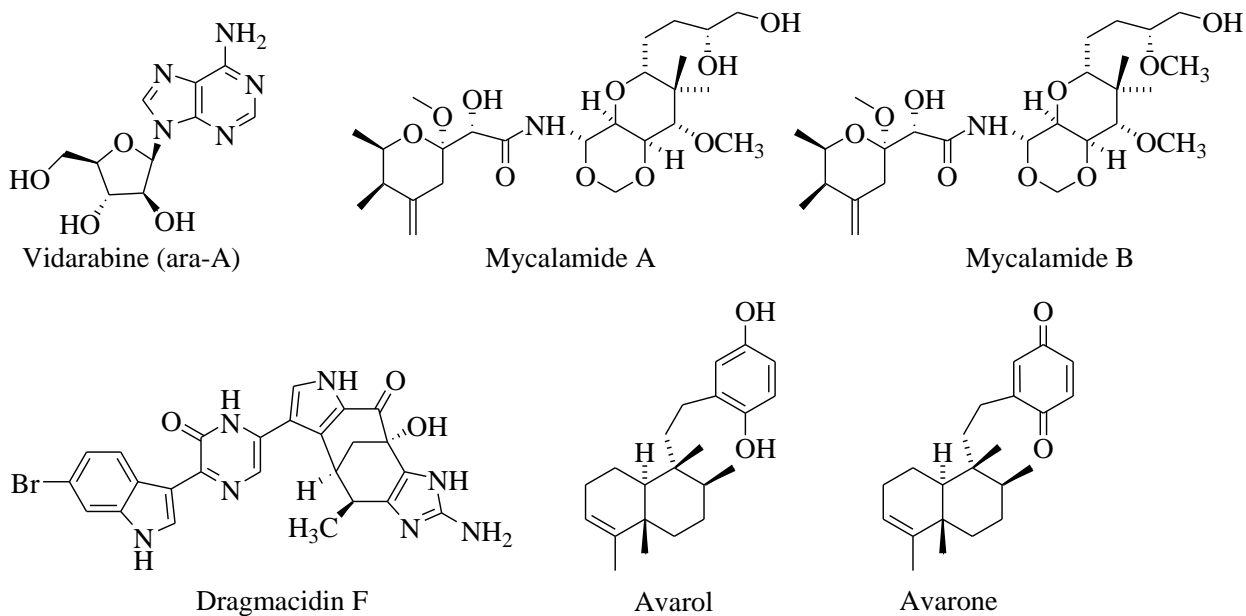


**Fig. 1.4. Selected metabolites with promising antiviral activity**

### 1.4.2. Neuronal cell protection and Anti Alzheimer compounds

JBIR-65, a new diterpene, isolated from a sponge derived *Actinomadura* sp. SpB081030SC-15, protects neuronal hybridoma N18-RE-105 cells from L-glutamate toxicity with an EC<sub>50</sub> value of 31 μM.<sup>28)</sup>

The alkaloid Manzamine Y isolated from an Indonesian sponge of the genus *Acanthostrongylophora* showed significant inhibitory activity of GSK3, an enzyme implicated in Alzheimer's disease pathology.<sup>29)</sup>

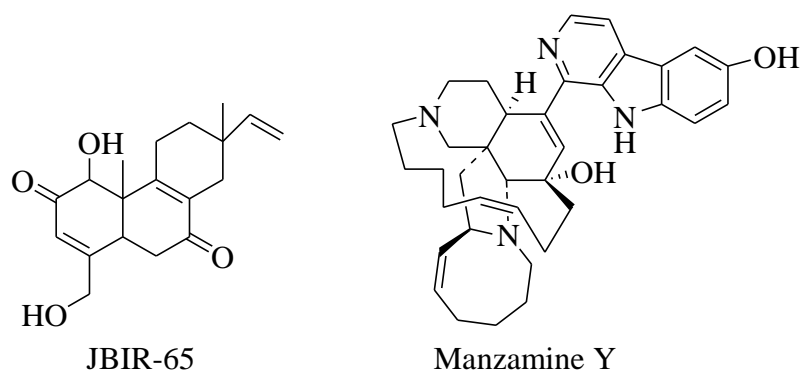


**Fig. 1.5. Selected metabolites with promising neuronal cell protection and anti-Alzheimer activity**

### 1.4.3. Anti cancer compounds

Cancer is one of the leading causes of death in the developed world. Carcinogenesis is a process by which normal cells are altered into cancer cells. It is characterized by a progression of changes at both, cellular and genetic level, that reprogram a cell to undergo uncontrolled division, thus forming a malignant mass (tumor) that can spread to distant locations.<sup>30)</sup>

An ideal anticancer agent is expected to inhibit, delay or reverse the progression of cancer through its cytotoxicity or apoptosis-inducing properties. Cytotoxic drugs are primarily used as anticancer drugs because they are toxic to cancer cells. These drugs have been associated with human cancers at high (therapeutic) levels of exposure and are carcinogens and teratogens in many animal species. Cytotoxic drugs have an effect of preventing the rapid growth and division (mitosis) of cancer cells.<sup>31)</sup>

Recent technological and methodological advances in structure elucidation, organic synthesis, and biological assay have resulted in the isolation and clinical evaluation of various novel anticancer agents.<sup>32)</sup>

From the marine Actinobacterium *Salinispora tropica*, Salinosporamide A (a novel bicyclic beta-lactone gamma-lactam) was isolated.<sup>33-34)</sup> Salinosporamide A is proteasome inhibitor which induces apoptosis in multiple myeloma cells.<sup>35)</sup> It is being developed by Nereus Pharmaceuticals, Inc. (as NPI-0052). NPI-0052 is being evaluated in phase I trials for solid tumors, lymphoma and multiple myeloma.<sup>36)</sup>

Bastadins-6, -9 and -16 isolated from the marine sponge *Ianthella basta* exhibited *in vitro* cytostatic and/or cytotoxic effects in six human and mouse cancer cell lines and DBHB (5,5'-dibromohemibastadin) exhibited both anti-angiogenic (HUVECs) and anti-migratory effects in mouse B16F10 melanoma cells.<sup>37)</sup>

From the Indonesian marine sponge *Luffariella variabilis*, two new  $\beta$ -carboline alkaloids, variabines A and B were isolated. Variabine B had interesting antitumor activity through inhibition of chymotrypsin-like activity of the proteasome and Ubc13 (E2)–Uev1A interaction with IC50 values of 4 and 5  $\mu\text{g}/\text{ml}$ , respectively. Variabine A which is a sulphonated derivative of Variabine B had little effect on the activity or interaction.<sup>38)</sup>

Eribulin is an anticancer drug under the trade name Halaven. Eribulin metylate was approved by the U.S. Food and Drug Administration on November 15, 2010, to treat patients with metastatic breast cancer who have received at least two prior chemotherapy regimens for late-stage disease, including both anthracycline- and taxane-based chemotherapies.<sup>39)</sup>

Eribulin is a fully synthetic macrocyclic ketone analogue of the marine sponge natural product halichondrin B.<sup>40)</sup>

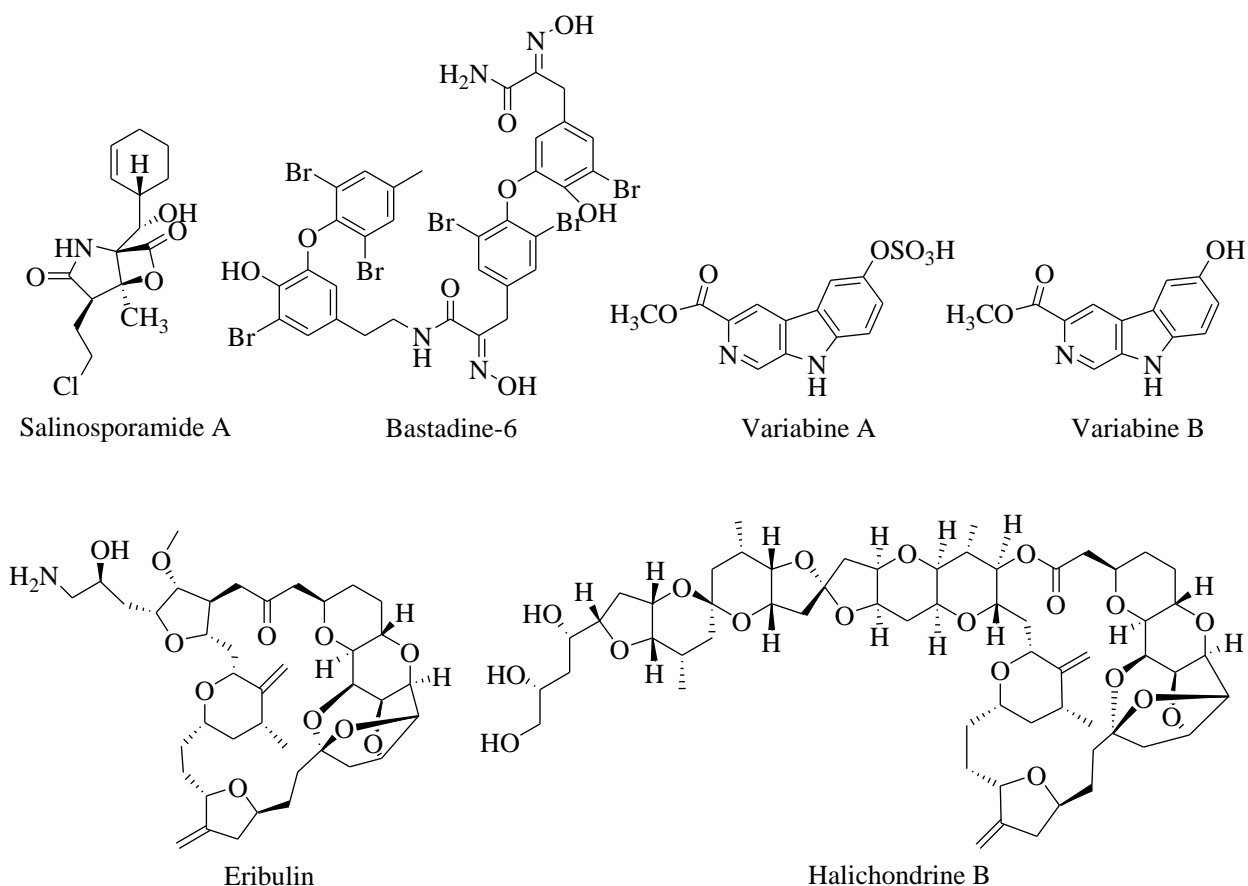


**Fig. 1.6. Selected metabolites with promising anti-cancer activity**

#### 1.4.4. Anti-inflammatory compounds

Many publications about identification of marine-derived metabolites with anti-inflammatory activity were reported.

Monoalide was extracted from sponges *Luffariella variabilis*.<sup>41)</sup> Monoalide inhibits A2 phospholipase enzyme and the hydrolytic elimination of arachidonic acid from phospholipids, demonstrating anti-inflammatory properties.<sup>42)</sup>

Cavernolide is a C21 terpene lactone obtained from the sponge *Fasciospongiacavernosa*. It acts as a potent inhibitor for the tumor necrosis factor- $\alpha$ , nitric oxide, and prostaglandin E2 *in vitro* due to its ability to inhibit the human synovial phospholipase A2 and inducible nitric oxide synthase (iNOS) and cyclooxygenase-2 (COX-2) gene expression in intact cells.<sup>43)</sup>



Tedanol, a brominated and sulfated pimarane diterpene, isolated from the Caribbean sponge *Tedania ignis* showed a potent anti-inflammatory activity at 1 mg/kg evaluated *in vivo* in a mouse model of inflammation. After a single intraperitoneal administration, tedanol significantly reduced both the acute and the subchronic phases of carrageenan-induced inflammation. The anti-inflammatory activity was coupled with a strong inhibition of COX-2 expression, inhibition of cellular infiltration measured as mieloperoxidase(MPO) levels, and inhibition of iNOS expression. These features make tedanol a promising template for the development of new anti-inflammatory molecules with low gastrointestinal toxicity.<sup>44)</sup>

Contignasterol<sup>45)</sup> an unusual steroid from the sponges *Petrosia contignata*, was studied under the code IZP 94005 as an anti-inflammatory agent. In contrast to drugs with analogous action, this compound is not an inhibitor of A2 phospholipase, but it inhibits the excretion of histamine by leukocytes and is referred to as a leukocyte-selective anti-inflammatory agent.<sup>46)</sup>Inflazyme Pharmaceutical Ltd. and Aventis Pharma (USA) were jointly developing a new drug on the basis of contignasterol. However, because of its extremely complicated structure, contignasterol was modified and replaced with the simpler, highly active, synthetic analogues IPL 576092 and IPL 512602 I.<sup>47)</sup>

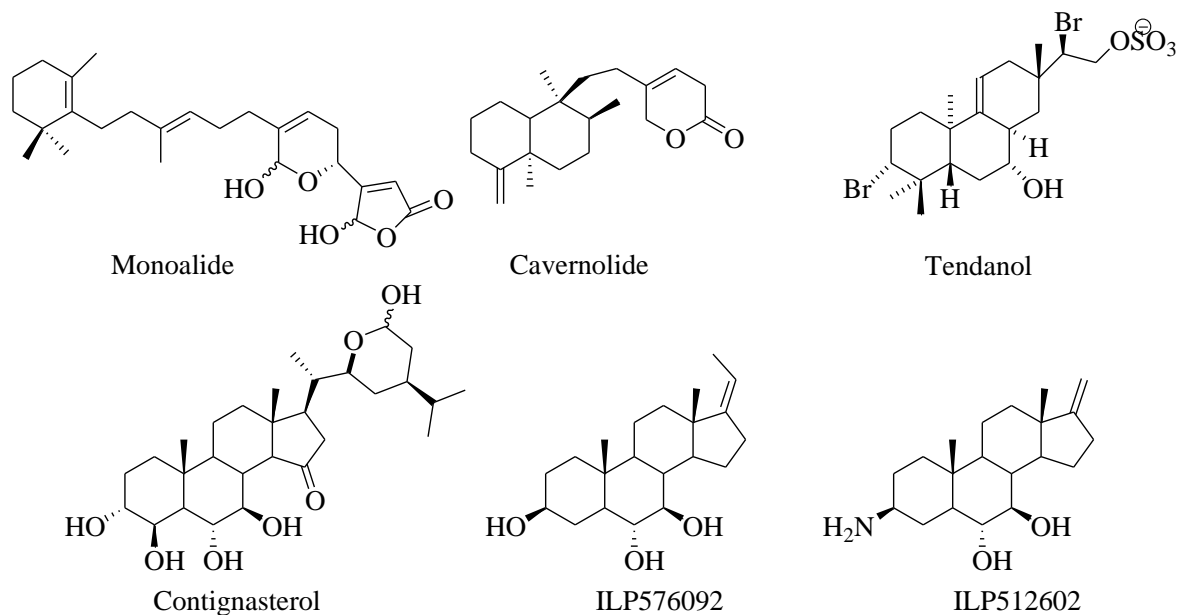


**Fig. 1.7. Selected metabolites with promising anti-inflammatory activity**

#### 1.4.5. Antibacterial and antifungal compounds

With respect to antibiotics and fungicides, similar multi resistance problems have concerned physicians for a long time. Many new molecules with antibiotic properties are discovered every year, but in marine sponges their ubiquity is remarkable. An early screening by Burkholder and coworker<sup>48)</sup> revealed that 18 of 31 sponges tested showed antimicrobial effects, of which some were very strong against a range of gram-positive and gram-negative bacteria.<sup>49)</sup>

Naamine D a novel imidazole alkaloid, isolated from the Red Sea sponge *Leucettacif. chagosensis*<sup>50)</sup> had a MIC of 6.25  $\mu\text{g/mL}$  against *Cryptococcus neoformans*. Interestingly, naamine D at 1  $\mu\text{M}$  competitively inhibited murine macrophage-inducible nitric oxide synthase by 50 %.

Two new alkaloids, hyrtimomines D and E, were isolated from an Okinawan marine sponge *Hyrtios sp.* Hyrtimomines D and E are unique bisindole alkaloids possessing the canthin-6-one skeleton with a hydroxyindole and an imidazolium units. Hyrtimomines D and E act as a potent inhibitors against *Cryptococcus neoformans* (IC<sub>50</sub>, 4 and 8  $\mu\text{g/ml}$ , respectively) and *Candida albicans* (IC<sub>50</sub>, 4 and 8  $\mu\text{g/ml}$ , respectively), while hyrtimomine D acts as a potent inhibitor

against *Trichophyton mentagrophytes* (MIC 16  $\mu\text{g/ml}$ ) and *Staphylococcus aureus* (MIC, 4  $\mu\text{g/ml}$ ).<sup>51)</sup>

Essramycin, a novel triazolopyrimidine antibiotic isolated from *Streptomyces* sp, showed a promising antibacterial activity with MIC of 2–8  $\mu\text{g/ml}$  against Gram-positive and Gram-negative bacteria.<sup>52)</sup>

Araguspongins C isolated from the marine sponge *Haliclona exigua*, showed a promising antifungal activity against *Cryptococcus neoformans*, *Sporothrix schenckii*, *Trichophyton mentagrophytes* and *Aspergillus fumigatus* with identical MIC of 50  $\mu\text{g/ml}$  against them.<sup>53)</sup>

N-(2-hydroxyphenyl)-2-phenazinamine (NHP) is a new antibiotic isolated from *Nocardia dassonvillei*. The new compound showed significant antifungal activity against *Candida albicans*, with a MIC of 64  $\mu\text{g/ml}$ .<sup>54)</sup>

Lynamicins, are chlorinated bisindole pyrroles, isolated from *Marinispora* sp. showed significant activity against drug-resistant pathogens such as methicillin-resistant *Staphylococcus aureus* and vancomycin-resistant *Enterococcus faecium*.<sup>55)</sup>

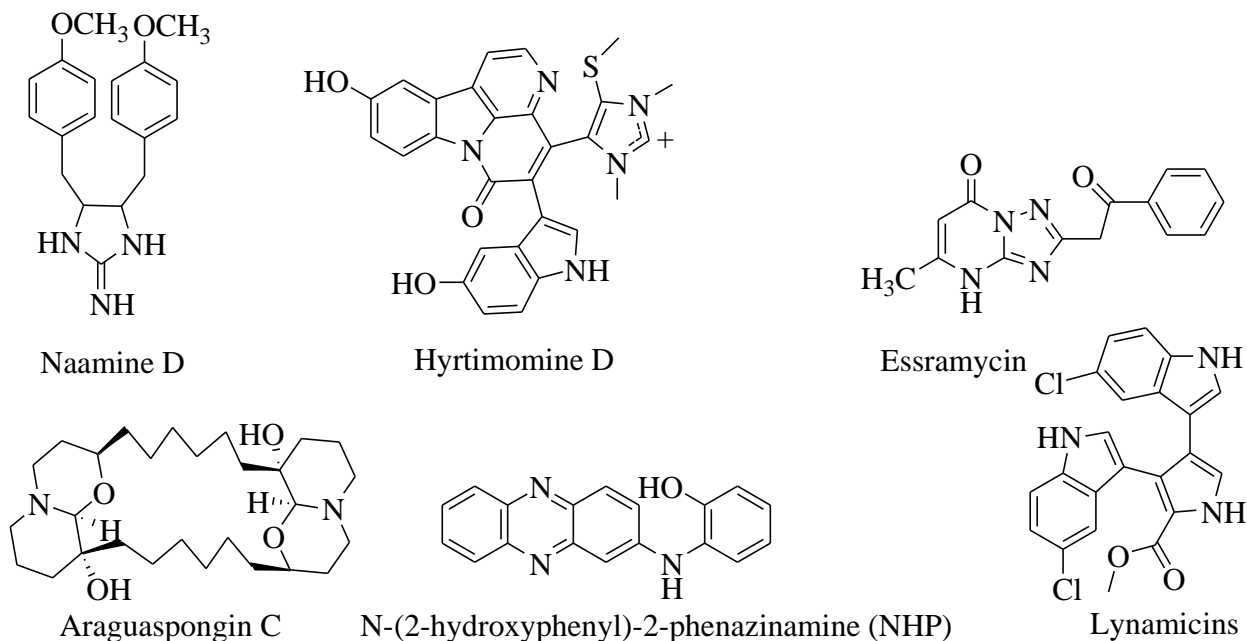


**Fig. 1.8. Selected metabolites with promising antibacterial and antifungal activity**

#### 1.4.6. Antiprotozoal compounds

Throughout the world, Many attempts have been developed to harvest marine natural products in fighting infectious diseases caused by parasites occur in human and animal.

Manzamine type alkaloids have been isolated from an Indonesian sponge and have shown effects against malaria, in addition to tuberculosis and leishmania.<sup>56)</sup>Manzamine A and selected derivatives are known to have a fast onset of action because of high degree of bioavailability and prolonged antiparasitic activity without obvious toxic effects.<sup>57)</sup> These compounds showed promising activity against *Leishmania Mexicana* protozoa which cause diseases like cutaneous ulcer and nasopharyngeal infections.

Gracilioethers A-C, isolated from marine sponge *Agelas gracilis* showed antimalarial activity against the parasite *P. falciparum*. In addition, Gracilioether B displayed antileishmanial activity (68% inhibition at 0.029  $\mu\text{M}$ ).<sup>58-59)</sup>

Pandarosides E-J, the new steroidal glycosides were reported from a Caribbean sponge *Pandora sacanthifolium*. These compounds as well as their methyl esters displayed promising antiprotozoal activity against *Trypanosoma bruceirhodesiense* and *Leishmania donovani*. Among these, Pandaroside G and its methyl derivative, exhibited the highest activity ( $\text{IC}_{50}$  = 0.038  $\mu\text{M}$  and 0.051  $\mu\text{M}$ , respectively). The other compound was also active against multidrug resistant malarial *Plasmodium falciparum* strain.<sup>59-60)</sup>

(2S,5R,6R)-2-hydroxy-3,5,6-trimethyloctan-4-one, isolated from marine *Streptomyces* sp. VITDDK3 possessed acaricidal and larvicidal activity against blood-sucking parasites.<sup>61)</sup>

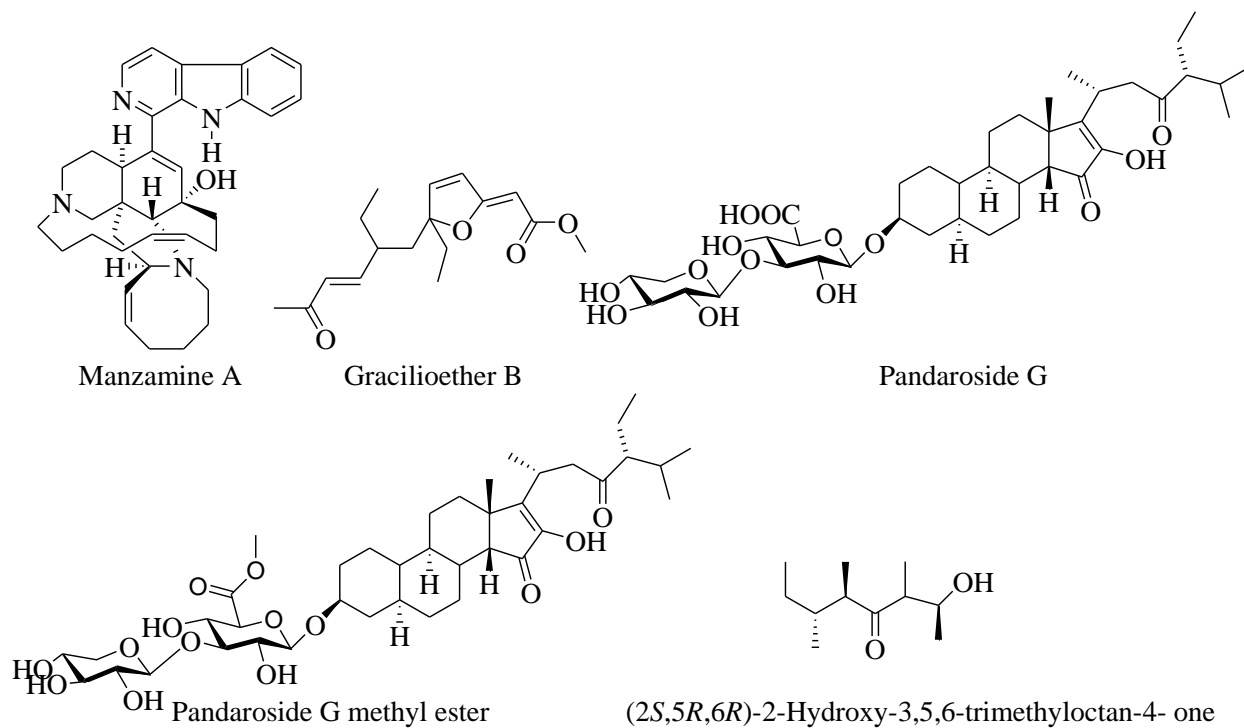


**Fig. 1.9. Selected metabolites with promising antiprotozoal activity**

#### 1.4.7. Anti-tuberculosis compounds

Some of the numerous marine antimicrobial compounds displayed high activity against the tuberculosis bacterium *Mycobacterium tuberculosis*.

For instance, pseudopteroxazol, benzoxazole diterpene alkaloid from the gorgonian coral *Pseudopterogorgia elisabethae*, inhibits the growth of this mycobacterium by 97% in a concentration of 12.5  $\mu\text{g/ml}$  in the absence of toxic effects, while (+)-8-hydroxymanzamine from the sponge *Pachypellina* sp has a minimum inhibiting concentration of 0.91  $\mu\text{g/ml}$ .<sup>62)</sup>

The known bromopyrrole alkaloids, hymenidin and monobromoisophakellin,<sup>63-64)</sup> are also reported in the marine sponge *Prosuberites laughlini*. Preliminary tests for anti-tuberculosis activity of these two alkaloids demonstrated that these compounds significantly inhibited the growth of *Mycobacterium tuberculosis* H37Rv (MIC values = 6.1 and 64.0  $\mu\text{g/mL}$ ).<sup>65)</sup>

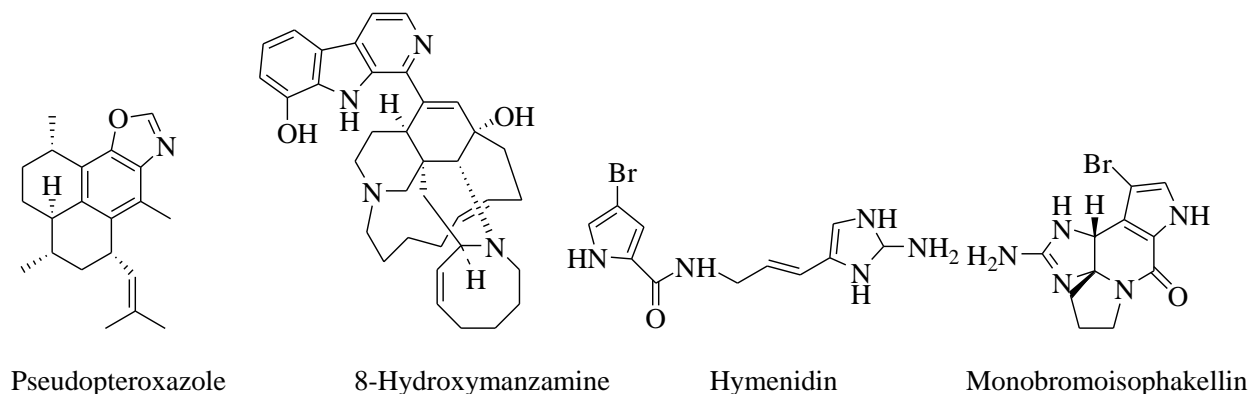


**Fig. 1.10. Selected metabolites with promising anti-tuberculosis activity**

#### 1.4.8. CNS depressant compounds

New anthramycin-type analogues, designated usabamycin A–C have been isolated from cultures of marine *Streptomyces* sp. NPS853. The usabamycins showed selective inhibition of serotonin (5 hydroxy tryptamine) 5-HT<sub>2B</sub> uptake.<sup>66)</sup>

An antiepileptic ceramide mixture was isolated from the Red Sea sponge *Negombata corticata*. The anticonvulsant activity of the ceramide mixture on male albino rats was measured using the pentylene tetrazole-induced seizure model. This finding has important implications for biological studies with this class of compounds.<sup>67)</sup>

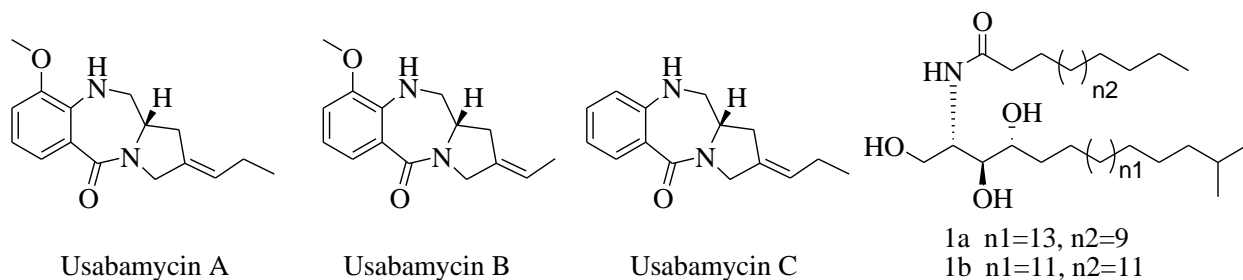


**Fig. 1.11. Selected metabolites with CNS activity**

### 1.5. Current status of natural products research

The growing interest in marine natural products has led to the discovery of an increasing number of potentially active metabolites considered worthy for clinical applications. A recent review provided an updated list of NP-derived drugs launched since 2008 (Table 1.1) and natural products which are currently under in late stage clinical development (Table 1.2).<sup>68)</sup>

**Table 1.1: NP-derived drugs launched since 2008 by year with reference to their lead compound, classification and disease area**

| Year | Generic name (trade name)                     | Lead compound (source)          | Classification | Disease area                |
|------|---|---------------------------------|----------------|-----------------------------|
| 2006 | Varenicline<br>(Chantix/Champix)              | (-)-Cytisine (plant)            | NP-derived     | Nicotine dependence         |
| 2008 | Ceftobiprolemedocartil<br>(Zeftera, Zevtera™) | Cephalosporin C (fungus)        | SS NP          | Antibacterial               |
| 2008 | Umirolimus (Biomatrix)                        | Sirolimus (actino)              | SS NP          | Cardiovascular surgery      |
| 2008 | Methylnaltrexone<br>(Relistor)                | Morphine (plant)                | NP derived     | Opioid-induced constipation |
| 2009 | Tebipenempivoxil<br>(Orapenem)                | Thienamycin (actino)            | SS NP          | Antibacterial               |
| 2009 | Telavancin (Vibativ)                          | Vancomycin (actino)             | SS NP          | Antibacterial               |
| 2009 | Romidepsin (Istodax)                          | Romidepsin (bacteria)           | NP             | Cancer                      |
| 2009 | Nalfurafine (Remitch)                         | Morphine (plant)                | SS NP          | Pruritus                    |
| 2010 | Cabazitaxel (Jevtana)                         | Paclitaxel (plant)              | SS NP          | Cancer                      |
| 2010 | Fingolimod (Gilenya)                          | Myricocin (fungus)              | NP-            | Multiple sclerosis          |
| 2010 | Ceftarolinefosamil<br>(Teflaro)               | Cephalosporin C (fungus)        | SS NP          | Antibacterial               |
| 2010 | Eribulin (Halaven)                            | Halichondrin B (sponge)         | NP-derived     | Cancer                      |
| 2010 | Mifamurtide (Mepact)                          | Muramyl dipeptide<br>(bacteria) | NP-derived     | Cancer                      |

|      |                                       |  |            |                           |
|------|---------------------------------------|--|------------|---------------------------|
| 2010 | Zucapsaicin (Zuacta)                  | Capsaicin (plant)                      | NP-derived | Pain                      |
| 2011 | Fidaxomicin (Difucid)                 | Fidaxomicin (actino)                   | NP         | Antibacterial             |
| 2011 | 2011 Spinosad (Natroba)               | Spinosyn A : D (actino)                | NP         | Antiparasitic             |
| 2011 | Brentuximabvedotin<br>(Adcetris)      | Dolastatin (sea<br>hare/cyanobacteria) | ADC        | Cancer                    |
| 2012 | Ingenolmebutate (Picato)              | Ingenolmebutate (plant)                | NP         | keratosis                 |
| 2012 | Dapagliflozin (Forxiga)               | Phlorizin (plant)                      | NP-derived | Type 2 diabetes           |
| 2012 | Carfilzomib (Kyprolis)                | Epoxomicin (actino)                    | NP-derived | Oncology                  |
| 2012 | Arterolane /piperazine<br>(Synriam)   | Artemisinin (plant)                    | NP-derived | Antiparasitic             |
| 2012 | Novolimus (DESyne)                    | Sirolimus (actino)                     | SS NP      | Cardiovascular<br>surgery |
| 2013 | Canagliflozin 43<br>(Invokana)        | Phlorizin (plant)                      | NP-derived | Type 2 diabetes           |
| 2013 | Ado-trastuzumabemtansine<br>(Kadcyla) | Maytansine<br>(bacteria/plant)         | ADC        | Cancer                    |

**Table 1.2: NP-derived drugs in late stage clinical development (NDA or equivalent and phase III) on 31 December 2013.**

| Compound                 | Classification | Disease area (therapeutic area)                             |
|--------------------------|----------------|---|
| <u>NDA or equivalent</u> |                |   |
| Dalbavancin              | SS NP          | Antibacterial (anti-infective)                              |
| Oritavancin              | SS NP          | Antibacterial (anti-infective)                              |
| Ipragliflozin            | NP-derived     | Type 2 diabetes (cardiovascular and metabolic)              |
| Luseogliflozin           | NP-derived     | Type 2 diabetes (cardiovascular and metabolic)              |
| Empagliflozin            | NP-derived     | Type 2 diabetes (cardiovascular and metabolic)              |
| Tofogliflozin            | NP-derived     | Type 2 diabetes (cardiovascular and metabolic)              |
| Vorapaxar                | NP-derived     | Anti-thrombotic (cardiovascular and metabolic)              |
| Naloxegol                | SS NP          | Opioid-induced constipation<br>(immunological,inflammatory) |



Phase III

|                         |            |   |
|-------------------------|------------|---|
| Plazomicin              | SS NP      | Antibacterial (anti-infective)                            |
| Surotomycin             | SS NP      | Antibacterial (anti-infective)                            |
| Solithromycin           | SS NP      | Antibacterial (anti-infective)                            |
| Ceftolozane/tazobactam  | SS NP      | Antibacterial (anti-infective)                            |
| Eravacycline            | NP-derived | Antibacterial (anti-infective)                            |
| Epigallocatechingallate | NP         | Alzheimer's disease (neurological)                        |
| Tetrodotoxin            | NP         | Pain (neurological)                                       |
| Ertugliflozin           | NP-derived | Type 2 diabetes (cardiovascular and metabolic)            |
| ATX-101                 | bile acid  | submental fat reduction (cardiovascular and metabolic)    |
| Migalastat              | SS NP      | Fabry disease (cardiovascular and metabolic)              |
| Naldemedine             | NP-derived | Opioid-induced constipation (immunological, inflammatory) |
| Recoflavone             | NP-derived | Gastritis/dye eye (immunological, inflammatory)           |
| Obeticholic acid        | SS NP      | Biliary cirrhosis (immunological, inflammatory)           |
| Siponimod               | NP-derived | Multiple sclerosis (immunological, inflammatory)          |
| Karenitecin             | SS NP      | Oncology  |
| Fosbretabulin           | SS NP      | Oncology  |
| Vintafolide             | NP-derived | Oncology  |
| Zoptarelin doxorubicin  | SS NP      | Oncology  |
| Lestaurtinib            | NP derived | Oncology  |
| Midostaurin             | NP derived | Oncology  |
| Tivantinib              | NP         | Oncology  |
| Plitidepsin             | NP         | Oncology  |
| Panobinostat            | NP derived | Oncology  |

### 1.6. Aim of the study

Marine secondly metabolites particularly those that can be utilized as medications have shown a noteworthy effect on the improvement of pharmaceutical industry.<sup>69)</sup> Many excellent reviews have been published on the compounds with potent pharmacological activity to fight several devastating diseases experienced nowadays including cancer, HIV, osteoporosis, and AD.<sup>69-71)</sup>

Previous study done by our group on the Red Sea grass *Thalassodendron ciliatum* showed that the crude extract of *T. ciliatum* possessed potent antiviral activity (100% inhibition at the concentration of 1 µg/mL).<sup>72)</sup> Further chemical investigation the crude extract of *T. ciliatum* led to the isolation of asebotin which showed a potent activity against H5N1 virus. It could reduce the virus titre by 53.81% inhibition at concentration of 1 ng mL<sup>-1</sup>.<sup>72)</sup>

Among marine organisms which were collected from the Red Sea, the marine sponge *Mycale euplectellioides*. To the best of my knowledge there is only one research paper related to the chemical study on the bioactive metabolites obtained from *Mycale euplectellioides*.

Although there are many chemical studies on the marine sponge *Stylissa carteri*, the sphingolipids composition of this marine sponge were not mentioned.

Based on the previous findings, this study has been focused on augmenting the efforts of providing chemical profiles of some Red Sea marine organisms through continuing the chemical investigation of the crude extract *T. ciliatum*, chemical investigation of the crude extract obtained from the marine sponge *M. euplectellioides* and Isolation and identification the sphingolipids composition of the marine sponge *Stylissa carteri*.

## 1.7. General thesis contents

The main target of my laboratory and of the research presented within this doctor thesis is to search for bioactive metabolites from different natural resources.

As such, the study outlined in this thesis involves isolation, structure elucidation and biological characterization of pure compounds isolated from sea grass and marine sponges.

This study showed that chemical investigation of the crude extract *T. ciliatum* led to the isolation of a new phytoceramide molecular species TCC-1, along with four known compounds: 7 $\beta$ -hydroxy cholesterol (**10**), 7 $\beta$ -hydroxysitosterol (**11**), stigmasterol glucoside (**12**),  $\beta$ -sitosterol glucoside (**13**) for the first time along with asebotin (**14**) which was previously isolated.

Different phytosphingosine and 2-hydroxy fatty acid residues constituted the phytoceramide molecular species TCC-1. Extra purification of TCC-1 afforded two new phytoceramides: TCC-1-5 (**5**), and TCC-1-7 (**7**), as well as the known ceramide TCC-1-6 (**6**). All these compounds are being reported for the first time in this genus.

The second organism in this study was the Red Sea sponge *Mycale euplectellioides*. Chemical investigation of the crude extract obtained from *Mycale euplectellioides* led to isolation of MEC-1 phytoceramide molecular species. Anti-choline esterase activity of the isolated MEC-1 was evaluated *in vitro* using microplate-based Ellman's assay; further purification of MEC-1 afforded three pure phytoceramides: MEC-1-4 (**15**), MEC-1-7 (**16**) and MEC-1-8 (**17**). Additional phytochemical study of the crude extract obtained from *Mycale euplectellioides* led to the isolation of six known compounds: chimyl alcohol (**18**), batyl alcohol (**19**), thymine (**20**), uracil (**21**), thymidine (**22**) and uridine(**23**).The structures of the isolated compounds elucidated on the basis of chemical methods, spectroscopic techniques (IR, NMR experiments and HRMS), and comparison with appropriate literature data. The molecular modeling studies using glide docking showed the tight binding of ceramides to acetylcholine esterase (AChE). Ceramides have achieved better docking score and glide Emodel compared to known AChE inhibitors. Ceramides interacted with aromatic residue of peripheral anionic site and penetrated deeply till catalytic triad residue of the active site. Overall, ceramides by the

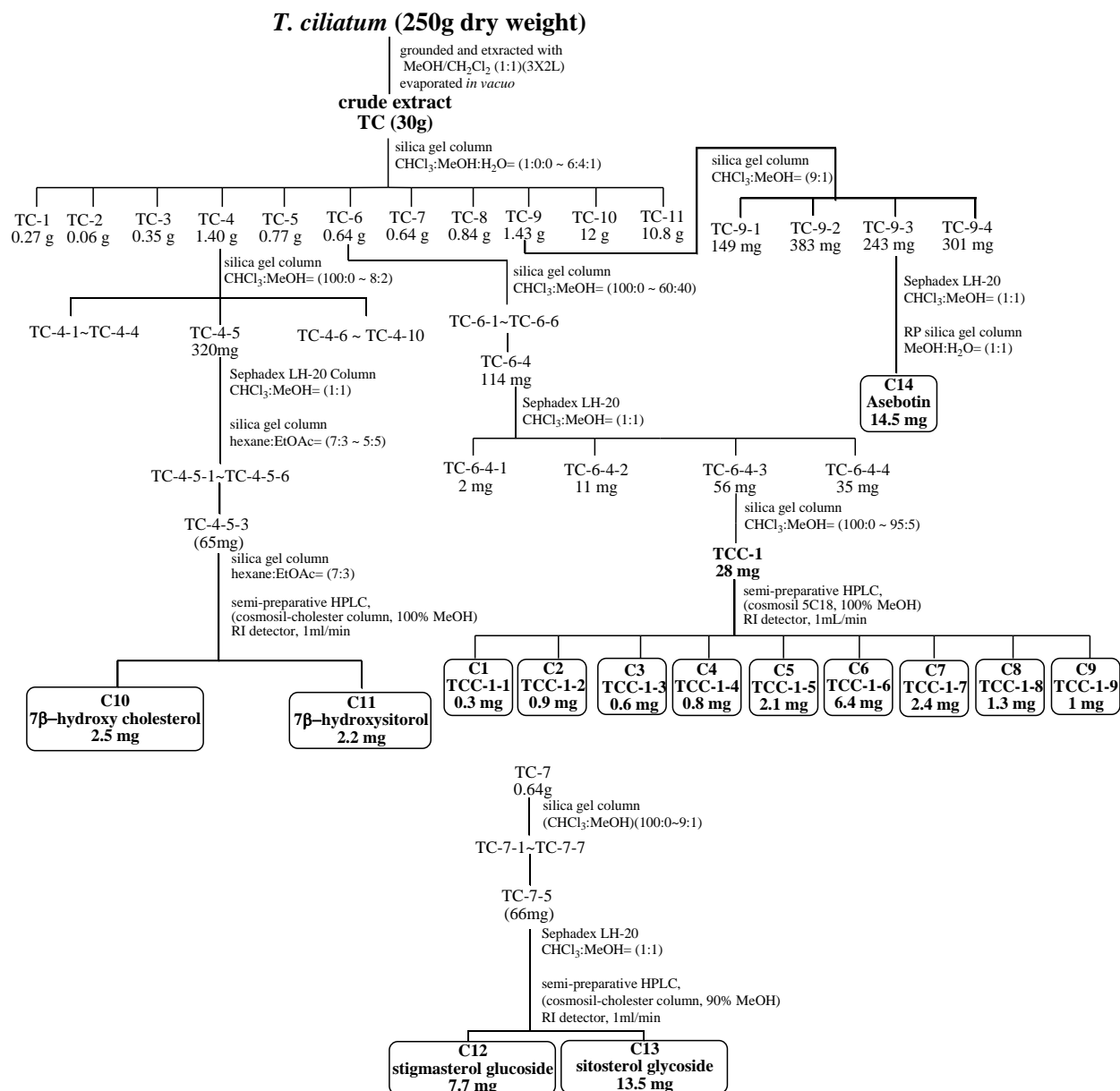
approaches used here could be considered promising lead compounds for discovery and design potent anti-choline esterase drug candidates which would be used for Alzheimer eradication.

The third marine sponge was *Stylissa carteri*. Chemical investigation of the *n*-hexane-chloroform fraction led to isolation of glycosphingolipids possessing  $\alpha$ -galactosyl ceramide structure (**24**) along with the bromopyrrole alkaloid, 2-bromo aldisine (**25**). The galactosyl ceramide molecular species is being reported for the first time in this genus. Based on the considerable importance of determining the sugar absolute configuration in natural product chemistry, one-pot reactions of the aldose obtained from SCC-1 after hydrolysis with L-cysteine methyl ester and *o*-tolylisothiocyanate yielded methyl 2-(polyhydroxyalkyl)-3-(*o*-tolylthiocarbamoyl)-thiazolidine-4(*R*)-carboxylates. Direct HPLC analysis of the reaction mixture and UV detection at 250 nm discriminated that the sugar moiety was D-galactose after comparing with the standard aldoses.

## 2. Results and discussion

### 2.1. Secondary metabolites isolated from *Thalassodendron ciliatum*

Previous study done by my group on the Red Sea grass *Thalassodendron ciliatum* showed that the crude extract of *T. ciliatum* possessed a potent antiviral activity (100% inhibition at the concentration of 1  $\mu$ g/mL). In the same previous study, chemical investigation of the crude extract led to the isolation of asebotin which showed a potent activity against H5N1 virus. In the current study, chemical research of the crude extract obtained from the same sea grass, led to the isolation of a new phytoceramide molecular species TCC-1, along with four known compounds: 7 $\beta$ -hydroxy cholesterol (**10**), 7 $\beta$ -hydroxysitosterol (**11**), stigmasterol glucoside (**12**),  $\beta$ -sitosterol glucoside (**13**) for the first time and asebotin (**14**) which was previously isolated. Different phytosphingosine and 2-hydroxy fatty acid residues constituted the phytoceramide molecular species TCC-1. Extra purification of TCC-1 afforded two new phytoceramides: TCC-1-5 (**5**), and TCC-1-7 (**7**), as well as the known ceramide TCC-1-6 (**6**). All these compounds are being reported for the first time in this genus. All structures were clarified on the basis of chemical methods, spectroscopic techniques (IR, NMR experiments and mass spectrometry), in addition to, the comparison with appropriate literature data. In this part, we would like to present the results of the chemical investigation of the natural products produced by *Thalassodendron ciliatum*.

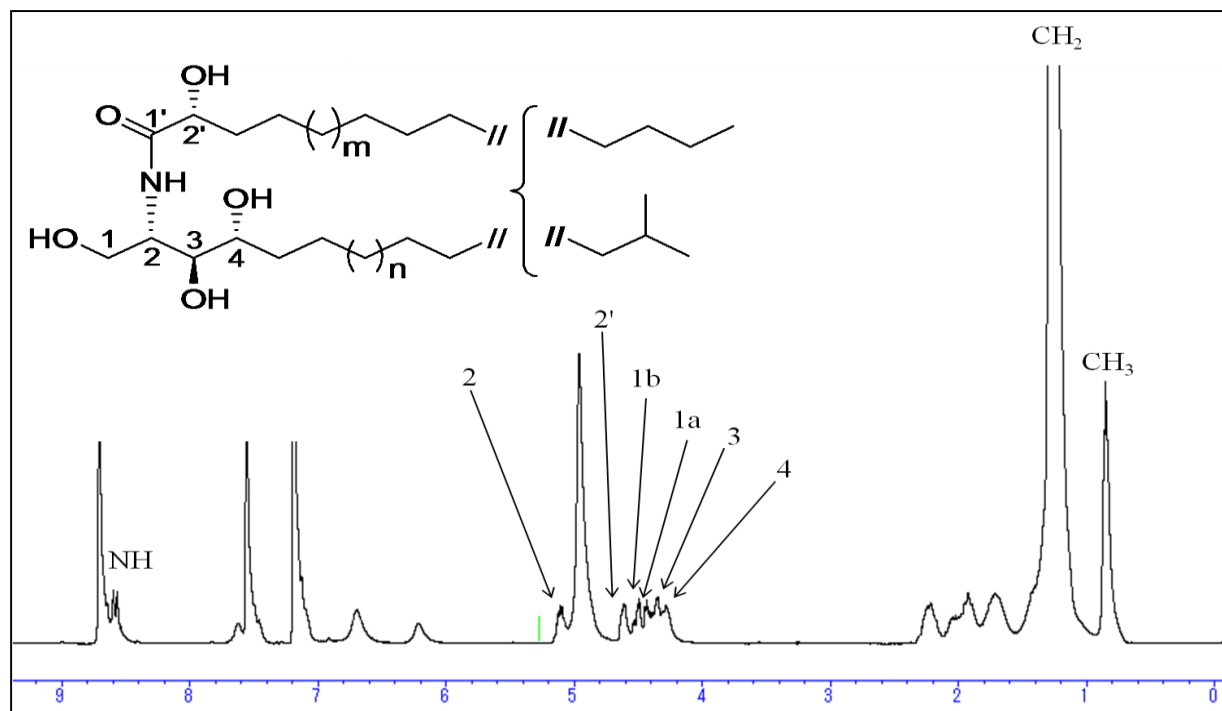
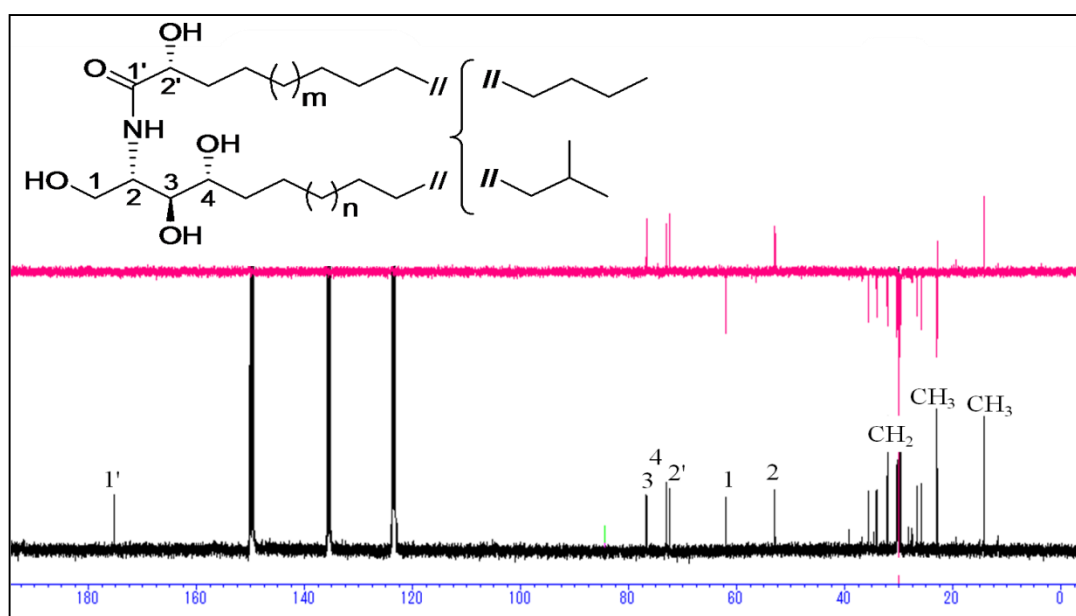


**Fig. 2.1. Extraction and isolation scheme of the Red Sea grass *T. ciliatum***

### 2.1.1. Compounds (1~9)

TCC-1 (28 mg) was obtained as a white amorphous solid, showing a single spot on silica gel thin layer chromatography (TLC) from TC-6 fraction of the crude extract obtained from *T. ciliatum*.

## Spectroscopic analysis

Fig. 2.2.  $^1\text{H-NMR}$  spectrum of TCC-1 (400 MHz,  $\text{C}_5\text{D}_5\text{N}$ )Fig. 2.3.  $^{13}\text{C-NMR}$  spectra of TCC-1 (400 MHz,  $\text{C}_5\text{D}_5\text{N}$ )

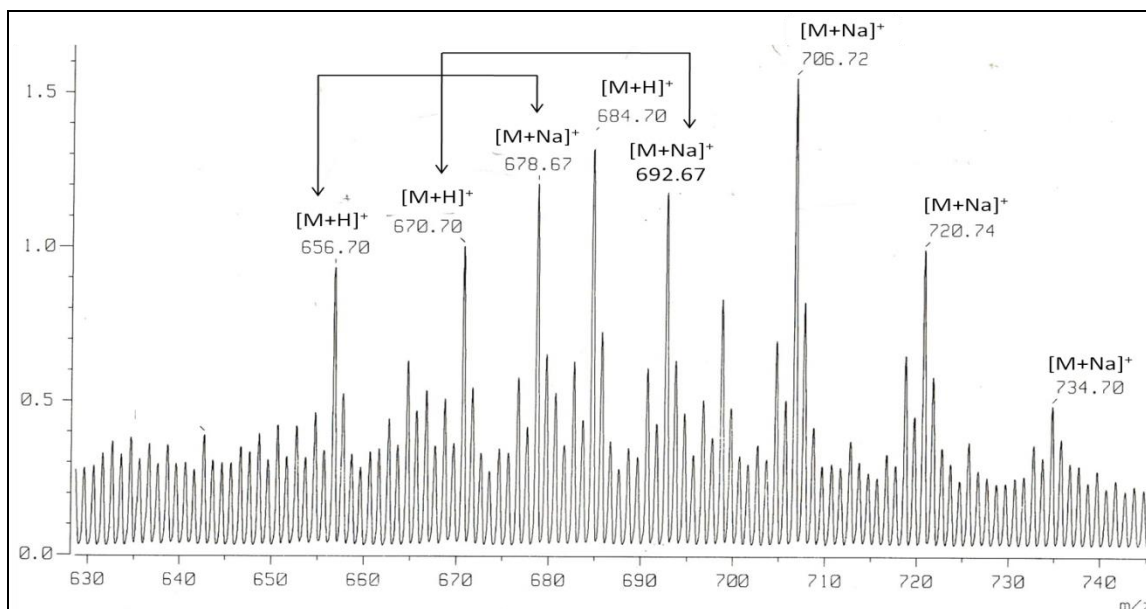


Fig. 2.4. FAB-MS (positive ion mode) of TCC-1

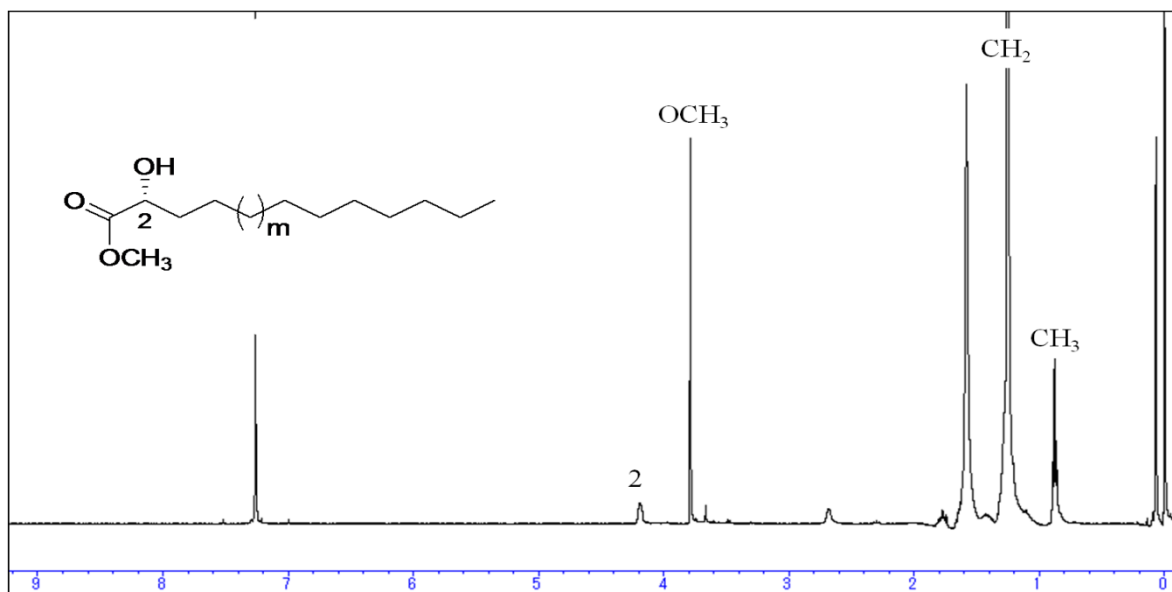
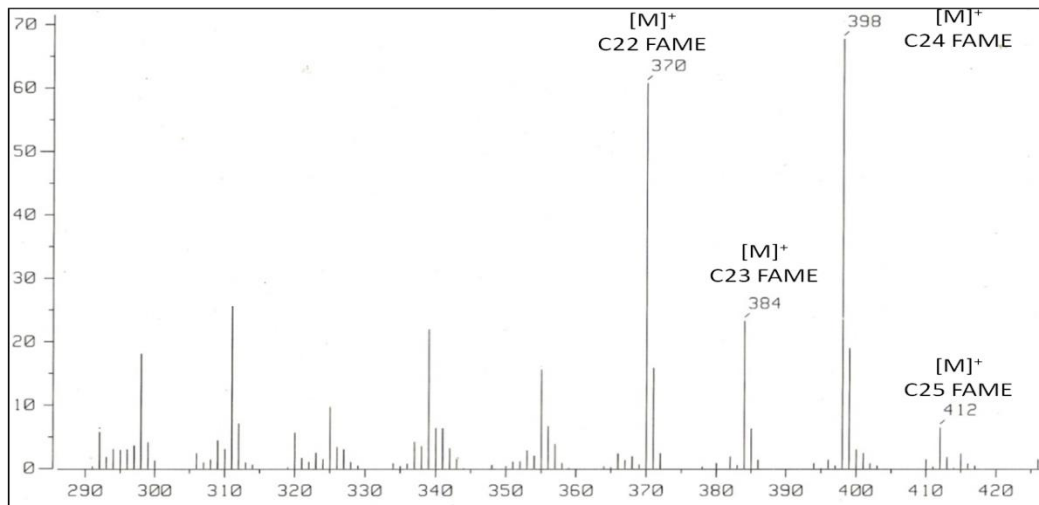


Fig. 2.5.  $^1\text{H-NMR}$  spectrum of FAMES after hydrolysis of TCC-1 (400 MHz,  $\text{CDCl}_3$ )





**Fig. 2.6.** EI-MS of FAMES after hydrolysis of TCC-1

$^1\text{H-NMR}$  (400 MHz) and  $^{13}\text{C-NMR}$  (100 MHz) data for TCC-1 in  $\text{C}_5\text{D}_5\text{N}$  are listed in **Table 2.1**.

**Table 2.1:**  $^{13}\text{C-NMR}$  (100 MHz) and  $^1\text{H-NMR}$  (400 MHz) spectroscopic data of TCC-1 ( $\text{C}_5\text{D}_5\text{N}$ ,  $\delta$  in ppm,  $J$  in Hz).

| <i>TCC-1</i>    |                        |   |
|-----------------|------------------------|---|
| <i>No.</i>      | $\delta_{\text{C}}$    | $\delta_{\text{H}}$ ( <i>No.</i> , <i>M</i> , $J_{\text{Hz}}$ ) |
| NH              |                        | 8.58 (1H, d, $J=8.9$ Hz)  |
| 1a              | 62.0 ( $\text{CH}_2$ ) | 4.43 (1H, dd, $J=10.8, 5.2$ Hz)                                 |
| 1b              |                        | 4.49 (1H, dd, $J=10.8, 4.6$ Hz)                                 |
| 2               | 52.9 (CH)              | 5.12 (1H, m)  |
| 3               | 76.7 (CH)              | 4.35 (1H, m)  |
| 4               | 73.0 (CH)              | 4.27 (1H, m)  |
| 1'              | 175.2 (C)              |   |
| 2'              | 72.4 (CH)              | 4.61 (1H, m)  |
| - $\text{CH}_3$ | 14.2 ( $\text{CH}_3$ ) | 0.88 (m)  |
|                 | 22.7 ( $\text{CH}_3$ ) |   |

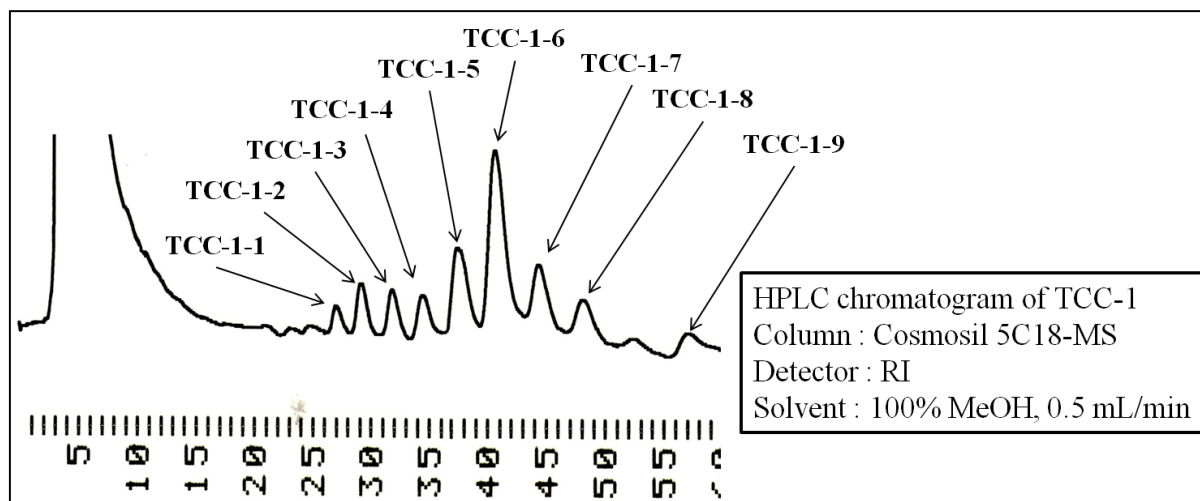


Fig. 2.7. Analytical HPLC chromatogram of TCC-1

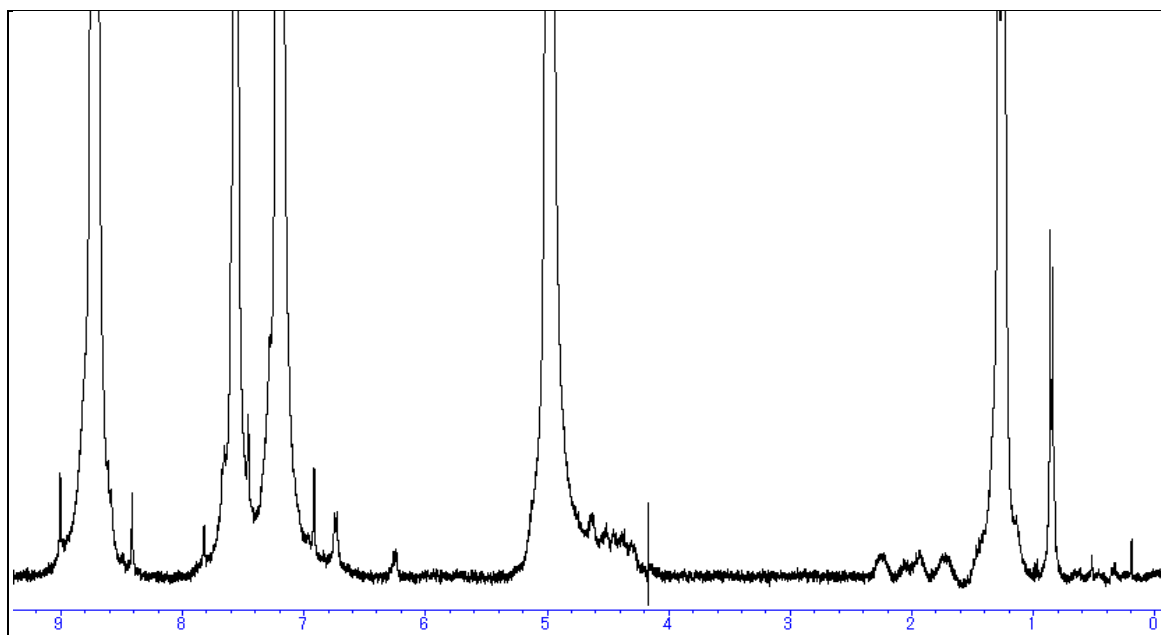
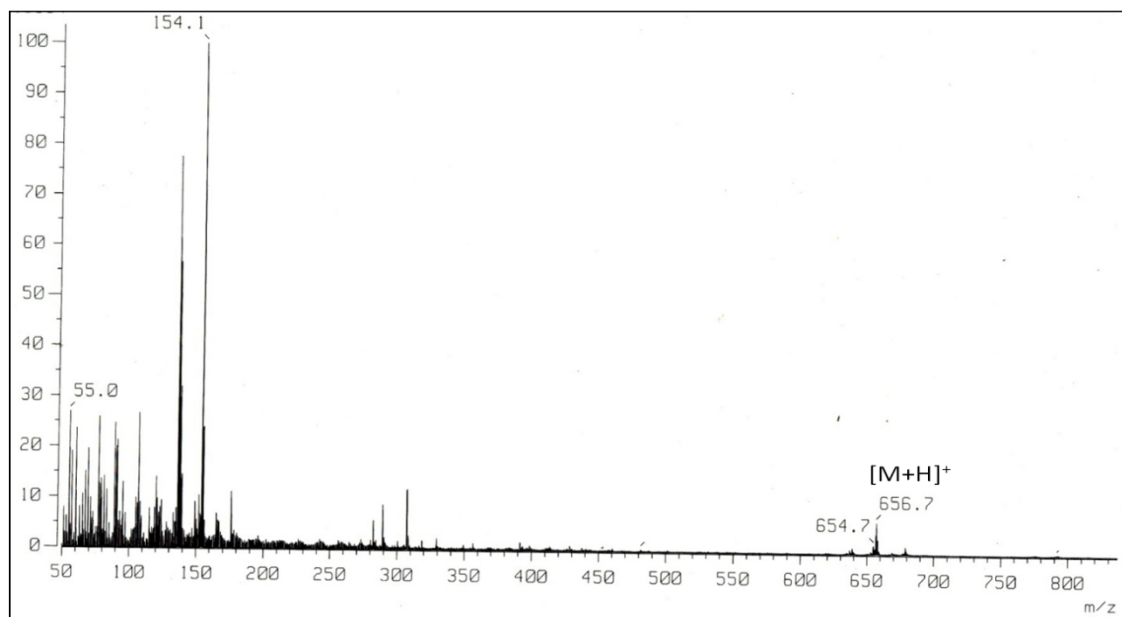
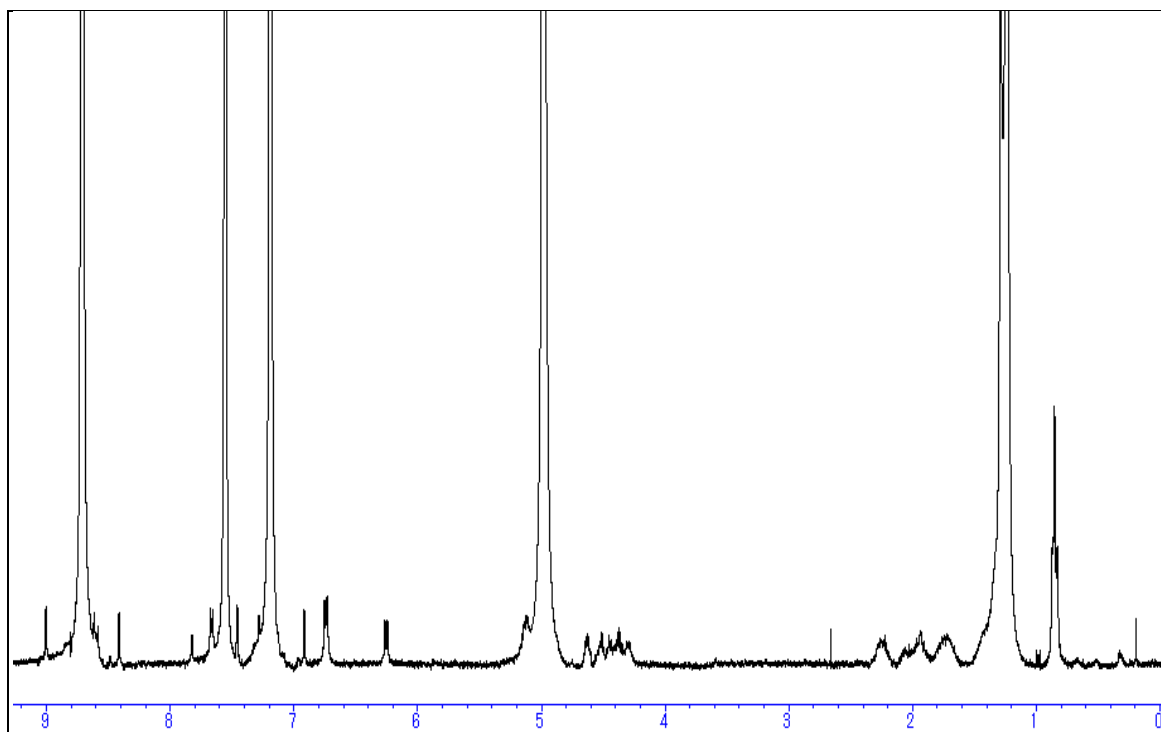


Fig. 2.8.  $^1\text{H-NMR}$  spectrum of TCC-1-1 (400 MHz,  $\text{C}_5\text{D}_5\text{N}$ )



**Fig. 2.9.** FAB-MS (positive ion mode) of TCC-1-1



**Fig. 2.10.**  $^1\text{H}$ -NMR spectrum of TCC-1-2 (400 MHz,  $\text{C}_5\text{D}_5\text{N}$ )

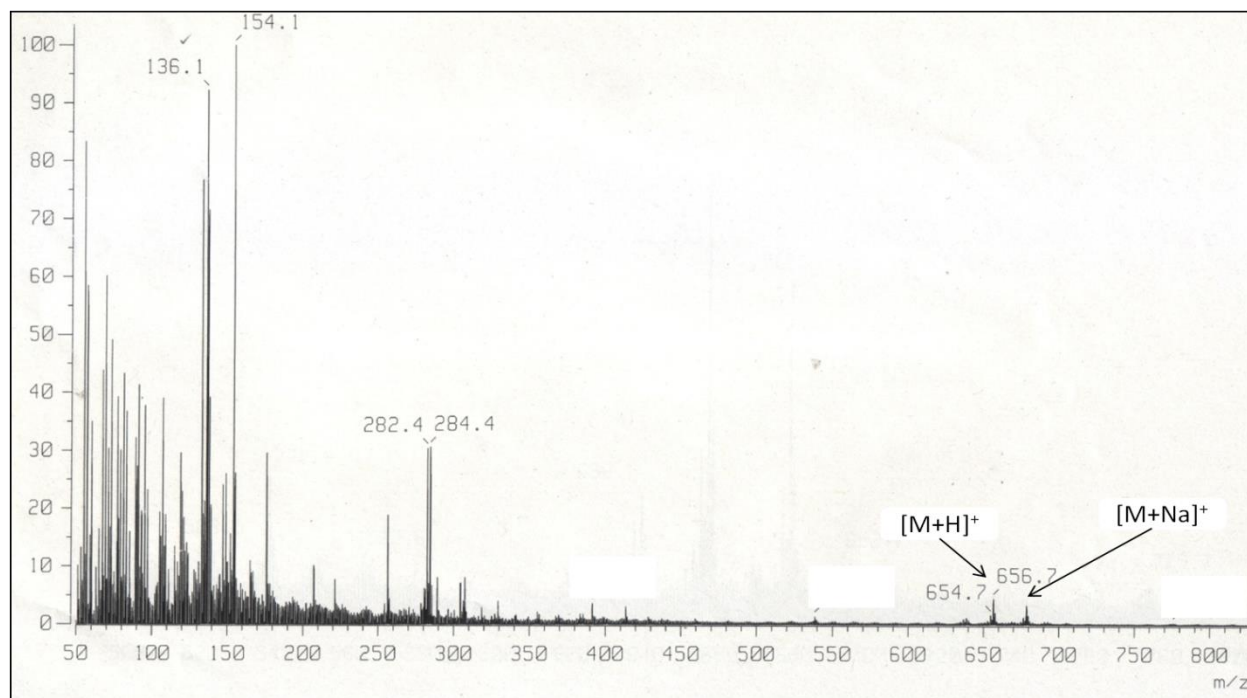


**Fig. 2.11.** FAB-MS (positive ion mode) of TCC-1-2

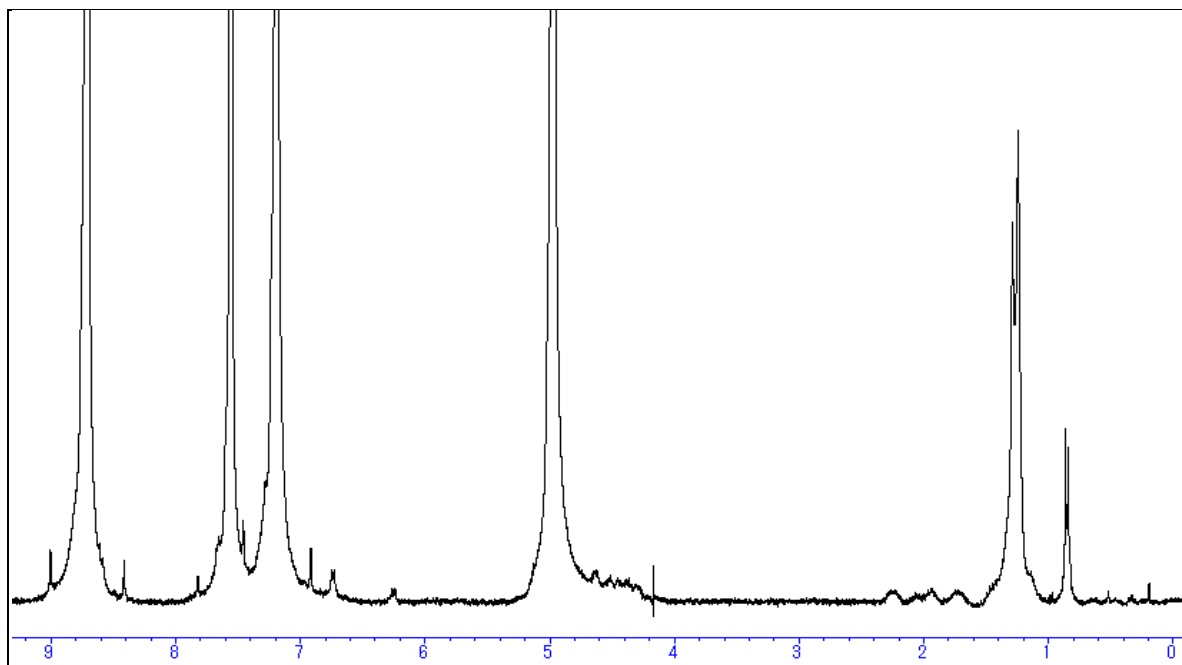


**Fig. 2.12.** <sup>1</sup>H-NMR spectrum of TCC-1-3 (400 MHz, C<sub>5</sub>D<sub>5</sub>N)

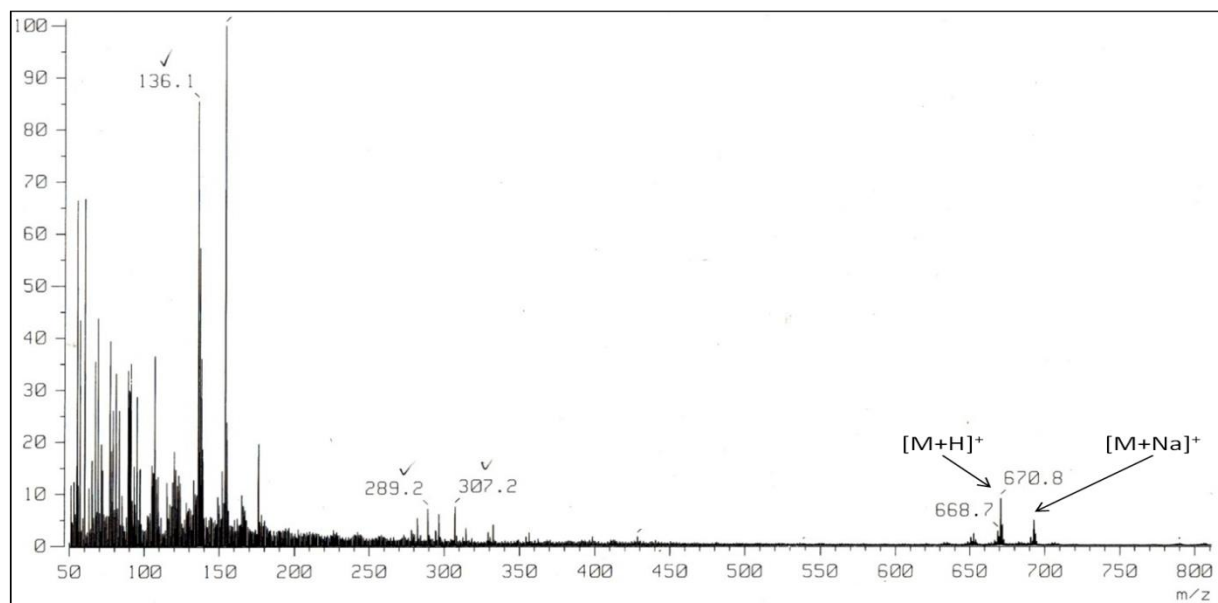


**Fig. 2.13.** FAB-MS (positive ion mode) of TCC-1-3

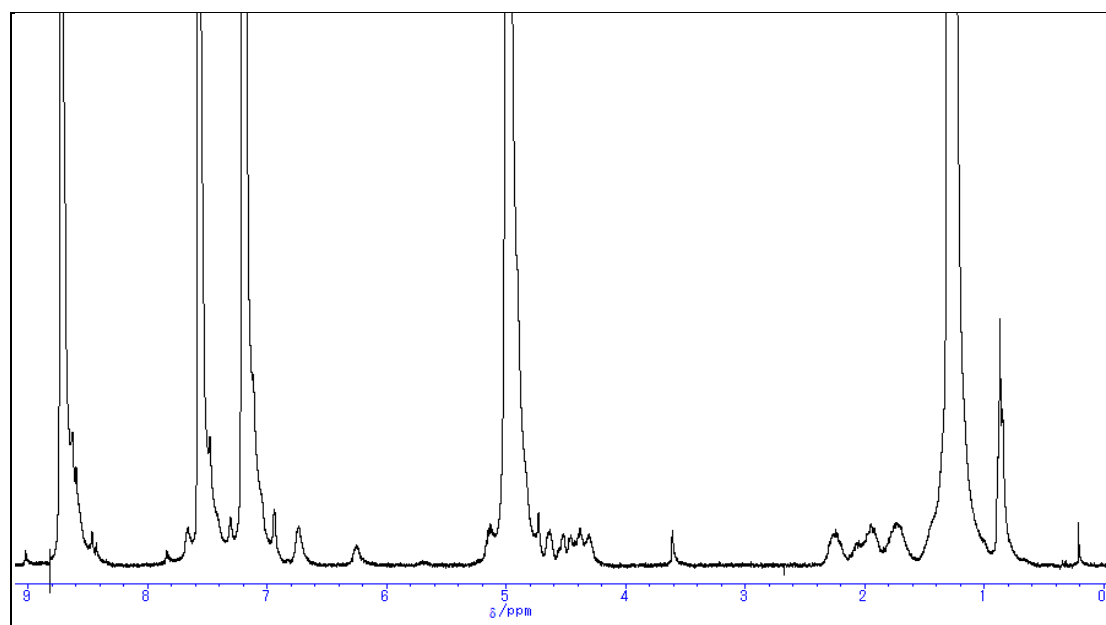


**Fig. 2.14.**  $^1\text{H-NMR}$  spectrum of TCC-1-4 (400 MHz,  $\text{C}_5\text{D}_5\text{N}$ )

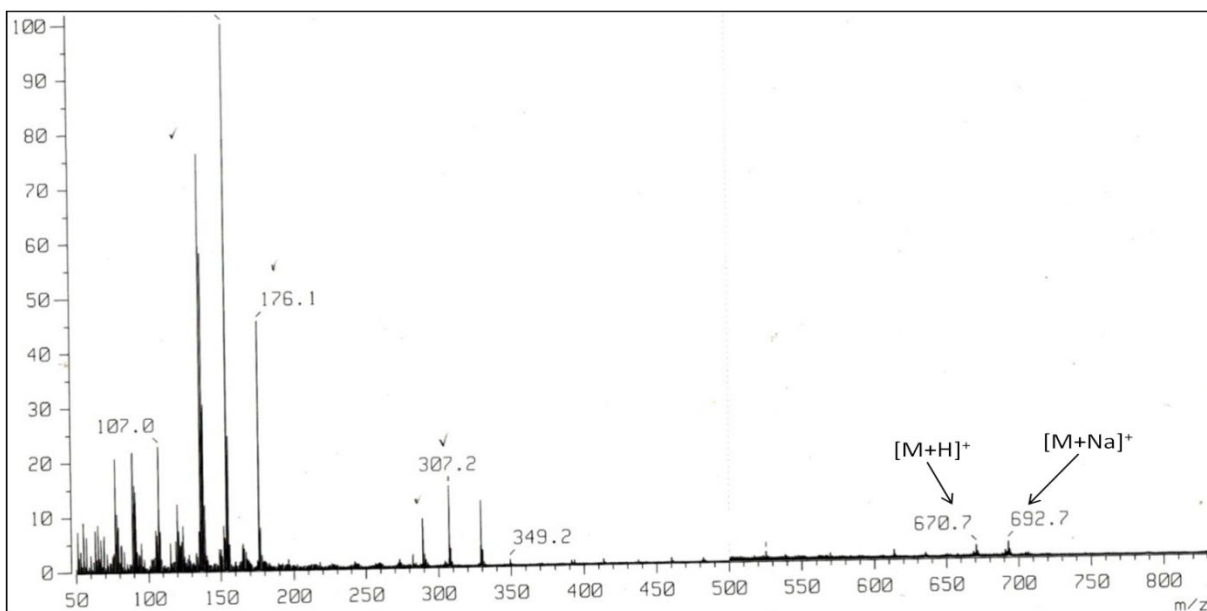


Fig. 2.15. FAB-MS (positive ion mode) of TCC-1-4

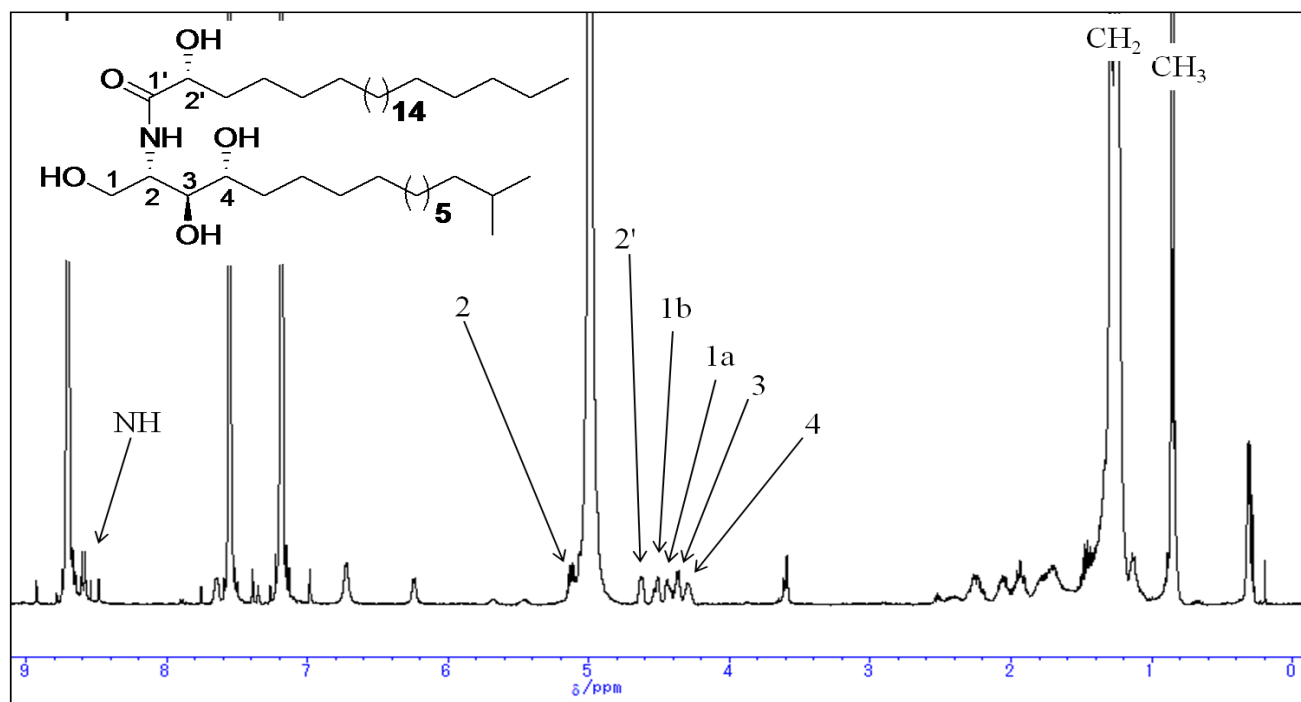


Fig. 2.16. <sup>1</sup>H-NMR spectrum of TCC-1-5 (400 MHz, C<sub>5</sub>D<sub>5</sub>N)

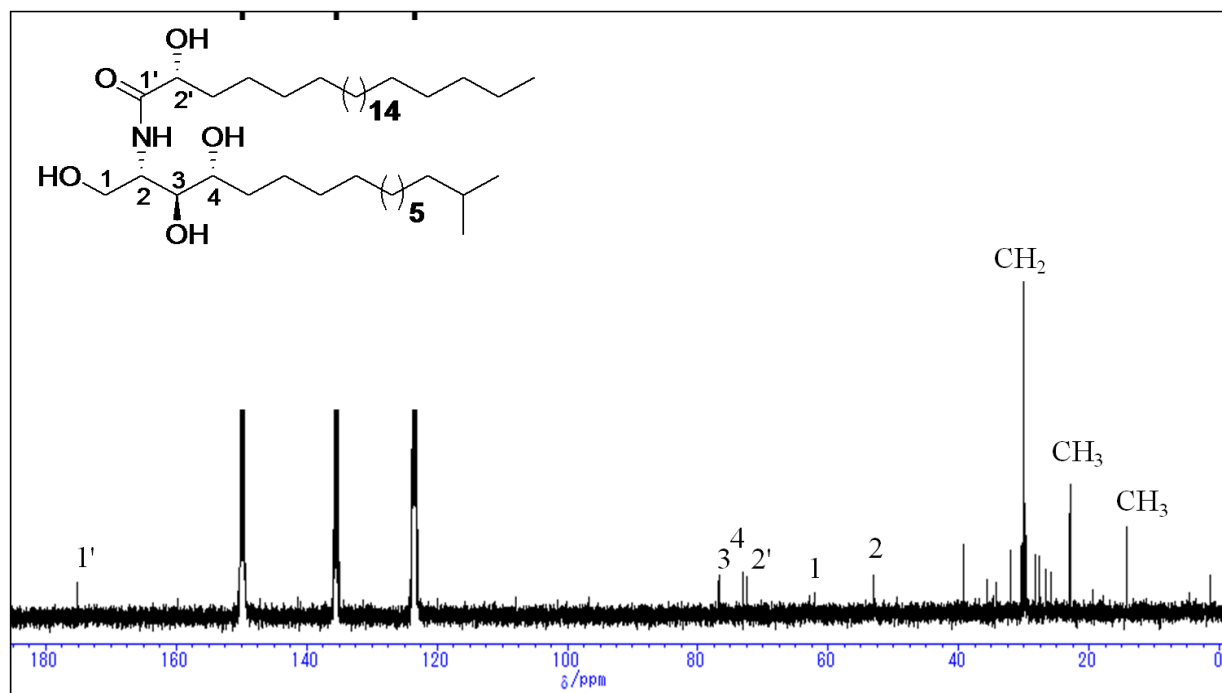


Fig. 2.17.  $^{13}\text{C}$ -NMR spectrum of TCC-1-5 (100 MHz,  $\text{C}_5\text{D}_5\text{N}$ )

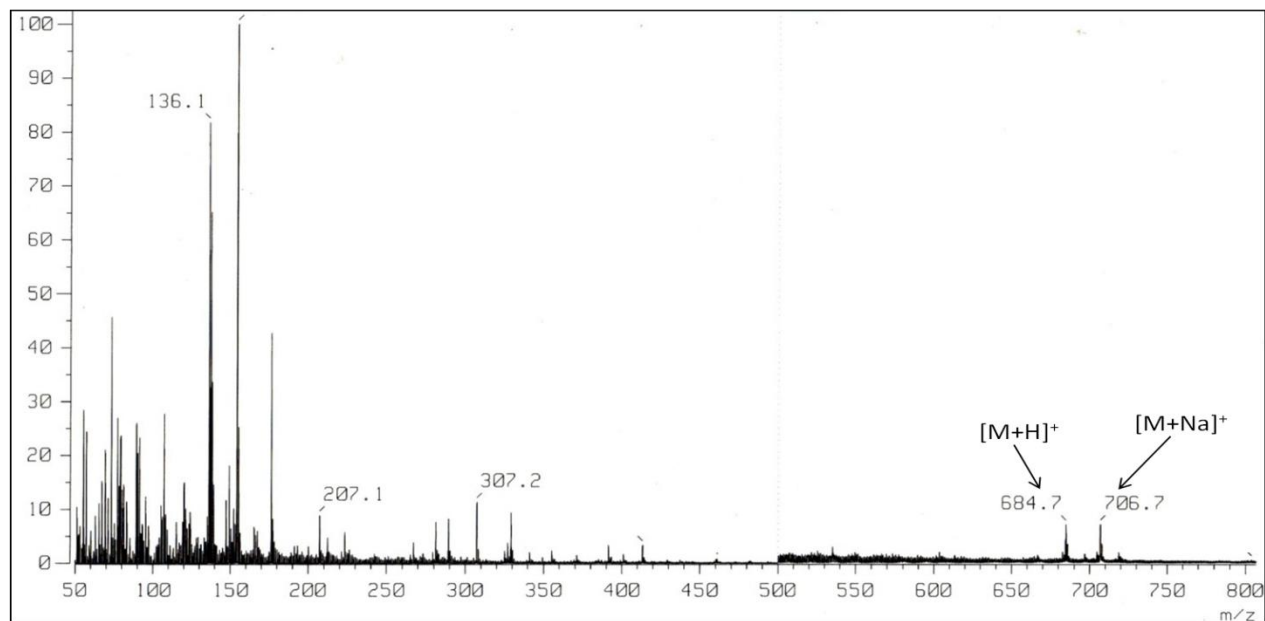


Fig. 2.18. FAB-MS (positive ion mode) of TCC-1-5

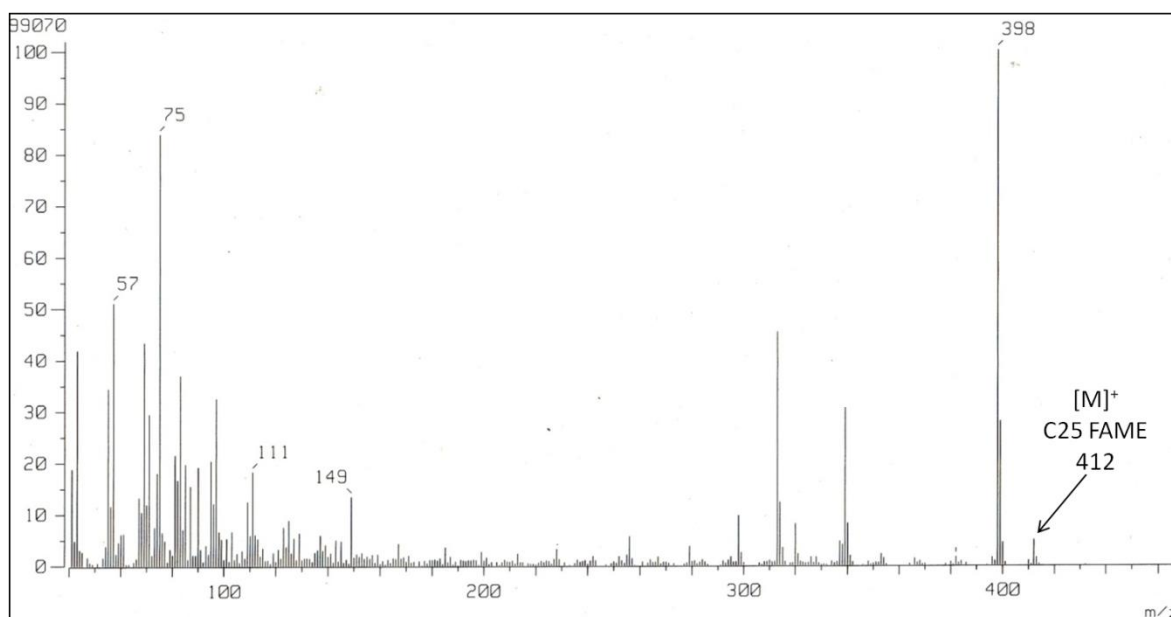


Fig. 2.19. EI-MS (positive ion mode) of TCC-1-5-FAME

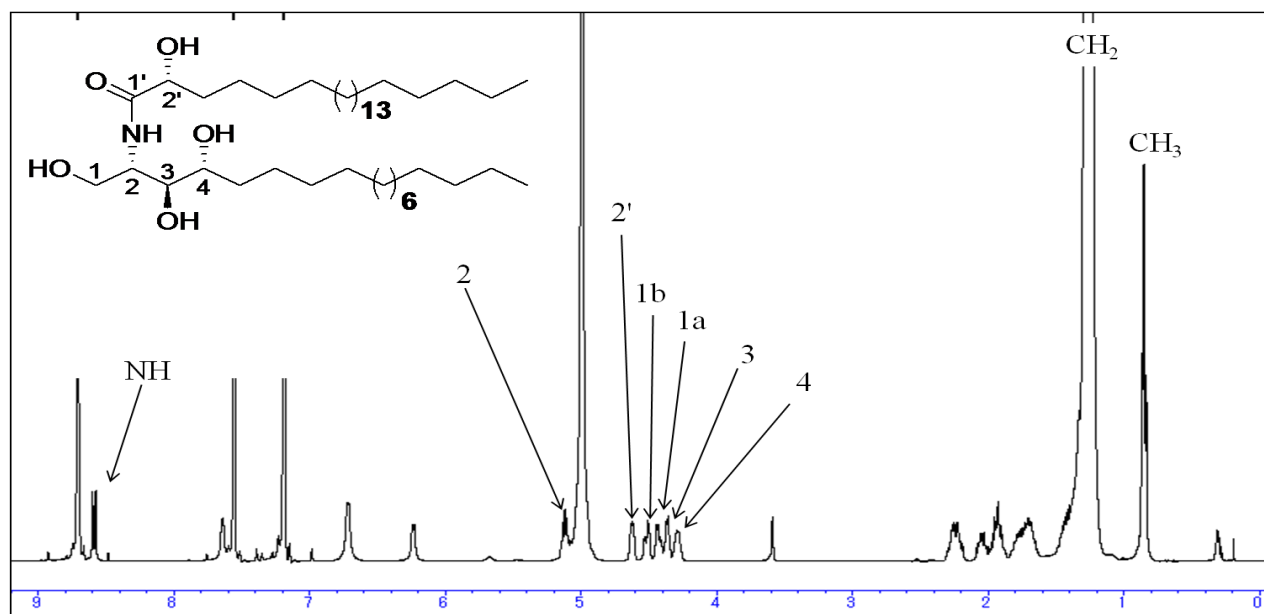


Fig. 2.20.  $^1\text{H-NMR}$  spectrum of TCC-1-6 (400 MHz,  $\text{C}_5\text{D}_5\text{N}$ )



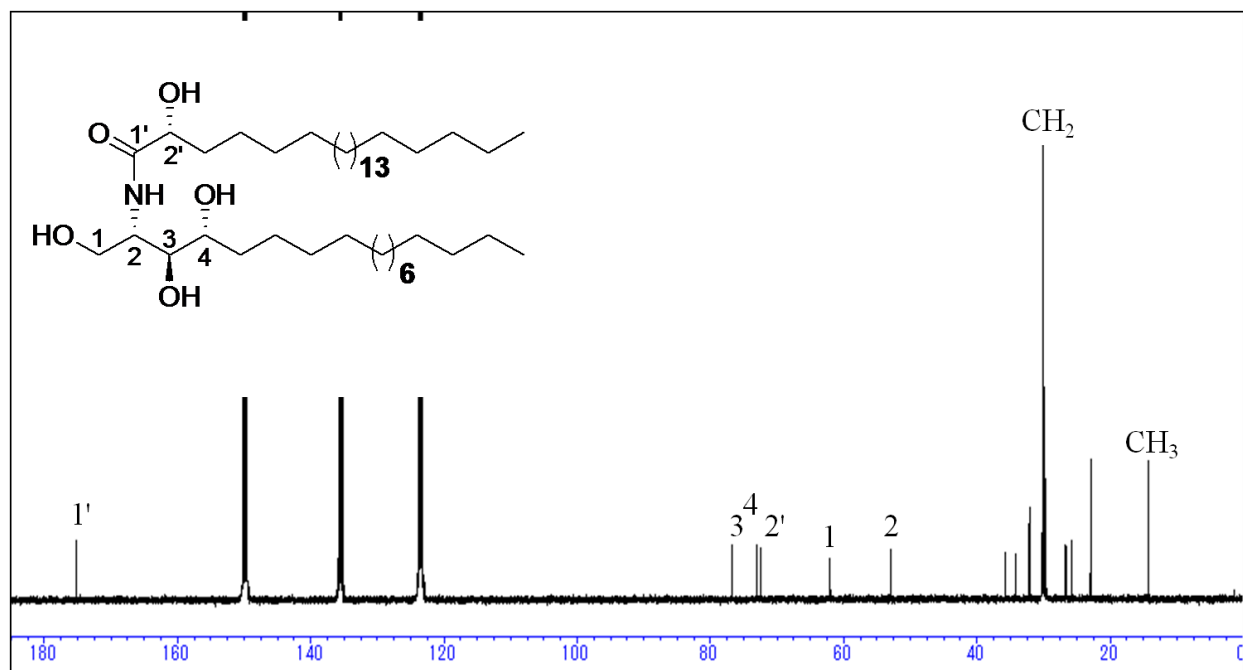


Fig. 2.21.  $^{13}\text{C}$ -NMR spectrum of TCC-1-6 (100 MHz,  $\text{C}_5\text{D}_5\text{N}$ )

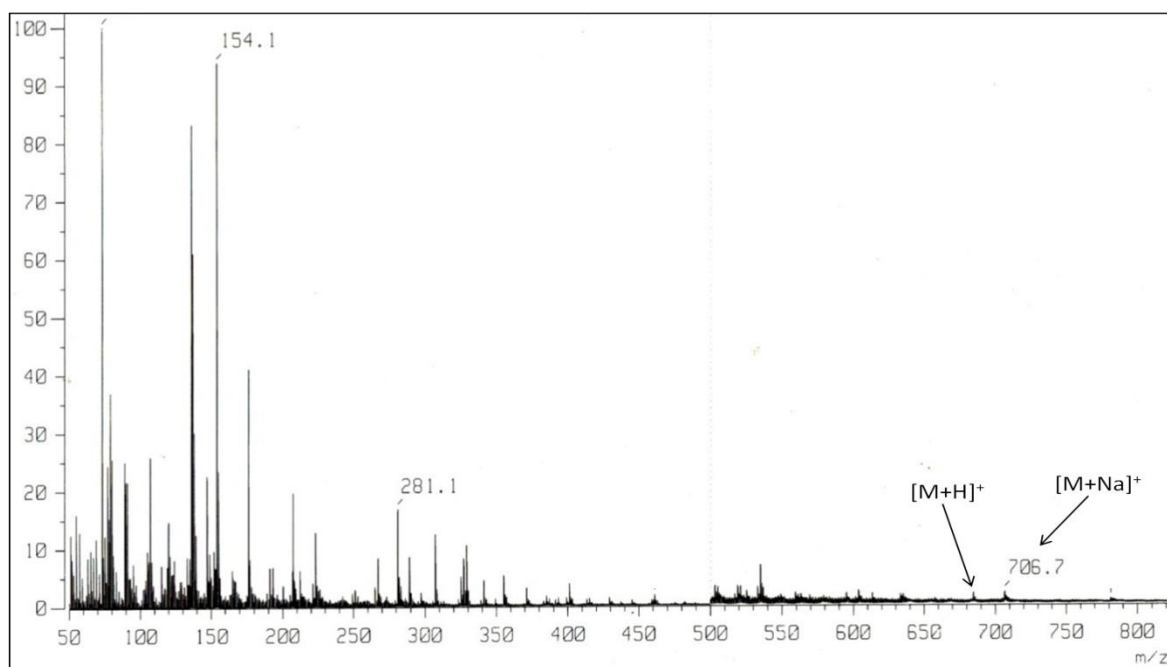


Fig. 2.22. FAB-MS (positive ion mode) of TCC-1-6

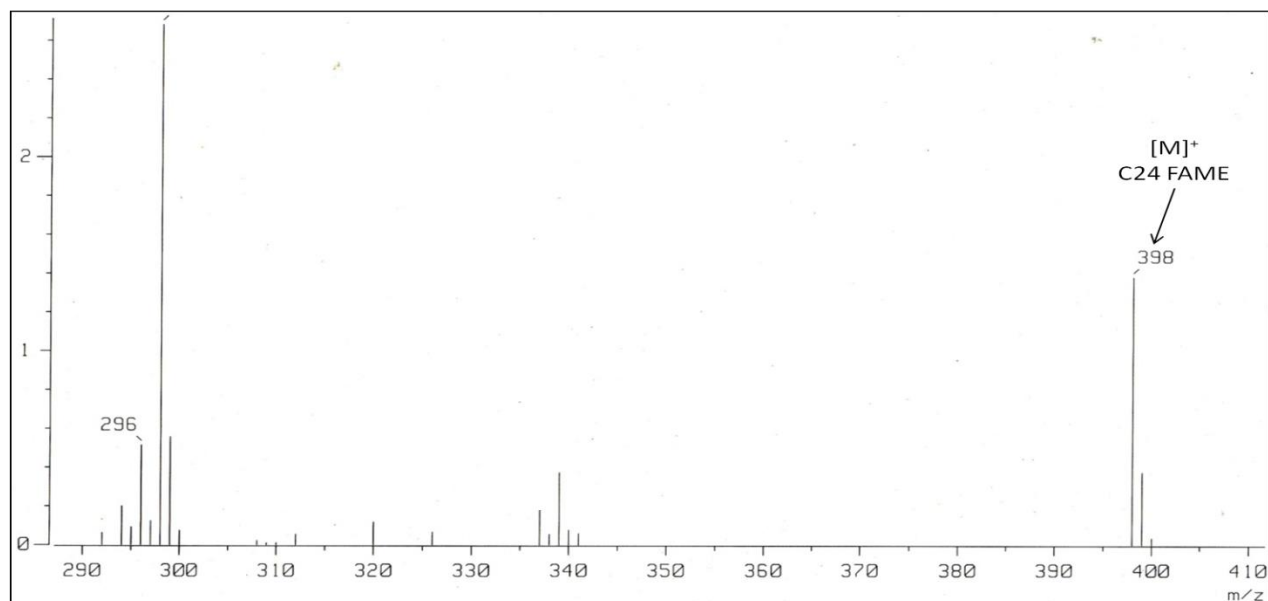


Fig. 2.23. EI-MS (positive ion mode) of TCC-1-6-FAME

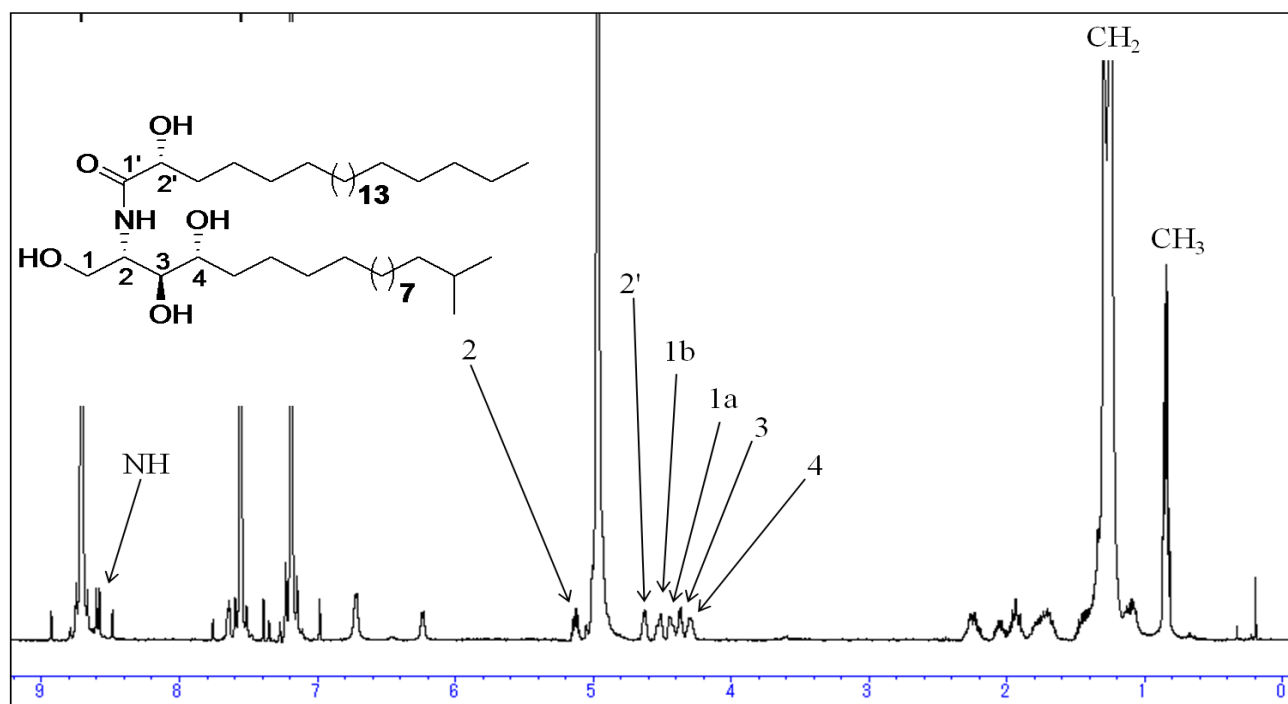


Fig. 2.24.  $^1\text{H-NMR}$  spectrum of TCC-1-7(400 MHz,  $\text{C}_5\text{D}_5\text{N}$ )

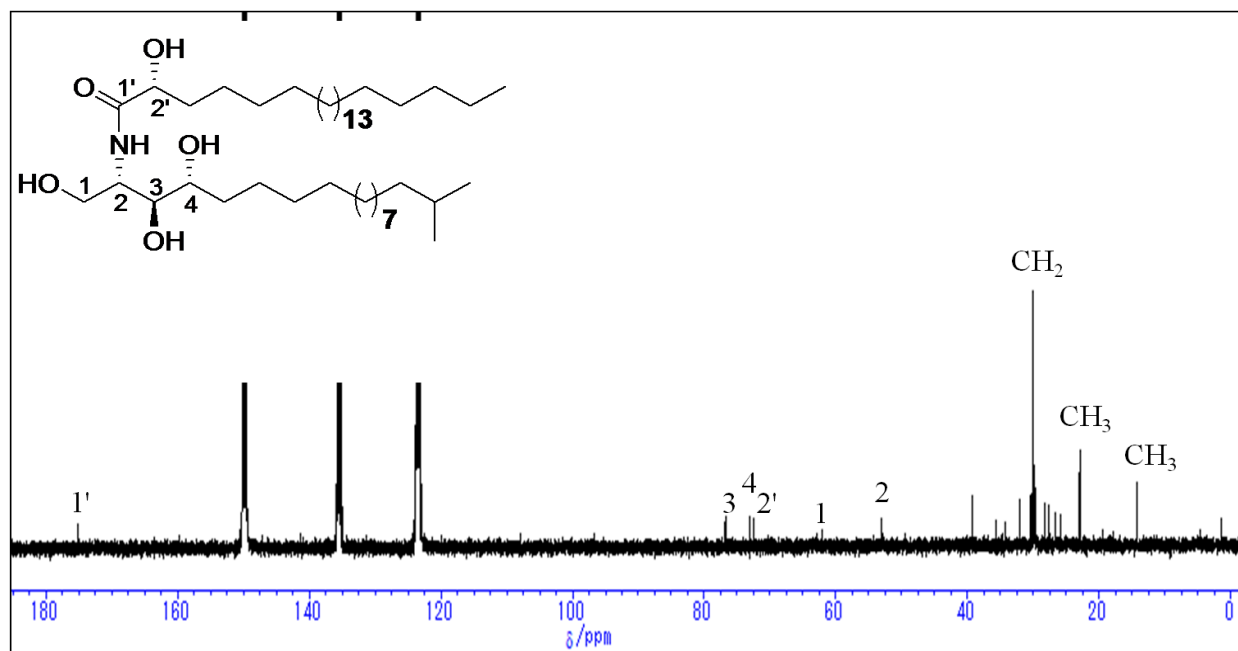


Fig. 2.25.  $^{13}\text{C}$ -NMR spectrum of TCC-1-7 (400 MHz,  $\text{C}_5\text{D}_5\text{N}$ )

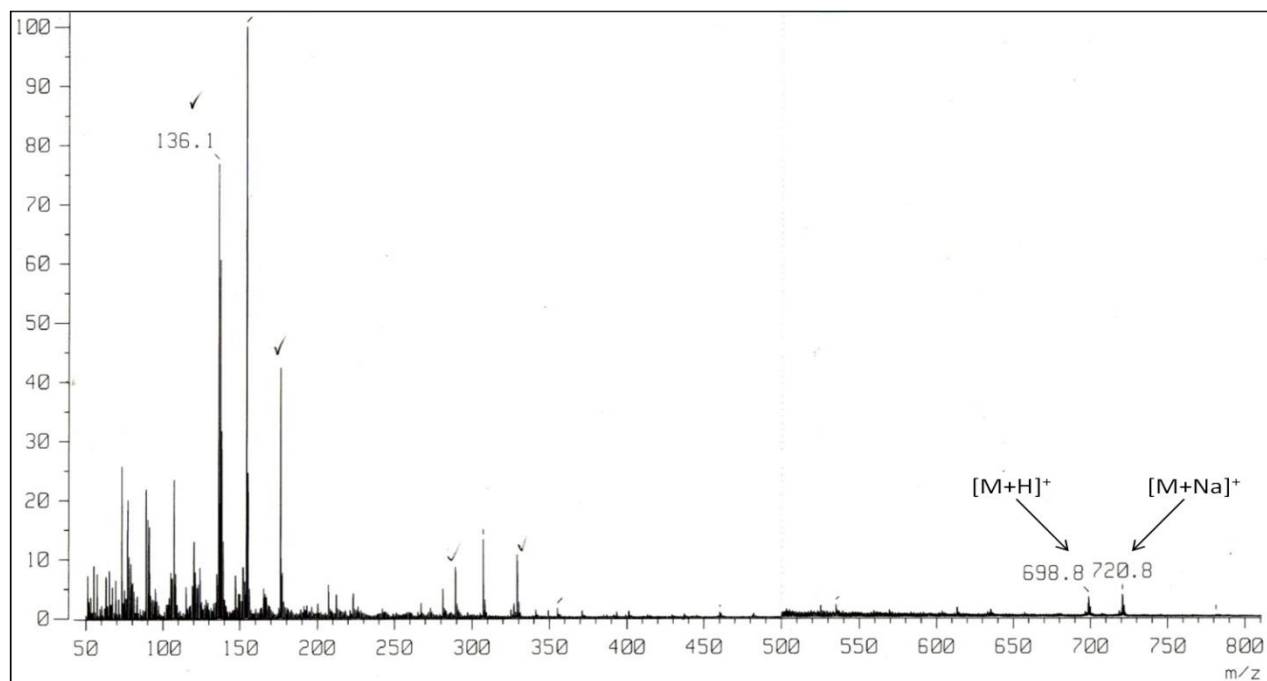


Fig. 2.26. FAB-MS (positive ion mode) of TCC-1-7

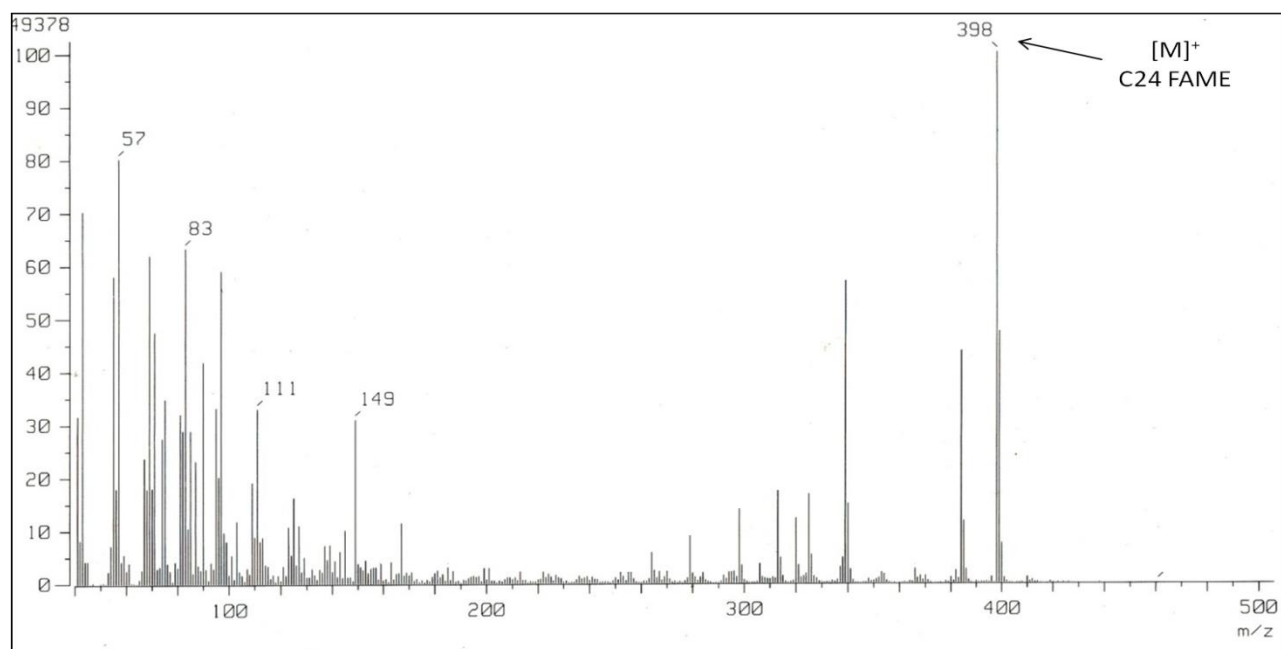


Fig. 2.27. EI-MS (positive ion mode) of TCC-1-7-FAME

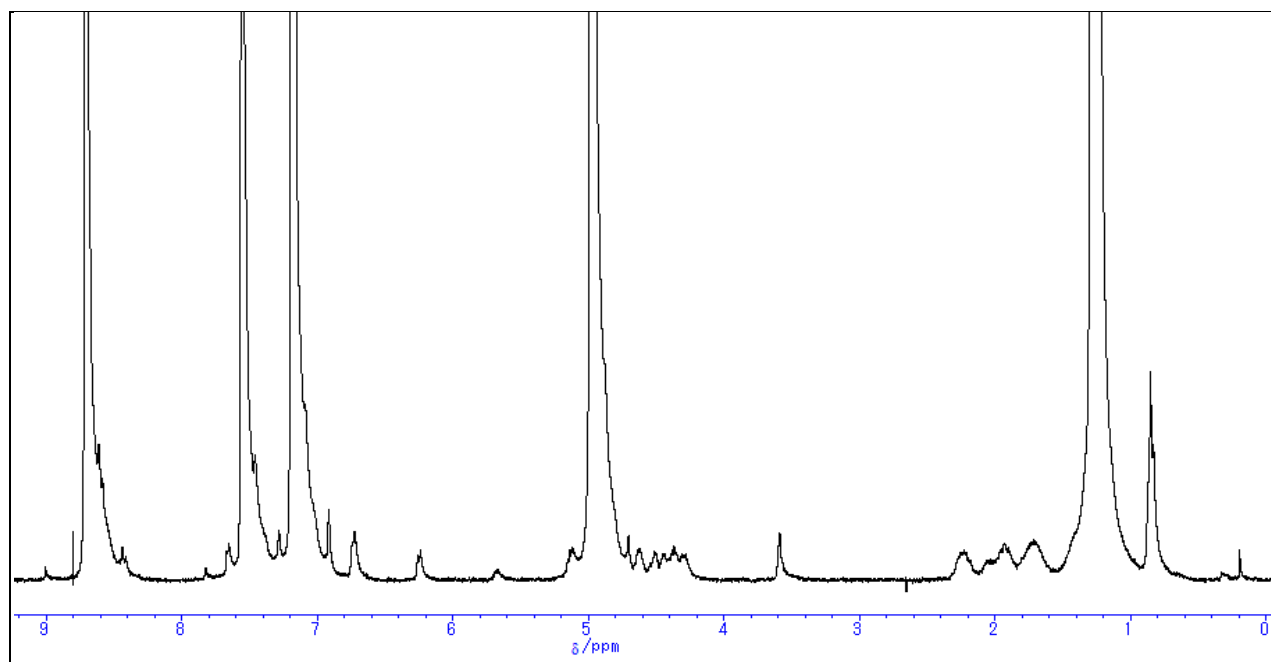
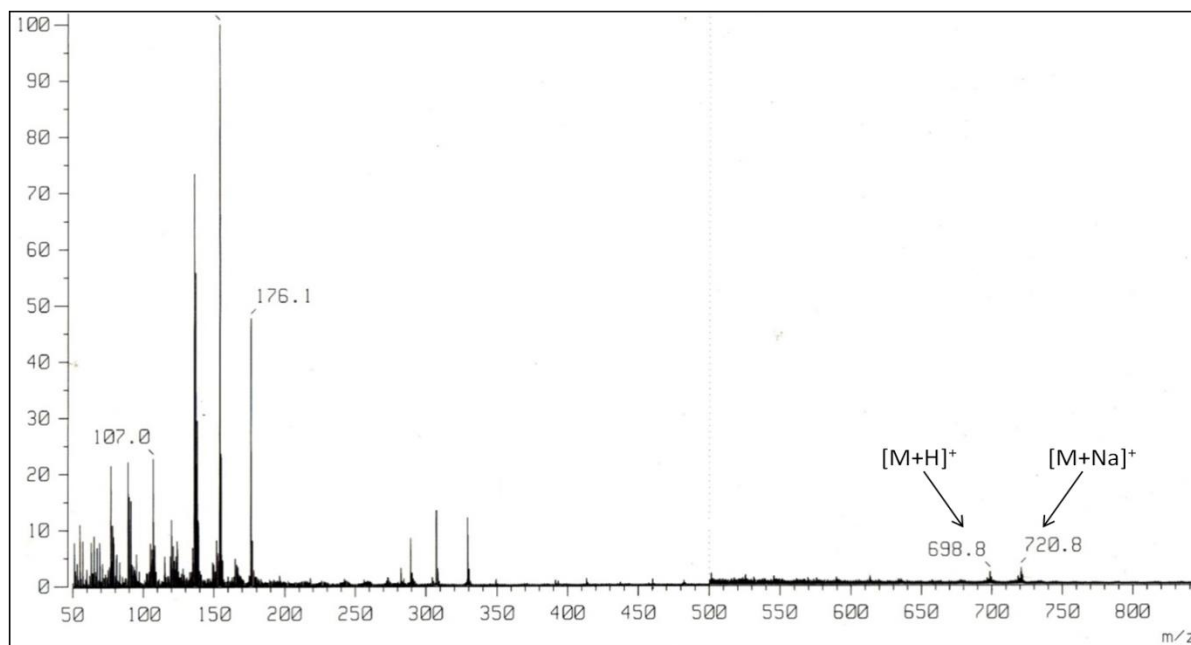
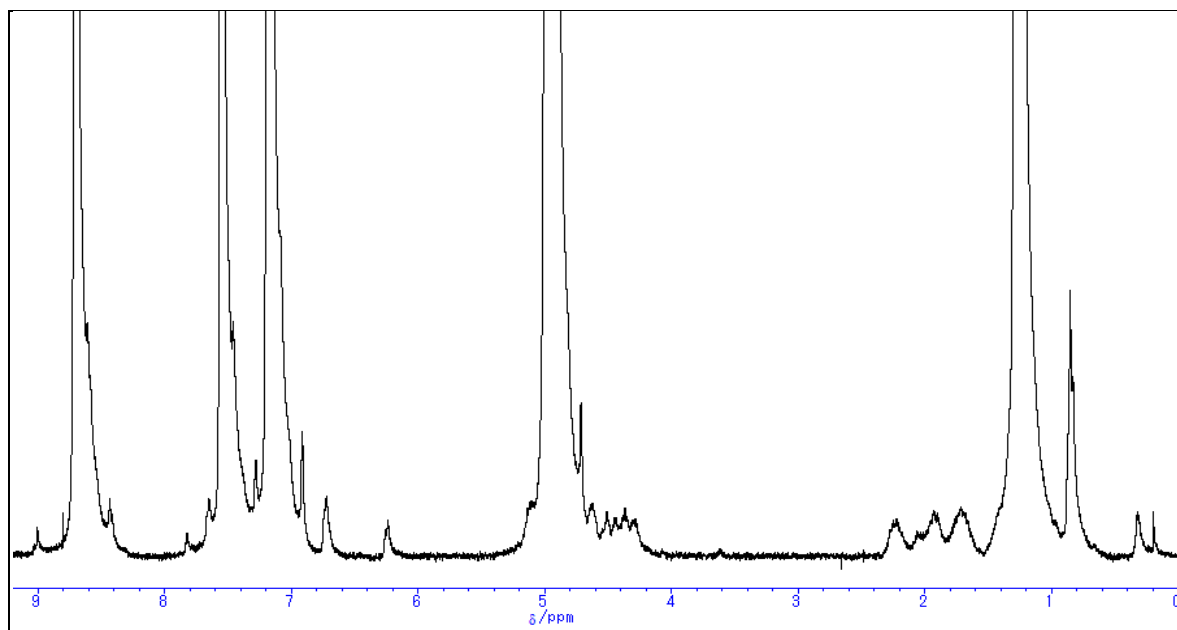


Fig. 2.28. <sup>1</sup>H-NMR spectrum of TCC-1-8 (400 MHz, C<sub>5</sub>D<sub>5</sub>N)



**Fig. 2.29:** FAB-MS (positive ion mode) of TCC-1-8



**Fig. 2.30.**  $^1\text{H-NMR}$  spectrum of TCC-1-9 (400 MHz,  $\text{C}_5\text{D}_5\text{N}$ )

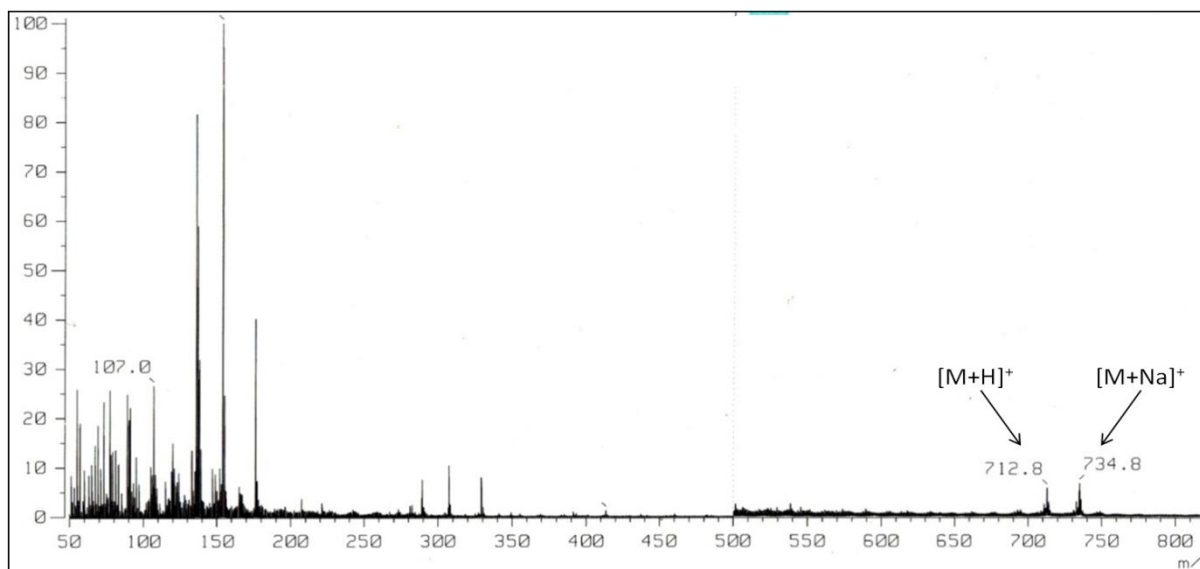


**Fig. 2.31. FAB-MS (positive ion mode) of TCC-1-9**

## Discussion

TCC-1 exhibited a characteristic absorption band for hydroxyl group ( $3300\text{ cm}^{-1}$ ), C-H ( $2900\text{ cm}^{-1}$ ) and amide absorption ( $1623, 1545\text{ cm}^{-1}$ ) in the IR spectrum.

The  $^1\text{H-NMR}$  spectrum in  $\text{C}_5\text{D}_5\text{N}$  showed resonances of an amide proton doublet at  $\delta_{\text{H}} 8.59$  (1H, d,  $J=8.9\text{ Hz}$ ), protons of a long methylene chain centered at  $\delta_{\text{H}} 1.27$ , and overlapped methyl groups at  $\delta_{\text{H}} 0.86$  indicating sphingolipid skeleton. The characteristic signals of 2-amino-1,3,4,2'-tetrol of the hydrocarbon chain were observed at  $\delta_{\text{H}} 5.11$  (1H, m, H-2), 4.61 (1H, m, H-2'), 4.49 (1H, m, H-1a), 4.43 (1H, m, H-1b), 4.34 (1H, m, H-3), and 4.28 (1H, m, H-4) in the  $^1\text{H-NMR}$  spectrum and at  $\delta_{\text{C}} 52.9$  (C-2), 72.4 (C-2'), 62.0 (C-1), 76.7 (C-3), 72.9 (C-4) and an amide carbonyl at  $\delta_{\text{C}} 175.2$  (C-1') in the  $^{13}\text{C-NMR}$  spectrum. A series of molecular ion peaks due to  $[\text{M}+\text{Na}]^+$  were observed in the positive ion FAB-MS spectrum at  $m/z$ : 678, 692, 706, 720, 734 (Fig. 2.4). Therefore, TCC-1 is regarded to be a molecular species of a phytosphingosine-type ceramide, possessing 2-hydroxy fatty acid groups. Furthermore, TCC-1 is suggested to have normal and iso type terminal methyl groups<sup>73)</sup> since the carbon signals for the terminal methyl groups were observed at  $\delta_{\text{C}} 14.2$  (normal type), 22.7 (iso type) in the  $^{13}\text{C-NMR}$  spectrum (Fig. 2.3, Table 2.1). The structure of TCC-1 (Fig. 2.32) was characterized by comparison of its  $^{13}\text{C-NMR}$  spectral data with that of known ceramides.<sup>74-76)</sup>

The absolute stereochemistry of the ceramide molecular species is suggested to be (2*S*, 3*S*, 4*R*, 2'*R*), since the aforementioned <sup>1</sup>H-NMR (H-2, H-3, H-4, H-2') and <sup>13</sup>C-NMR signals (C-2, C-3, C-4, C-2') were in good agreement with those of phytosphingosine-type ceramide molecular species possessing (2*S*, 3*S*, 4*R*, 2'*R*) configurations.<sup>77-79)</sup>

According to the results of TCC-1 methanolysis with methanolic hydrochloric acid followed by <sup>1</sup>H-NMR, <sup>13</sup>C-NMR, and FAB-MS analysis, the length and branching pattern of the long chain bases and fatty acids could be determined. The *n*-hexane layer afforded a mixture of fatty acid methyl esters (FAMEs), which were subjected to <sup>1</sup>H-NMR and EI-MS analysis. EI-MS analysis of the FAMEs mixture showed the presence of four components at *m/z*: 370, 384, 398 and 412, which were characterized as FAM-1, FAM-2, FAM-3, and FAM-4 indicating C-22, C-23, C-24 and C-25 fatty acid methyl esters, respectively (Fig. 2.6).

Furthermore, FAMEs mixture was thought to possess normal terminal methyl groups, since the protons signals for the terminal methyl groups in the <sup>1</sup>H-NMR spectrum were observed at  $\delta_{\text{H}} = 0.85$  (3H, t, *J*=8).<sup>74)</sup>

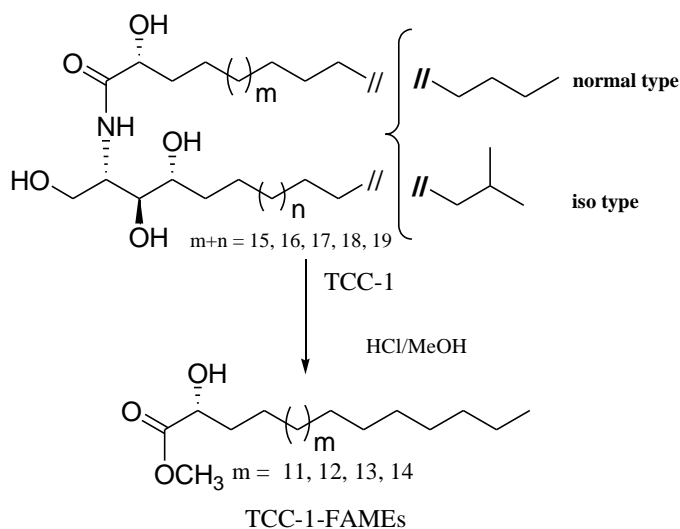


**Fig. 2.32. Structure of TCC-1**

The determination of the molecular species composition of sphingolipids was essential to this study, which was characterized by the isolation and structure elucidation of the ceramide components in TCC-1. Through using reversed phase HPLC, TCC-1 was separated into nine peaks which were recovered to give nine isolates (TCC-1-1 ~ TCC-1-9). On the basis of their

molecular masses, (TCC-1-1  $m/z$  678  $[M+Na]^+$ , TCC-1-2  $m/z$  678  $[M+Na]^+$ , TCC-1-3  $m/z$  692  $[M+Na]^+$ , TCC-1-4  $m/z$  692  $[M+Na]^+$ , TCC-1-5  $m/z$  706  $[M+Na]^+$ , TCC-1-6  $m/z$  706  $[M+Na]^+$ , TCC-1-7  $m/z$  720  $[M+Na]^+$ , TCC-1-8  $m/z$  720  $[M+Na]^+$ , and TCC-1-9  $m/z$  734  $[M+Na]^+$ ) the structures of these compounds were determined (Fig. 2.2).

The  $^1H$ -NMR spectra of TCC-1-1, TCC-1-3, TCC-1-5 and TCC-1-7 showed the characteristic signals of normal and iso-type terminal methyl groups at  $\delta_H = 0.85$  (3H, t,  $J=8$ ) and  $\delta_H = 0.85$  (6H, d,  $J=8$ ), respectively, while TCC-1-2, TCC-1-4, TCC-1-6, TCC-1-8, TCC-1-9 showed the signals of normal type terminal methyl groups  $\delta_H = 0.85$  (6H, t,  $J=8$ ). The presence of the iso-type methyl in the LCB of TCC-1-5, TCC-7 was further confirmed by the characteristic carbon signals in their  $^{13}C$ -NMR spectra at  $\delta_C$  22.7 (iso type). Further hydrolysis of TCC-1-5, TCC-1-6 and TCC-1-7 followed by EI-MS analysis of their FAMES, afforded homogenous FAMES  $m/z$  412, 398, 398  $[M]^+$ , respectively indicating C25, C24, C24 fatty acid methyl esters.

Taking in consideration the biosynthetic pathway of phytosphingosines<sup>80-81</sup>) and by comparing the optical rotation values of TCC-1-5, TCC-1-6, and TCC-1-7 [+8.4, +7.2, +26.3 respectively] with analogs reported in the literature,<sup>82</sup>) the proposed absolute configuration of TCC-1 was confirmed.

On the basis of the above findings and the molecular mass of TCC-1-5  $m/z$  (706  $[M+Na]^+$ , 684  $[M+H]^+$ ), TCC-1-6  $m/z$  (706  $[M+Na]^+$ , 684  $[M+H]^+$ ) and TCC-1-7  $m/z$  (720  $[M+Na]^+$ , 698  $[M+H]^+$ ), the length of the hydrocarbon chain and the structure of TCC-1-5, TCC-1-6 and TCC-1-7 were finally elucidated as shown in Fig. 2.33.

## Conclusion

From the above data and discussion, the structure of TCC-1 was found to be a molecular species of phytoceramides. Further purification of TCC-1 led to isolation of TCC-1-1~TCC-1-9 (**1~9**) as shown in Fig. 2.33.



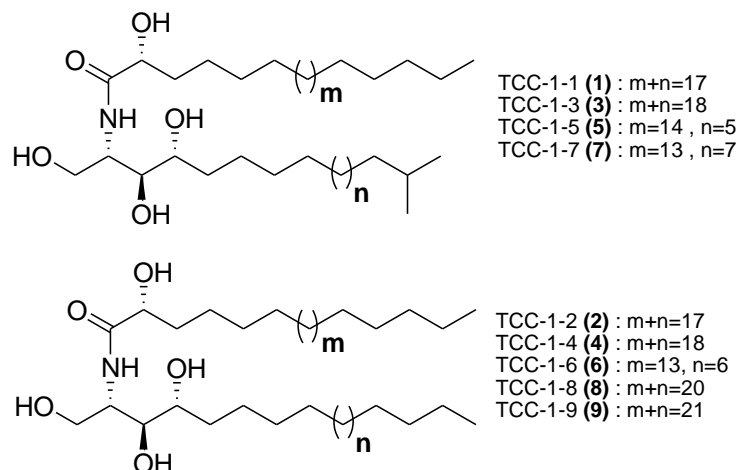


Fig. 2.33. Structure of the isolated phytoceramides from TCC-1

### 2.2.2. Compound 10

Compound **10** was isolated as a white amorphous powder from TC-4 fraction of the Red Sea grass *Thalassodendron ciliatum*.

### Spectroscopic analysis

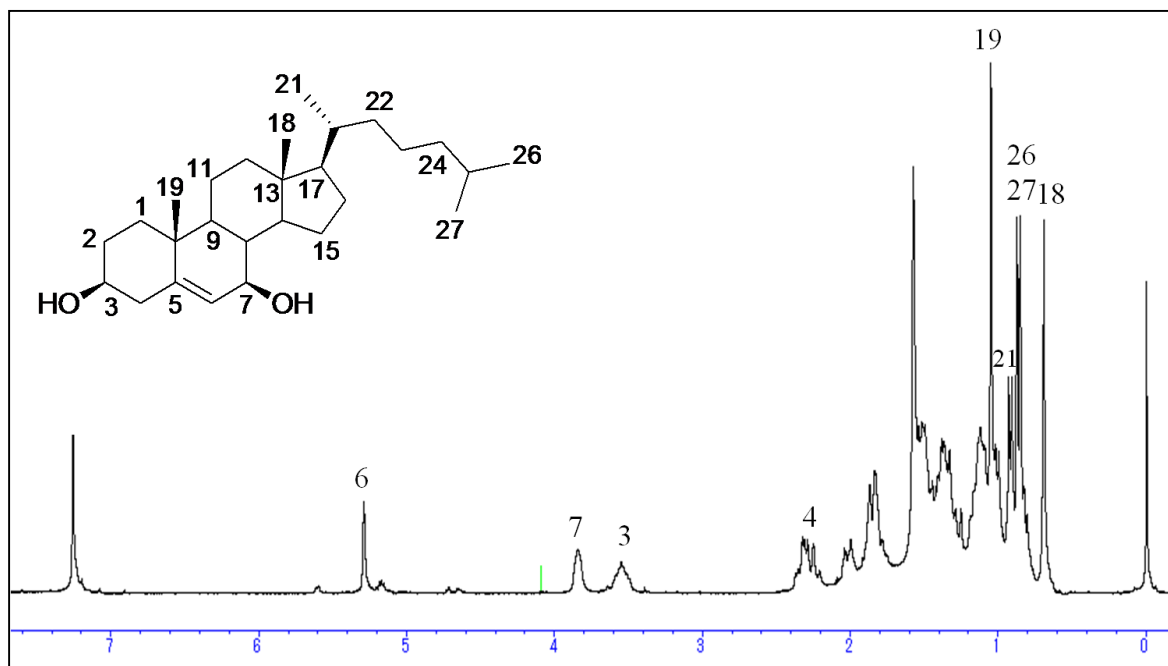


Fig. 2.34.  $^1\text{H-NMR}$  spectrum of compound **10** (400 MHz,  $\text{CDCl}_3$ )

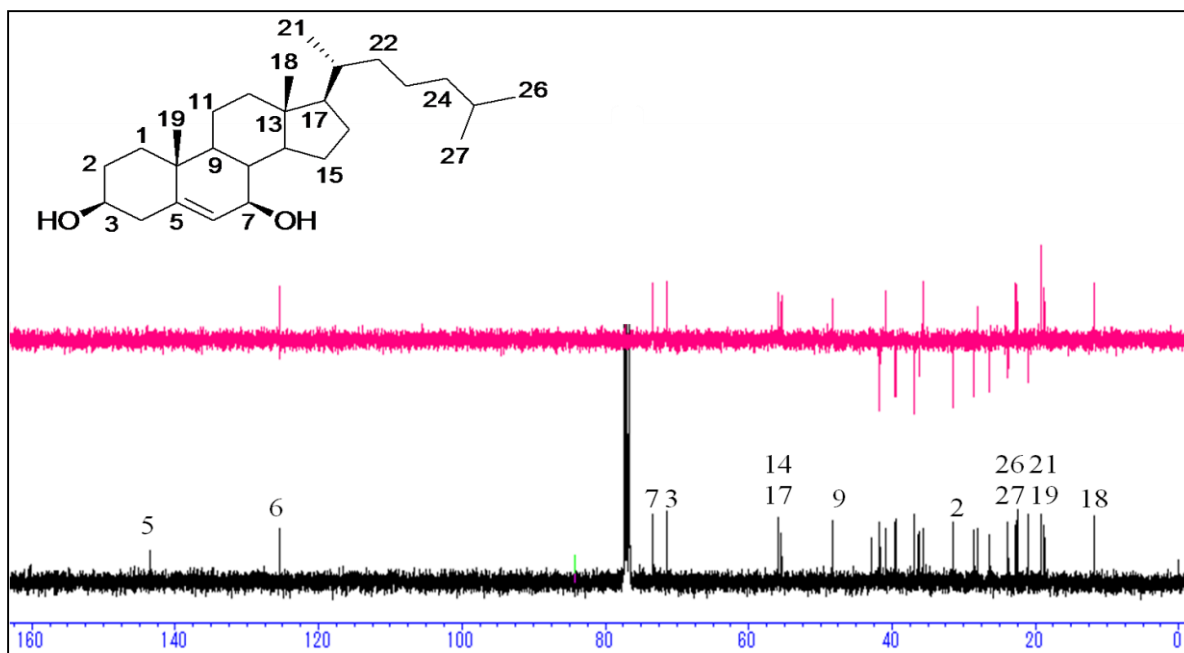


Fig. 2.35.  $^{13}\text{C}$ -NMR spectrum of compound **10** (100 MHz,  $\text{CDCl}_3$ ).

$^{13}\text{C}$ -NMR (100 MHz) and  $^1\text{H}$ -NMR (400 MHz) data for **10** in  $\text{CDCl}_3$  are listed in **Table 2.2**.

**Table 2.2:**  $^{13}\text{C}$ -NMR (100 MHz) and  $^1\text{H}$ -NMR (400 MHz) spectroscopic data of **10** ( $\text{CDCl}_3$ ,  $\delta$  in ppm,  $J$  in Hz).

| No. | $\delta_{\text{C}}$     | $\delta_{\text{H}}$ (No., $M$ , $J_{\text{Hz}}$ ) | No. | $\delta_{\text{C}}$     | $\delta_{\text{H}}$ (No., $M$ , $J_{\text{Hz}}$ ) |
|-----|-------------------------|---|-----|-------------------------|---|
| 1   | 36.9 (CH <sub>2</sub> ) |   | 15  | 26.3 (CH <sub>2</sub> ) |   |
| 2   | 31.5 (CH <sub>2</sub> ) |   | 16  | 28.5 (CH <sub>2</sub> ) |   |
| 3   | 71.4 (CH)               | 3.55 (1H, m)                                      | 17  | 55.9 (CH)               |   |
| 4   | 41.7 (CH <sub>2</sub> ) |   | 18  | 11.8 (CH <sub>3</sub> ) | 0.69 (3H, s)                                      |
| 5   | 143.4 (C)               |   | 19  | 19.1 (CH <sub>3</sub> ) | 1.05 (3H, s)                                      |
| 6   | 125.4 (CH)              | 5.29 (1H, brs)                                    | 20  | 36.1 (CH)               |   |
| 7   | 73.3 (CH)               | 3.84 (1H, brs)                                    | 21  | 18.7 (CH <sub>3</sub> ) | 0.92 (3H, d, $J=6.5$ Hz)                          |
| 8   | 40.9 (CH)               |   | 22  | 35.7 (CH <sub>2</sub> ) |   |
| 9   | 48.2 (CH)               |   | 23  | 23.8 (CH <sub>2</sub> ) |   |
| 10  | 36.4 (C)                |   | 24  | 39.5 (CH <sub>2</sub> ) |   |
| 11  | 21.0 (CH <sub>2</sub> ) |   | 25  | 28.01 (CH)              |   |
| 12  | 39.4 (CH <sub>2</sub> ) |   | 26  | 22.5 (CH <sub>3</sub> ) | 0.86 (3H, d, $J=6.5$ Hz)                          |
| 13  | 42.9 (C)                |   | 27  | 22.8 (CH <sub>3</sub> ) | 0.86 (3H, d, $J=6.5$ Hz)                          |
| 14  | 55.4 (CH)               |   |     |                         |   |

## Discussion

Compound **10** was obtained as a white amorphous powder from TC-4 fraction of the marine sea grass *Thalassodendron ciliatum*. The structure elucidation of **10** began with the analysis of its  $^1\text{H-NMR}$ ,  $^{13}\text{C-NMR}$  spectrum and DEPT experiment. The  $^1\text{H-NMR}$  spectrum showed the chemical shift at  $\delta$  0.69 and 1.05 indicated the presence of two angular methyl signals at position 18 and 19 of the structure. The  $^1\text{H-NMR}$  spectrum also exhibited one olefinic double bond proton at  $\delta$  5.29, along with one up field signal at  $\delta$  0.86 due to the presence of two secondary methyl groups at position 26 and 27 of the skeleton. The up field chemical shift at  $\delta$  0.92 as a doublet and coupling constant of  $J = 6.5$  Hz with the intensity of 3H was assigned for the terminal methyl group of 21 of **10**. The down field chemical shift at  $\delta$  3.55 and  $\delta$  3.84 indicated the presence of two carbinol protons at position 3 and 7 of the isolated compound.

The  $^{13}\text{C-NMR}$  spectra of **10** showed the presence of 27 carbons, five characteristic signals at  $\delta$  11.8, 19.1, 18.7, 22.5, 22.8, were assigned for two angular methyl groups and three terminal methyl groups at position 18, 19, 21, 26 and 27 respectively, of the structure. Two downfield signals at  $\delta$  143.4, 125.4 respectively, were assigned for the olefinic carbons at C-5 and C-6 position. Similarly, the relative down field chemical shifts at  $\delta$  71.4 and 73.3 were assigned for the oxymethines at positions C-3 and C-7, respectively. The relative stereo chemistry of the hydroxyl group at C-7 was proposed to be  $\beta$  oriented, since the chemical shifts of the C-7 attached to  $\alpha$  oriented hydroxyl group appeared at  $\delta$  65.3 as mentioned in the reference compound,<sup>83)</sup> while **10** showed a characteristic signal at  $\delta$  73.3.

The molecular formula of **10** was deduced as  $\text{C}_{27}\text{H}_{46}\text{O}_2$  based on the NMR spectra and further confirmed by the mass spectra with the appearance of the molecular ion peak at  $m/z$ , 402  $[\text{M}]^+$  in the EI-MS spectrum. The NMR data of **10** was compared with a reference data and found to be matched.<sup>83)</sup>

## Conclusion

From the above data and discussion the structure of **10** was assigned as

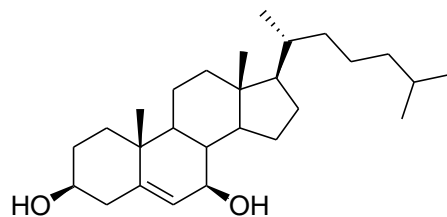


Fig. 2.36. Structure of 7 $\beta$ -hydroxy cholesterol (**10**)

### 2.2.3. Compound 11

Compound **11** was isolated as a white amorphous powder from TC-4 fraction of the Red Sea grass *Thalassodendron ciliatum*.

#### Spectroscopic analysis

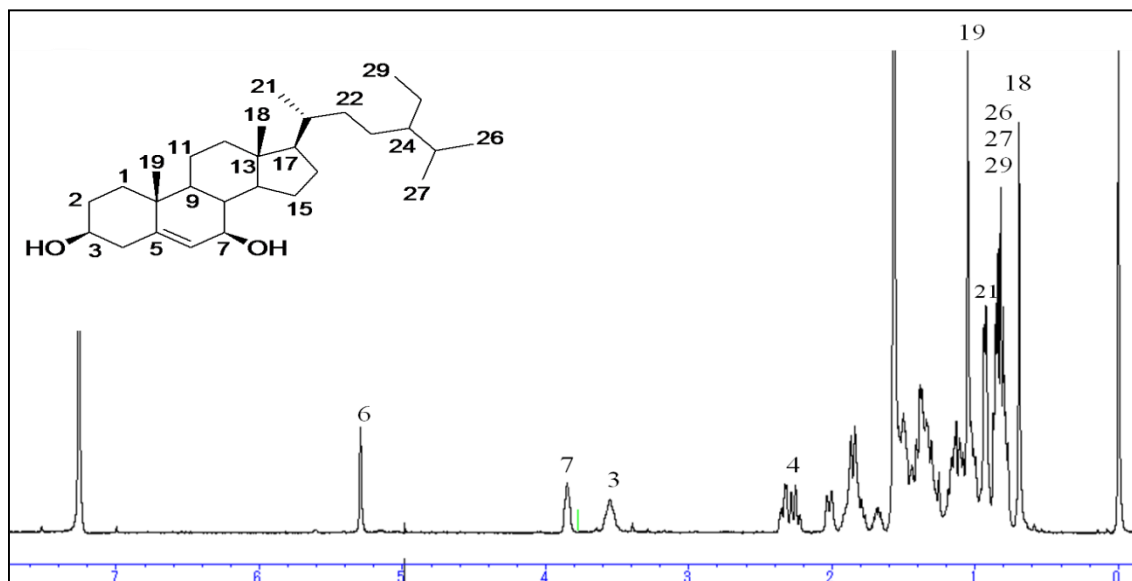


Fig. 2.37.  $^1\text{H-NMR}$  spectrum of compound **11** (400 MHz,  $\text{CDCl}_3$ ).

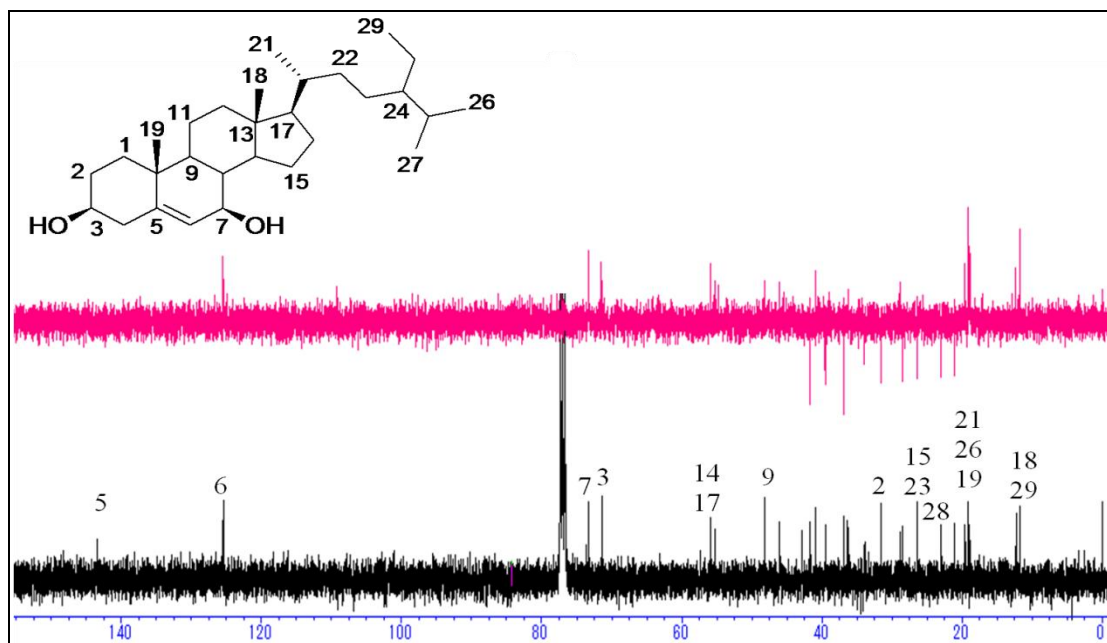


Fig. 2.38.  $^{13}\text{C}$ -NMR spectrum of compound **11** (100 MHz,  $\text{CDCl}_3$ ).

$^{13}\text{C}$ -NMR (100 MHz) and  $^1\text{H}$ -NMR (400 MHz) data for **11** in  $\text{CDCl}_3$  are listed in Table 2.3.

Table 2.3:  $^{13}\text{C}$ -NMR (100 MHz) and  $^1\text{H}$ -NMR (400 MHz) spectroscopic data of compound **11** ( $\text{CDCl}_3$ ,  $\delta$  in ppm,  $J$  in Hz).

| No. | $\delta_{\text{C}}$     | $\delta_{\text{H}}$ (No., $M$ , $J_{\text{Hz}}$ ) | No. | $\delta_{\text{C}}$     | $\delta_{\text{H}}$ (No., $M$ , $J_{\text{Hz}}$ ) |
|-----|-------------------------|---|-----|-------------------------|---|
| 1   | 36.9 (CH <sub>2</sub> ) |   | 16  | 28.5 (CH <sub>2</sub> ) |   |
| 2   | 31.5 (CH <sub>2</sub> ) |   | 17  | 55.9 (CH)               |   |
| 3   | 71.4 (CH)               | 3.55 (1H, m)                                      | 18  | 11.8 (CH <sub>3</sub> ) | 0.69 (3H, s)                                      |
| 4   | 41.7 (CH <sub>2</sub> ) |   | 19  | 19.1 (CH <sub>3</sub> ) | 1.05 (3H, s)                                      |
| 5   | 143.4 (C)               |   | 20  | 36.2 (CH)               |   |
| 6   | 125.4 (CH)              | 5.29 (1H, brs)                                    | 21  | 18.8 (CH <sub>3</sub> ) | 0.94 (3H, d, $J=6.5$ Hz)                          |
| 7   | 73.3 (CH)               | 3.85 (1H, brs)                                    | 22  | 33.9 (CH <sub>2</sub> ) |   |
| 8   | 40.9 (CH)               |   | 23  | 26.3 (CH <sub>2</sub> ) |   |
| 9   | 48.2 (CH)               |   | 24  | 46.0 (CH)               |   |
| 10  | 36.4 (C)                |   | 25  | 28.8 (CH)               |   |
| 11  | 21.0 (CH <sub>2</sub> ) |   | 26  | 18.9 (CH <sub>3</sub> ) | 0.82 (3H, d, $J=6.5$ Hz)                          |
| 12  | 39.5 (CH <sub>2</sub> ) |   | 27  | 19.5 (CH <sub>3</sub> ) | 0.82 (3H, d, $J=6.5$ Hz)                          |
| 13  | 42.9 (C)                |   | 28  | 22.9 (CH <sub>2</sub> ) |   |
| 14  | 55.3 (CH)               |   | 29  | 12.3 (CH <sub>3</sub> ) | 0.86 (3H, t, $J=7.5$ Hz)                          |
| 15  | 26.3 (CH <sub>2</sub> ) |   |     |                         |   |

## Discussion

Compound **11** was obtained as a white amorphous powder from TC-4 fraction of the marine sea grass *Thalassodendron ciliatum*. The structure elucidation of **11** began with the analysis of its  $^1\text{H}$ - and  $^{13}\text{C}$ -NMR spectra exhibited the structure of a steroidal nucleus.<sup>84)</sup> Compound **11** exhibited almost similar  $^1\text{H}$ - and  $^{13}\text{C}$ -NMR spectra as compound (**10**) except for the presence of characteristic signals at [ $\delta_{\text{H}}$ 1.25 (2H, m), 0.86 (3H, t,  $J = 7.5\text{Hz}$ );  $\delta_{\text{C}}$  22.9, 12.3], assigned for extra ethyl moiety at position 28 and 29 in **11**. The other characteristic signals were almost same since the  $^1\text{H}$ -NMR spectrum showed the chemical shift at  $\delta$  0.69 and 1.05 indicated the presence of two angular methyl signals at position 18 and 19 of the molecule. The  $^1\text{H}$ -NMR spectrum also exhibited one olefinic double bond proton at  $\delta$  5.29, along with one up field signal at  $\delta$  0.82 due to the presence of two secondary methyl groups at position 26 and 27 of the skeleton. The up field chemical shift at  $\delta$  0.94 as a doublet and coupling constant of  $J = 6.5\text{ Hz}$  with the intensity of 3H was assigned for the terminal methyl group of 21 of **11**. The down field chemical shift at  $\delta$  3.55 and  $\delta$  3.85 indicated the presence of two carbinol protons at position 3 and 7 of the proposed skeleton.

The  $^{13}\text{C}$ -NMR spectra of **11** showed the presence of 29 carbons, six characteristic signals at  $\delta$  11.8, 12.3, 18.8, 18.9, 19.1, 19.5, were assigned for the methyl groups at positions 18, 29, 21, 26, 19 and 27 respectively, of the structure. Two downfield signals at  $\delta$  143.4, 125.4 respectively, were assigned for the olefinic carbons at C-5 and C-6 position. Similarly, the relative down field chemical shifts at  $\delta$  71.4 and 73.3 were assigned for the oxymethines at positions C-3 and C-7, respectively. The relative stereo chemistry of the hydroxyl group at C-7 was proposed to be  $\beta$  oriented due to the characteristic signal at  $\delta$  73.3 since the chemical shifts of the C-7 attached to  $\alpha$  oriented hydroxyl group appeared at  $\delta$  65.3 as shown in the reference compound.<sup>82)</sup>

The molecular formula of **11** was deduced as  $\text{C}_{29}\text{H}_{50}\text{O}_2$  based on the NMR spectra and further confirmed by the mass spectra with the appearance of the molecular ion peak at  $m/z$ , 430  $[\text{M}]^+$  in the EI-MS spectrum showing 28 mass per unit increase than compound **10** confirming the presence of the ethyl moiety. The NMR data of **11** was compared with a reference data and found to be matched.<sup>83)</sup>

## Conclusion

From the above data and discussion the structure of **11** was assigned as

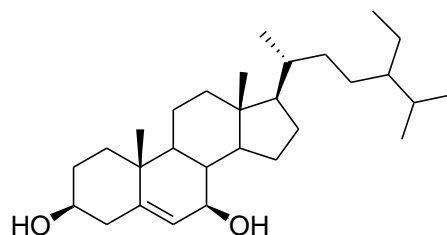


Fig. 2.39. Structure of 7 $\beta$ -hydroxy sitosterol (**11**)

### 2.2.4. Compound 12

Compound **12** was isolated as a white amorphous powder from TC-7 fraction of the Red Sea grass *Thalassodendron ciliatum*.

### Spectroscopic analysis

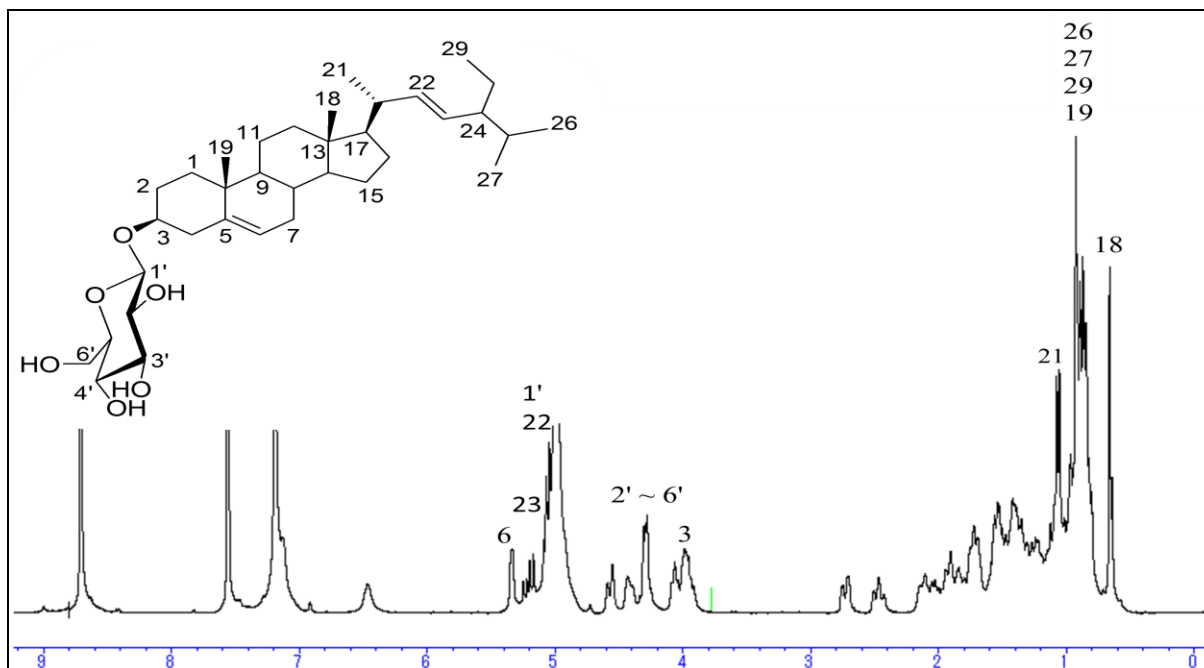


Fig. 2.40.  $^1\text{H-NMR}$  spectrum of compound **12** (400 MHz,  $\text{C}_5\text{D}_5\text{N}$ )

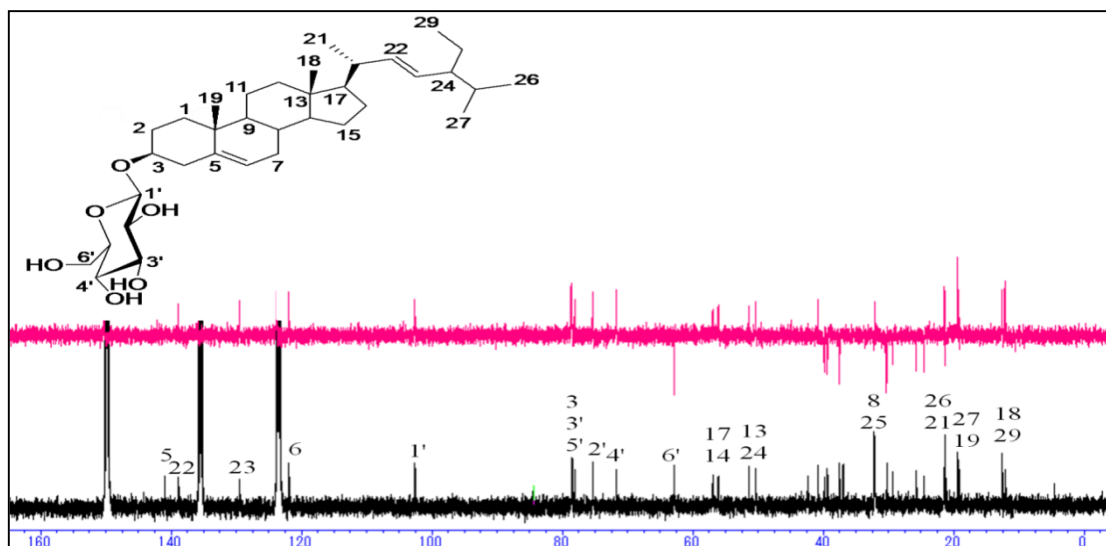


Fig. 2.41.  $^{13}\text{C}$ -NMR spectrum of compound 12 (100 MHz,  $\text{C}_5\text{D}_5\text{N}$ ).

Table 2.4:  $^{13}\text{C}$ -NMR (100 MHz) and  $^1\text{H}$ -NMR (400 MHz) spectroscopic data of 12 (pyridine- $d_5$ ,  $\delta$  in ppm,  $J$  in Hz)

| No. | $\delta_{\text{C}}$     | $\delta_{\text{H}}$ (No., $M$ , $J_{\text{Hz}}$ ) | No. | $\delta_{\text{C}}$     | $\delta_{\text{H}}$ (No., $M$ , $J_{\text{Hz}}$ ) |
|-----|-------------------------|---|-----|-------------------------|---|
| 1   | 37.4 (CH <sub>2</sub> ) |   | 19  | 19.4 (CH <sub>3</sub> ) | 0.95 (3H, s)                                      |
| 2   | 30.2 (CH <sub>2</sub> ) |   | 20  | 40.7 (CH)               |   |
| 3   | 78.6 (CH)               | 4.06 (1H, m)                                      | 21  | 21.4 (CH <sub>3</sub> ) | 1.09 (3H, d, $J=6.5$ Hz)                          |
| 4   | 39.3 (CH <sub>2</sub> ) |   | 22  | 138.8 (CH)              | 5.07 (1H, dd, $J=8.7$ Hz, $J=15.1$ Hz)            |
| 5   | 140.9 (C)               |   | 23  | 129.4 (CH)              | 5.23 (1H, dd, $J=8.7$ Hz, $J=15.1$ Hz)            |
| 6   | 121.9 (CH)              | 5.33 (1H, brs)                                    | 24  | 51.4 (CH)               |   |
| 7   | 32.1 (CH <sub>2</sub> ) |   | 25  | 32.1 (CH)               |   |
| 8   | 32.0 (CH)               |   | 26  | 21.2 (CH <sub>3</sub> ) | 0.85 (3H, d, $J=6.5$ Hz)                          |
| 9   | 50.3 (CH)               |   | 27  | 19.1 (CH <sub>3</sub> ) | 0.87 (3H, d, $J=6.5$ Hz)                          |
| 10  | 36.9 (C)                |   | 28  | 25.7 (CH <sub>2</sub> ) |   |
| 11  | 21.2 (CH <sub>2</sub> ) |   | 29  | 12.5 (CH <sub>3</sub> ) | 0.88 (3H, t, $J=7.5$ Hz)                          |
| 12  | 39.8 (CH <sub>2</sub> ) |   | 1'  | 102.5 (CH)              | 5.07 (1H, d, $J=7.2$ Hz)                          |
| 13  | 42.3 (C)                |   | 2'  | 75.3 (CH)               |   |
| 14  | 56.9 (CH)               |   | 3'  | 78.1 (CH)               |   |
| 15  | 24.5 (CH <sub>2</sub> ) |   | 4'  | 71.7 (CH)               |   |
| 16  | 29.3 (CH <sub>2</sub> ) |   | 5'  | 78.4 (CH)               |   |
| 17  | 56.0 (CH)               |   | 6'  | 62.8 (CH <sub>2</sub> ) |   |
| 18  | 12.1 (CH <sub>3</sub> ) | 0.65 (3H, s)                                      |     |                         |   |



## Discussion

Compound **12** was obtained as a white amorphous powder from TC-7 fraction of the Red Sea grass *Thalassodendron ciliatum*. The structure elucidation of **12** began with the analysis of its  $^1\text{H-NMR}$ ,  $^{13}\text{C-NMR}$  spectrum and DEPT experiment exhibited the structure of steroids.<sup>84)</sup> The  $^1\text{H-NMR}$  spectrum of **12**, (Table 2.4), showed six methyl resonances, two of them are connected to quaternary carbon atom at  $\delta_{\text{H}}$  0.65 (s) and 0.95 (s) assigned to H<sub>3</sub>-18 and H<sub>3</sub>-19 respectively. Three of them are connected to methine carbon at  $\delta_{\text{H}}$  0.85, 0.87, and 1.09 assigned to H<sub>3</sub>-26, H<sub>3</sub>-27, and H<sub>3</sub>-21. The last methyl is attached to methylene carbon at  $\delta_{\text{H}}$  0.88 assigned to H<sub>3</sub>-29. In addition, a resonance at  $\delta_{\text{H}}$  5.33 of the most downfield chemical shift was assigned to H-6 which demonstrates that it is attached to an olefinic carbon. The chemical shift at  $\delta$  4.06 indicated the presence of one carbinol proton at position 3 of the proposed skeleton. One anomeric proton at  $\delta_{\text{H}}$  5.07 indicated the presence of the sugar moiety.

The  $^{13}\text{C-NMR}$  spectra of **12** (Table 2.4) showed there are 35 carbon atoms in the molecule. The olefinic resonance at  $\delta$  121.9, 138.8, and 129.4 corresponded to C-6, C-22 and C-23 methine carbons, and a signal at  $\delta$  140.9 corresponded to the C-5 quaternary carbon of the sterol moiety. An anomeric carbon signal at  $\delta$  102.5 indicated the presence of a sugar moiety. The four methine resonances at  $\delta$  75.3, 78.1, 71.7, and 78.4 as well as the methylene resonance at  $\delta$  62.8 were due to C-2', C-3', C-4', C-5' and C-6', respectively of the  $\beta$ -glucopyranoside. The value of  $J = 7.2$  on 1' (anomeric proton) reflected that the proton is the axial-axial to C-2' proton which means glucopyranoside moiety binds to the sterol moiety  $\beta$  position.<sup>85-86)</sup>

The molecular formula of **12** was deduced as C<sub>35</sub>H<sub>58</sub>O<sub>6</sub> based on the NMR spectra and further confirmed by the mass spectra with the appearance of the molecular ion peak at  $m/z$ , 574 [M]<sup>+</sup> in the EI-MS spectrum. The NMR data of **12** was compared with a reference data and found to be matched.<sup>87)</sup>

## Conclusion

From the above data and discussion the structure of compound **12** was assigned as

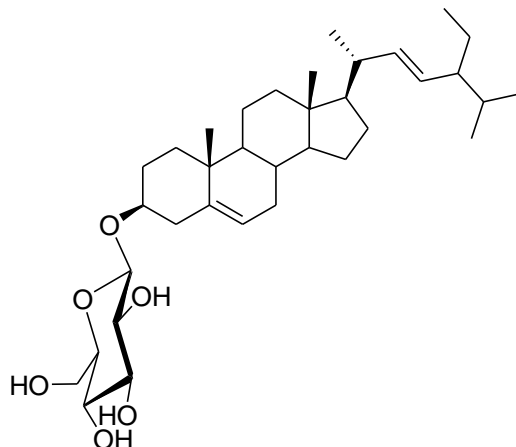


**Fig. 2.42.** Structure of stigmasterol glucoside (**12**)

### 2.2.5. Compound 13

Compound **13** was isolated as a white amorphous powder from the major fraction TC-7 of the Red Sea grass *Thalassodendron ciliatum*.

### Spectroscopic analysis

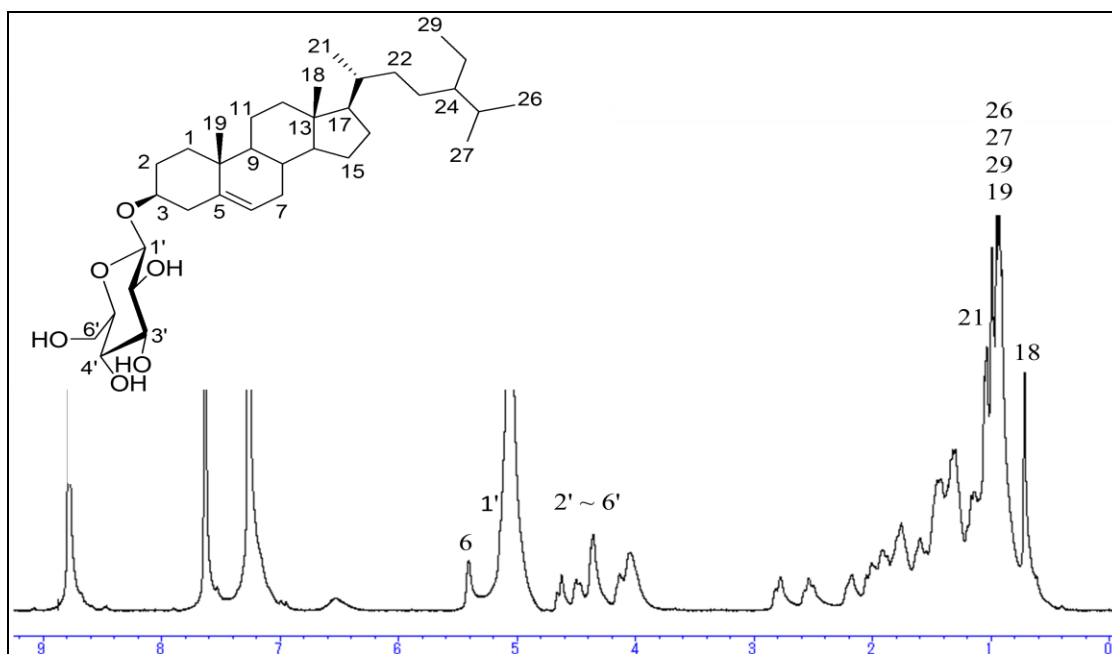


**Fig. 2.43.**  $^1\text{H-NMR}$  spectrum of compound **13** (400 MHz,  $\text{C}_5\text{D}_5\text{N}$ ).

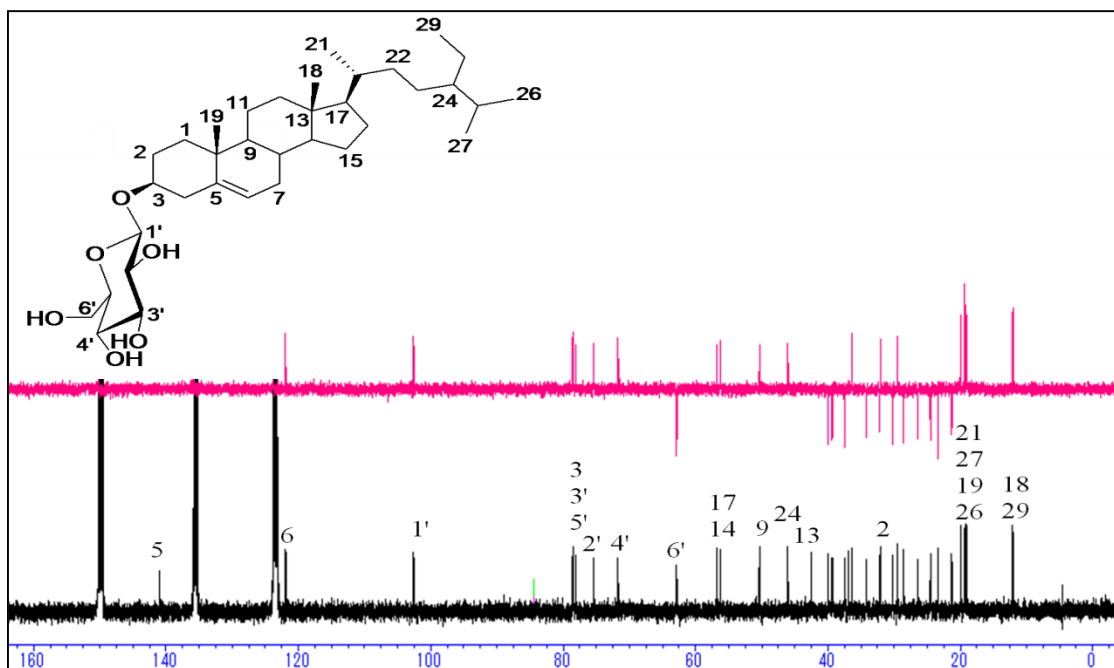


Fig. 2.44.  $^{13}\text{C}$ -NMR spectrum of compound 13 (100 MHz,  $\text{C}_5\text{D}_5\text{N}$ ).

Table 2.5:  $^{13}\text{C}$ -NMR (100 MHz) and  $^1\text{H}$ -NMR (400 MHz) spectroscopic data of compound 13 (pyridine- $d_5$ ,  $\delta$  in ppm,  $J$  in Hz)

| No. | $\delta_C$             | $\delta_H$ (No., $M$ , $J_{\text{Hz}}$ ) | No. | $\delta_C$             | $\delta_H$ (No., $M$ , $J_{\text{Hz}}$ ) |
|-----|------------------------|--|-----|------------------------|--|
| 1   | 37.4 ( $\text{CH}_2$ ) |  | 19  | 19.4 ( $\text{CH}_3$ ) | 0.92 (3H, s)                             |
| 2   | 30.2 ( $\text{CH}_2$ ) |  | 20  | 36.3 (CH)              |  |
| 3   | 78.4 (CH)              | 4.06 (1H, m)                             | 21  | 19.0 ( $\text{CH}_3$ ) | 0.97 (3H, d, $J=6.5$ Hz)                 |
| 4   | 39.3 ( $\text{CH}_2$ ) |  | 22  | 34.2 ( $\text{CH}_2$ ) |  |
| 5   | 140.9 (C)              |  | 23  | 26.4 ( $\text{CH}_2$ ) |  |
| 6   | 121.9 (CH)             | 5.33 (1H, brs)                           | 24  | 46.0 (CH)              |  |
| 7   | 32.0 ( $\text{CH}_2$ ) |  | 25  | 29.4 (CH)              |  |
| 8   | 32.1 (CH)              |  | 26  | 19.9 ( $\text{CH}_3$ ) | 0.85 (3H, d, $J=6.5$ Hz)                 |
| 9   | 50.3 (CH)              |  | 27  | 19.2 ( $\text{CH}_3$ ) | 0.87 (3H, d, $J=6.5$ Hz)                 |
| 10  | 36.9 (C)               |  | 28  | 23.4 ( $\text{CH}_2$ ) |  |
| 11  | 21.2 ( $\text{CH}_2$ ) |  | 29  | 12.1 ( $\text{CH}_3$ ) | 0.88 (3H, t, $J=7.5$ Hz)                 |
| 12  | 39.9 ( $\text{CH}_2$ ) |  | 1'  | 102.6 (CH)             | 5.06 (1H, d, $J=7.2$ Hz)                 |
| 13  | 42.5 (C)               |  | 2'  | 75.3 (CH)              |  |
| 14  | 56.8 (CH)              |  | 3'  | 78.1 (CH)              |  |
| 15  | 24.5 ( $\text{CH}_2$ ) |  | 4'  | 71.7 (CH)              |  |
| 16  | 28.5 ( $\text{CH}_2$ ) |  | 5'  | 78.4 (CH)              |  |
| 17  | 56.2 (CH)              |  | 6'  | 62.8 ( $\text{CH}_2$ ) |  |
| 18  | 11.9 ( $\text{CH}_3$ ) | 0.65 (3H, s)                             |     |                        |  |

## Discussion

Compound **13** was obtained as a white amorphous powder from the major fraction TC-7 of the Red Sea grass *Thalassodendron ciliatum*. The structure elucidation of compound **13** began with the analysis of its  $^1\text{H-NMR}$ ,  $^{13}\text{C-NMR}$  spectrum and DEPT experiment. Compound **13** exhibited almost similar  $^1\text{H-NMR}$  and  $^{13}\text{C-NMR}$  spectrum as compound **12** except for the absence of the characteristic signals at [ $\delta_{\text{H}}$  5.07(1H, dd,  $J=8.7$  Hz,  $J=15.1$  Hz ), 5.23 (1H, dd,  $J=8.7$  Hz,  $J=15.1$  Hz );  $\delta_{\text{C}}$  138.8, 129.4], assigned for olefinic moiety at position 22 and 23 in compound **12**, and the appearance of two new methylene signals at  $\delta_{\text{C}}$  34.2, 26.4 assigned to C-22, C-23 carbons in compound **13**. The other characteristic signals were almost same since the  $^1\text{H-NMR}$  spectrum of compound **13**, (Table 2.5), showed six methyl resonances, two of them are connected to quaternary carbon atom at  $\delta_{\text{H}}$  0.65(s) and 0.92 (s) assigned to H<sub>3</sub>-18 and H<sub>3</sub>-19 respectively. Three of them are connected to methine carbon at  $\delta_{\text{H}}$  0.85, 0.87, and 0.97 assigned to H<sub>3</sub>-26, H<sub>3</sub>-27, and H<sub>3</sub>-21. The last methyl is attached to methylene carbon at  $\delta_{\text{H}}$  0.88 assigned to H<sub>3</sub>-29 which were corresponding to the steroidal nucleus.<sup>83)</sup> In addition, a resonance at  $\delta_{\text{H}}$  5.33 of the most downfield chemical shift was assigned to H-6 which demonstrates that it is attached to an olefinic carbon. The chemical shift at  $\delta$  4.06 indicated the presence of one carbinol proton at position 3 of the proposed skeleton. One anomeric proton at  $\delta_{\text{H}}$  5.06 indicated the presence of the sugar moiety.

The  $^{13}\text{C-NMR}$  spectrum of **13** (Table 2.5) showed there are 35 carbon atoms in the molecule. The olefinic resonance at  $\delta$  121.9 corresponded to C-6 methine carbon, and a signal at  $\delta$  140.9 corresponded to the C-5 quaternary carbon of the sterol moiety. An anomeric carbon signal at  $\delta$  102.6 indicated the presence of a sugar moiety. The four methine resonances at  $\delta$  75.3, 78.1, 71.7, and 78.4 as well as the methylene resonance at  $\delta$  62.8 were due to C-2', C-3', C-4', C-5' and C-6', respectively of the  $\beta$ -glucopyranoside. The value of  $J = 7.2$  on 1' (anomeric proton) reflected that the proton is the axial-axial to C-2' proton which means glucopyranoside moiety binds to the sterol moiety  $\beta$  position.<sup>85,86)</sup>

The molecular formula of compound **13** was deduced as  $\text{C}_{35}\text{H}_{60}\text{O}_6$  based on the NMR spectra and further confirmed by the mass spectra with the appearance of the molecular ion peak at  $m/z$ , 576  $[\text{M}]^+$  in the EI-MS spectrum showing 2 mass per unit increase than compound **12** confirming the absence of one degree of unsaturation. The NMR data of compound **13** was compared with a reference data and found to be matched.<sup>87)</sup>

## Conclusion

From the above data and discussion the structure of compound **13** was assigned as

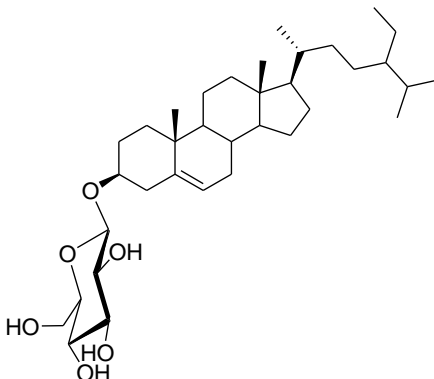


Fig. 2.45. Structure of  $\beta$ -sitosterol glucoside (**13**)

### 2.2.6. Compound 14

Compound **14** was isolated as white solid from the major fraction TC-9 of the Red Sea grass *Thalassodendron ciliatum*.

### Spectroscopic analysis

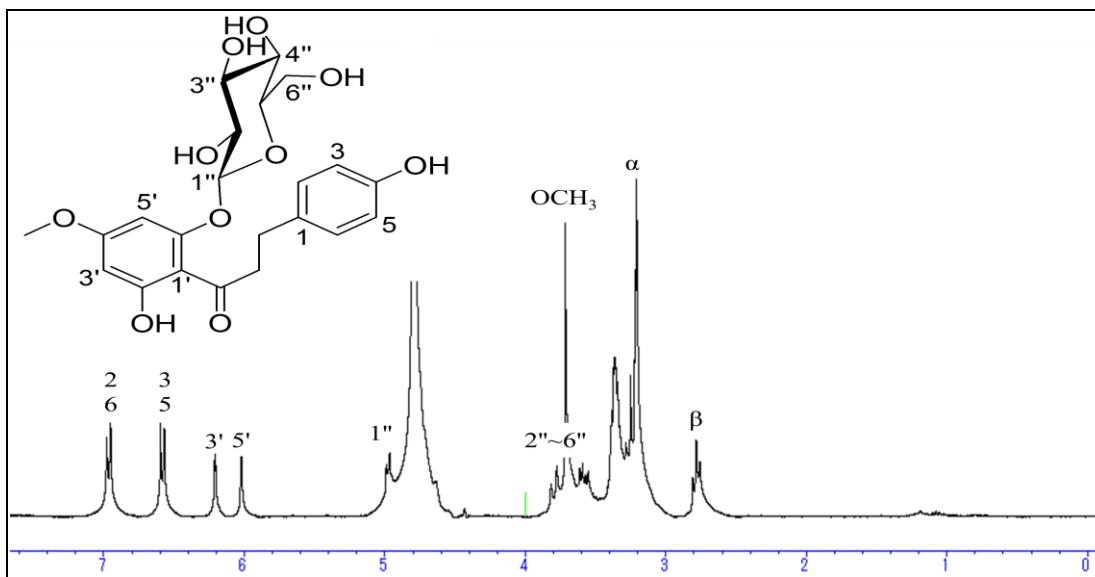


Fig. 2.46.  $^1\text{H-NMR}$  spectrum of compound **14** (400 MHz,  $\text{CDCl}_3$ ).

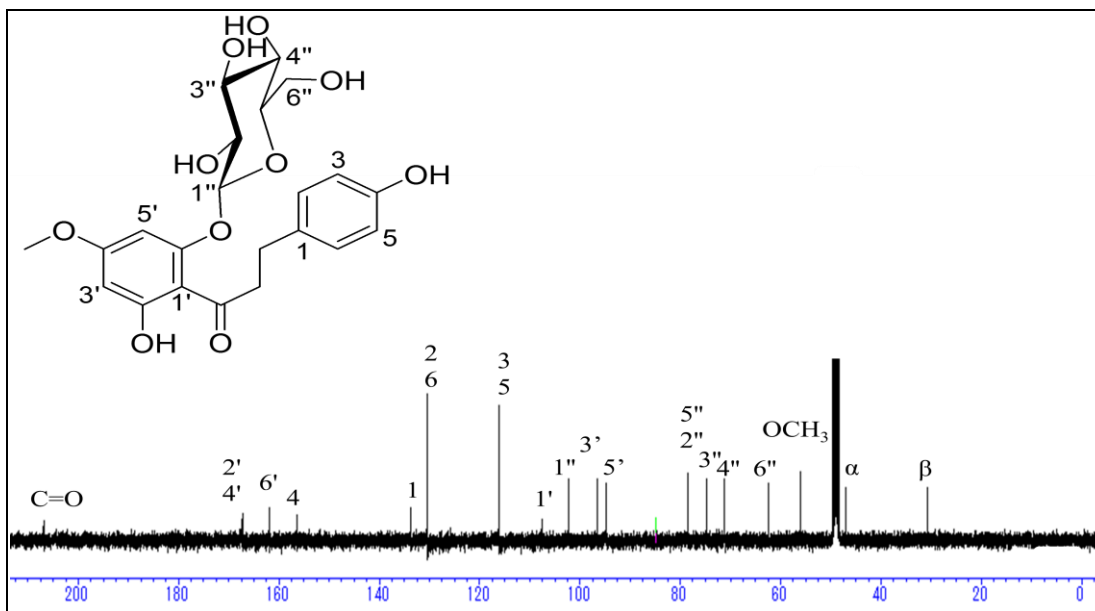


Fig. 2.47.  $^{13}\text{C}$ -NMR Spectrum of compound **14** (100 MHz,  $\text{CDCl}_3$ ).

$^{13}\text{C}$ -NMR (100 MHz) and  $^1\text{H}$ -NMR (400 MHz) data for compound **14** in  $\text{CD}_3\text{OD}$  are listed in Table 2.6.

Table 2.6:  $^{13}\text{C}$ -NMR (100 MHz) and  $^1\text{H}$ -NMR (400 MHz) spectroscopic data of compound **14** ( $\text{CD}_3\text{OD}$ ,  $\delta$  in ppm,  $J$  in Hz)

| No. | $\delta_{\text{C}}$ | $\delta_{\text{H}}$ (No., $M$ , $J_{\text{Hz}}$ ) | No.      | $\delta_{\text{C}}$    | $\delta_{\text{H}}$ (No., $M$ , $J_{\text{Hz}}$ ) |
|-----|---------------------|---|----------|------------------------|---|
| 1   | 133.8 (C)           |   | 6'       | 161.9 (C)              |   |
| 2   | 130.4 (CH)          | 6.96 (1H, d, $J=8.4$ Hz)                          | 1''      | 102.6 (CH)             | 4.98 (1H, d, $J=5.4$ Hz)                          |
| 3   | 114.9 (CH)          | 6.58 (1H, d, $J=8.4$ Hz)                          | 2''      | 78.4 (CH)              |   |
| 4   | 156.4 (C)           |   | 3''      | 74.7 (CH)              |   |
| 5   | 114.9 (CH)          | 6.58 (1H, d, $J=8.4$ Hz)                          | 4''      | 71.2 (CH)              | 3.55~3.88 (5H, m, glucosyl protons)               |
| 6   | 130.4 (CH)          | 6.96 (1H, d, $J=8.4$ Hz)                          | 5''      | 78.5 (CH)              |   |
| 1'  | 107.6 (C)           |   | 6''      | 62.4 ( $\text{CH}_2$ ) |   |
| 2'  | 167.2 (C)           |   | $\alpha$ | 47.0 ( $\text{CH}_2$ ) | 3.21 (2H, t, $J=7.2$ Hz)                          |
| 3'  | 96.5 (CH)           | 6.21 (1H, d, $J=2.4$ Hz)                          | $\beta$  | 30.7 ( $\text{CH}_2$ ) | 2.78 (2H, t, $J=7.2$ Hz)                          |
| 4'  | 167.4 (C)           |   | OMe      | 56.1 ( $\text{CH}_3$ ) | 3.72 (3H, s)                                      |
| 5'  | 94.8 (CH)           | 6.02 (1H, d, $J=2.4$ Hz)                          | C=O      | 206.9 (C)              |   |

## Discussion

Compound **14** was obtained as a white solid from TC-9 fraction of the marine sea grass *Thalassodendron ciliatum*. The structure elucidation of compound **14** began with the analysis of its  $^1\text{H}$ -NMR,  $^{13}\text{C}$ -NMR spectrum and DEPT experiment exhibited the structure of asebogenin

derivative which was composed of 1 methyl, 3 methylene, 11 methine and 7 quaternary carbons, with the characteristic signals as follow; two triplet signals appeared at  $\delta_{\text{H}}$  2.78 (2H, t,  $J = 7.2$  Hz,  $\text{CH}_2\text{-}\beta$ ) and at  $\delta_{\text{H}}$  3.21 (2H, t,  $J = 7.2$  Hz,  $\text{CH}_2\text{-}\alpha$ ), which are characteristic for the dihydrochalcones,<sup>87)</sup> two ortho-coupled doublets correlated together and appeared at  $\delta_{\text{H}}$  6.96 (2H, d,  $J = 8.4$  Hz, H-2 and H-6) and at  $\delta_{\text{H}}$  6.58 (2H, d,  $J = 8$  Hz, H-3 and H-5) which are indicating an oxygen substitution at the 4-position, another correlated meta-coupled doublets appeared at  $\delta_{\text{H}}$  6.21 (1H, d,  $J = 2.4$  Hz, H-3') and at  $\delta_{\text{H}}$  6.02 (1H, d,  $J = 2$  Hz, H-5').

Furthermore, a sharp singlet signal typical for an aromatic methoxyl group appeared at  $\delta_{\text{H}}$  3.72 (3H, s,  $\text{H}_3\text{CO-4'}$ ) and at  $\delta_{\text{C}}$  56.1 as confirmed from  $^{13}\text{C}$  NMR spectrum (Table 2.6). Moreover, a doublet signal appeared at  $\delta_{\text{H}}$  4.98 (1H, d,  $J = 7$  Hz, H-1'') characteristic for the anomeric proton of a hexose moiety identified to be glucose as shown in the  $^{13}\text{C}$ -NMR spectrum (Table 2.6). In addition to, a number of multiplets appeared between  $\delta_{\text{H}}$  3.55–3.88 (5H, m) are corresponding to the remaining sugars protons.

The molecular formula of compound **14** was deduced as  $\text{C}_{22}\text{H}_{26}\text{O}_{10}$  based on the NMR spectra. The NMR data of compound **14** was compared with a reference data and found to be matched.<sup>89,90)</sup>

## Conclusion

From the above data and discussion the structure of compound **14** was assigned as

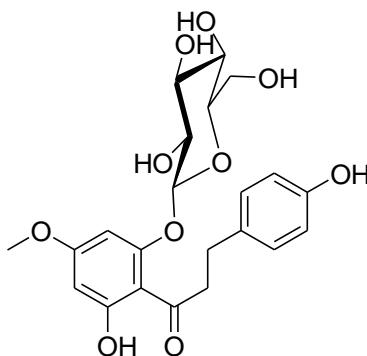


**Fig. 2.48. Structure of Asebotin (14)**

## 2.2. Secondary metabolites isolated from *Mycale euplectellioides*

Chemical investigation of the crude extract obtained from the marine sponge *Mycale euplectellioides* led to isolation of MEC-1 phytoceramide molecular species. Anti-choline esterase activity of the isolated MEC-1 was evaluated *in vitro* using microplate-based Ellman's assay; further purification of MEC-1 afforded three pure phytoceramides: MEC-1-4(**15**), MEC-1-7 (**16**) and MEC-1-8 (**17**). Additional phytochemical study of the crude extract obtained from *Mycale euplectellioides* led to the isolation of six known compounds: chimyl alcohol (**18**), batyl alcohol (**19**), thymine (**20**), uracil (**21**), thymidine (**22**) and uridine (**23**) for the first time. The structures of the isolated compounds elucidated on the basis of chemical methods, spectroscopic techniques (IR, NMR experiments and HRMS), and comparison with appropriate literature data. The molecular modeling studies using glide docking showed the tight binding of ceramides to acetylcholine esterase (AChE). Ceramides have achieved better docking score and glide Emodel compared to known AChE inhibitors. Ceramides interacted with aromatic residue of peripheral anionic site and penetrated deeply till catalytic triad residue of the active site. Overall, ceramides by the approaches used here could be considered promising lead compounds for discovery and design potent anti-choline esterase drug candidates, which would be used for Alzheimer eradication. In this part, we would show the results of the chemical investigation of the marine sponge *Mycale euplectellioides*.



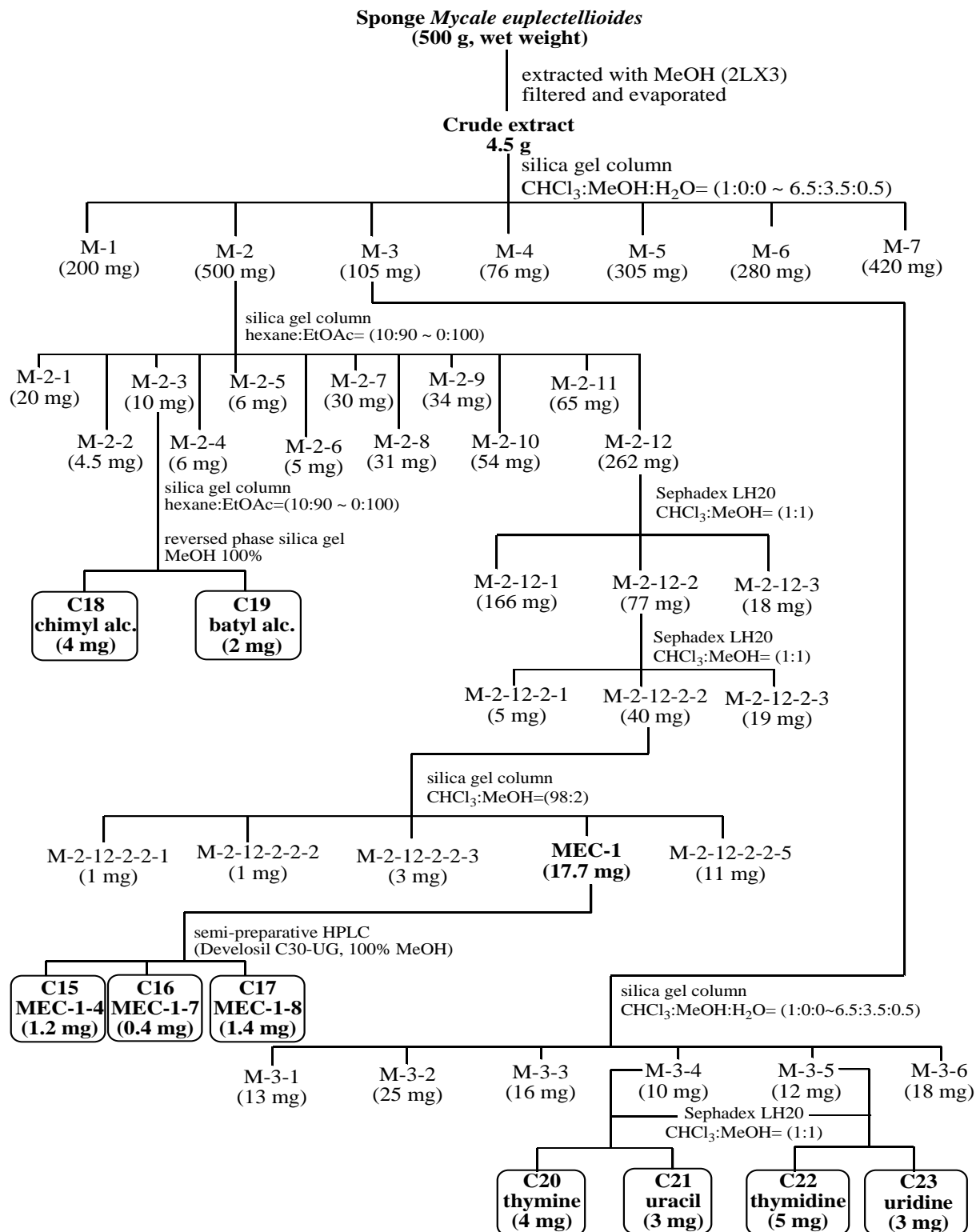


**Fig. 2.49.** Extraction and isolation scheme from *Mycale euplectellioides*

### 2.2.1. Compounds 15~17

MEC-1 (17.7 mg) was obtained as a white amorphous solid, showing a single spot on silica gel thin layer chromatography (TLC).

#### Spectroscopic analysis

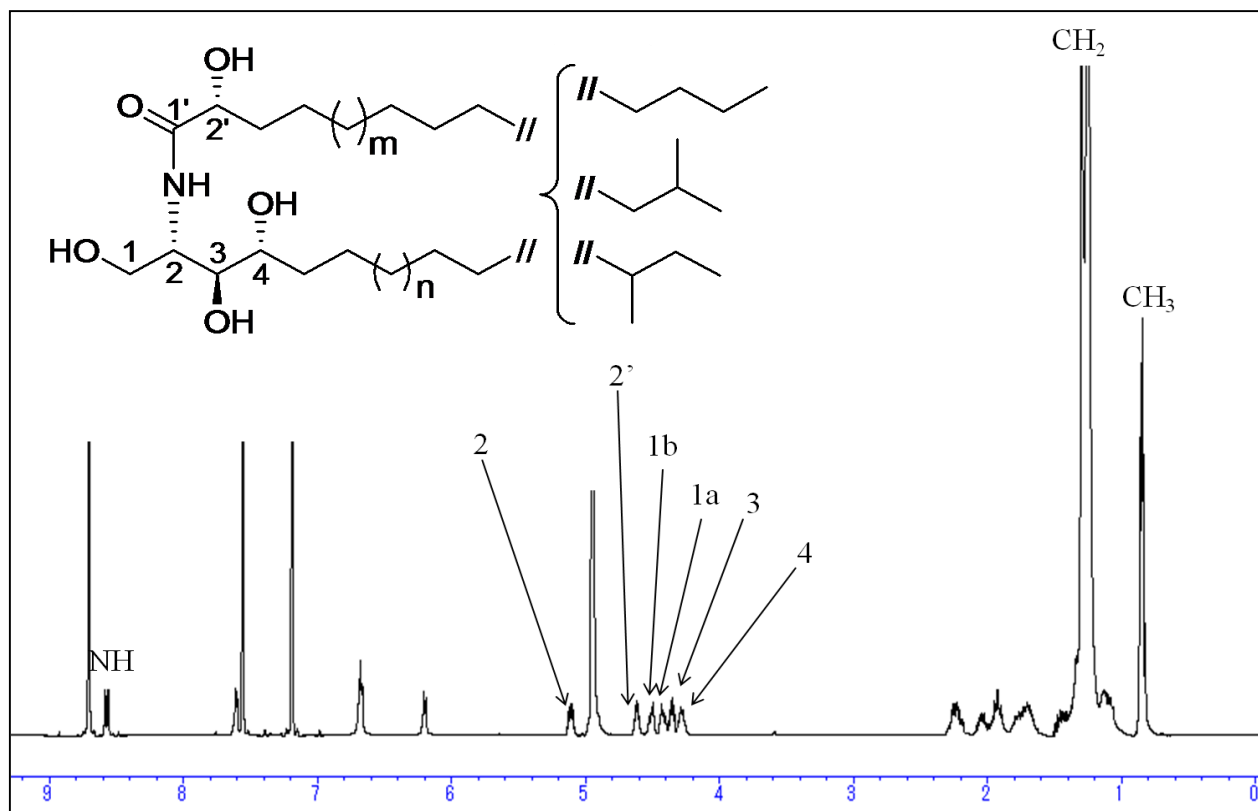


Fig. 2.50. <sup>1</sup>H-NMR spectrum of MEC-1 (400 MHz, C<sub>5</sub>D<sub>5</sub>N)

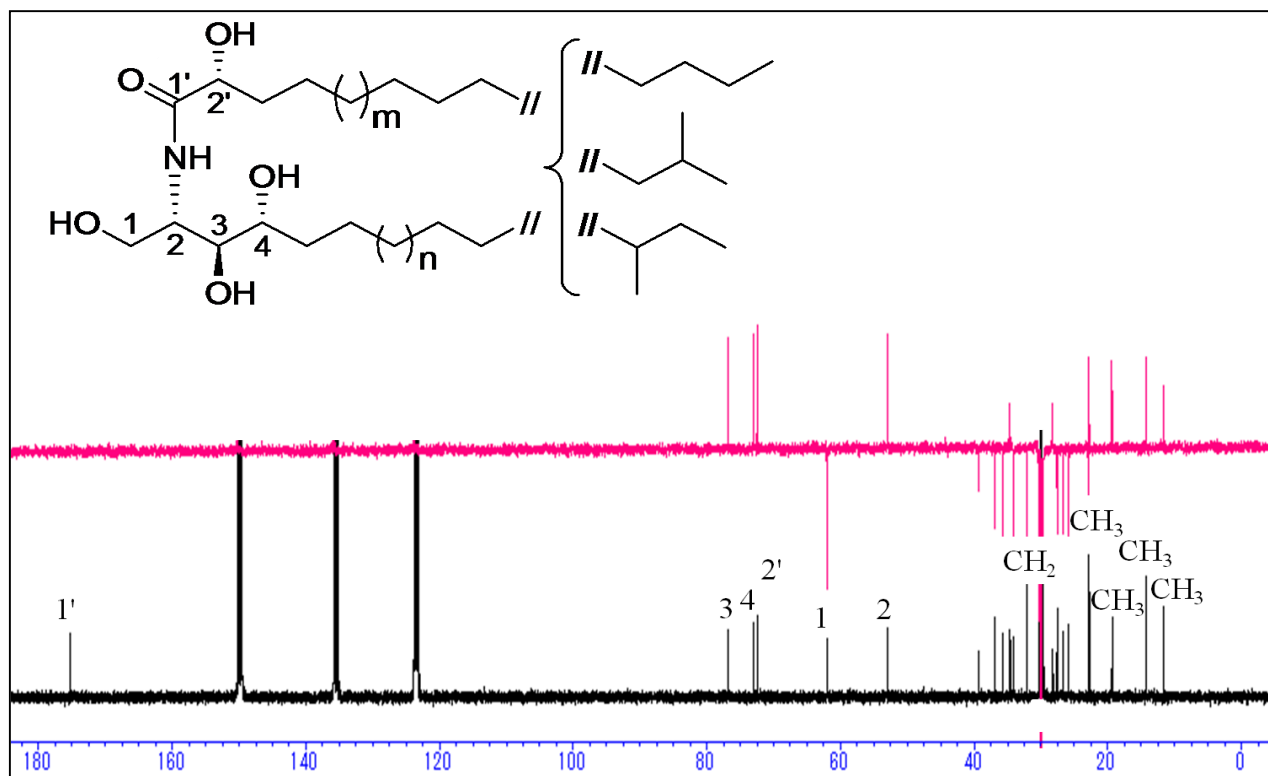


Fig. 2.51.  $^{13}\text{C}$ -NMR spectra of MEC-1 (400 MHz,  $\text{C}_5\text{D}_5\text{N}$ )

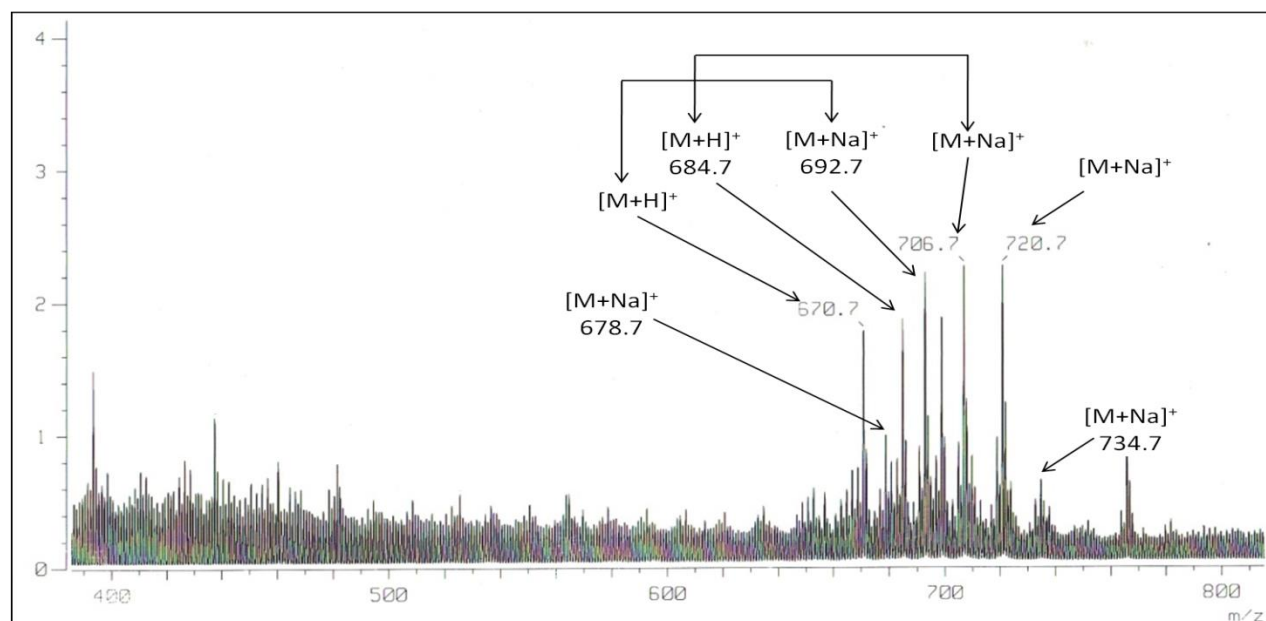


Fig. 2.52. FAB-MS (positive ion mode) of MEC-1

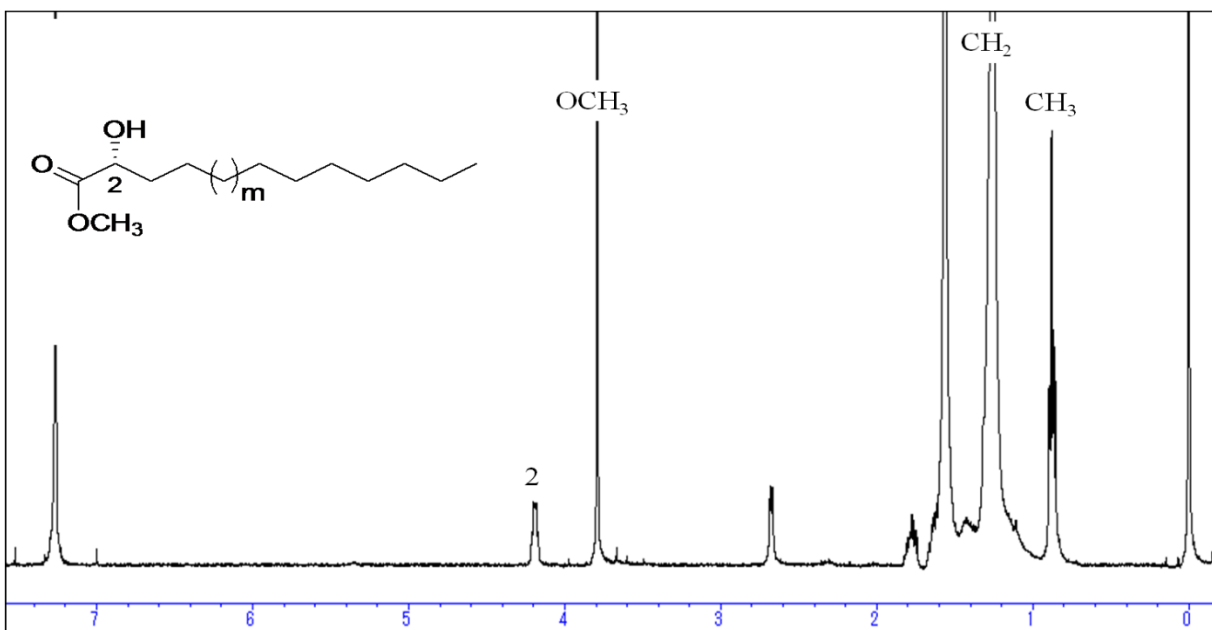


Fig. 2.53. <sup>1</sup>H-NMR spectrum of FAMEs after hydrolysis of MEC-1 (400 MHz, CDCl<sub>3</sub>)

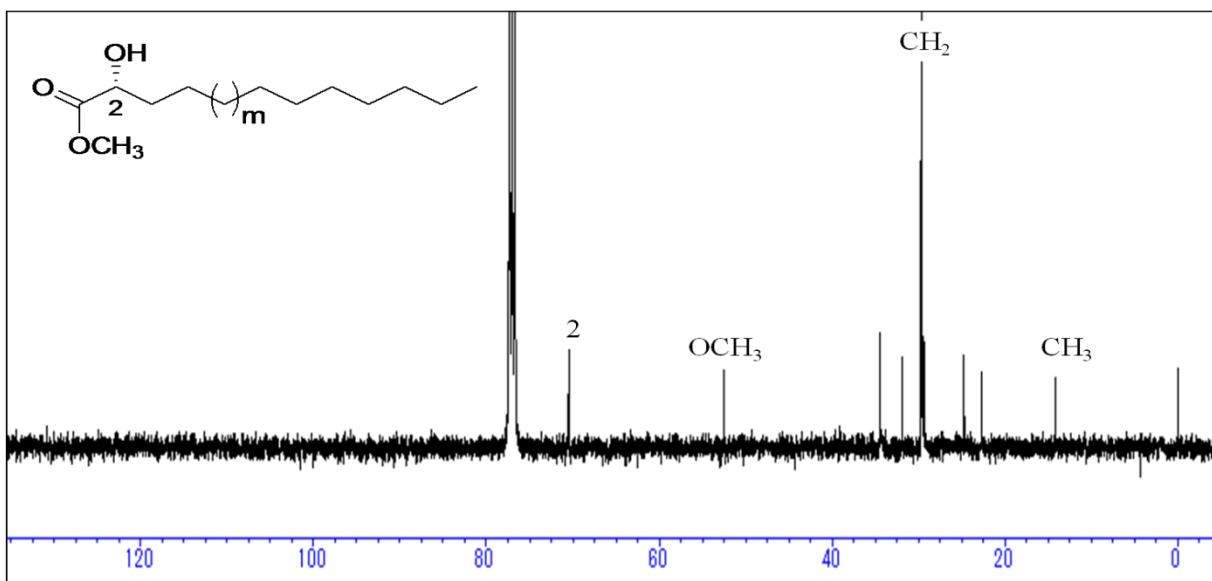


Fig. 2.54. <sup>13</sup>C-NMR spectrum of FAMEs after hydrolysis of MEC-1 (400 MHz, CDCl<sub>3</sub>)

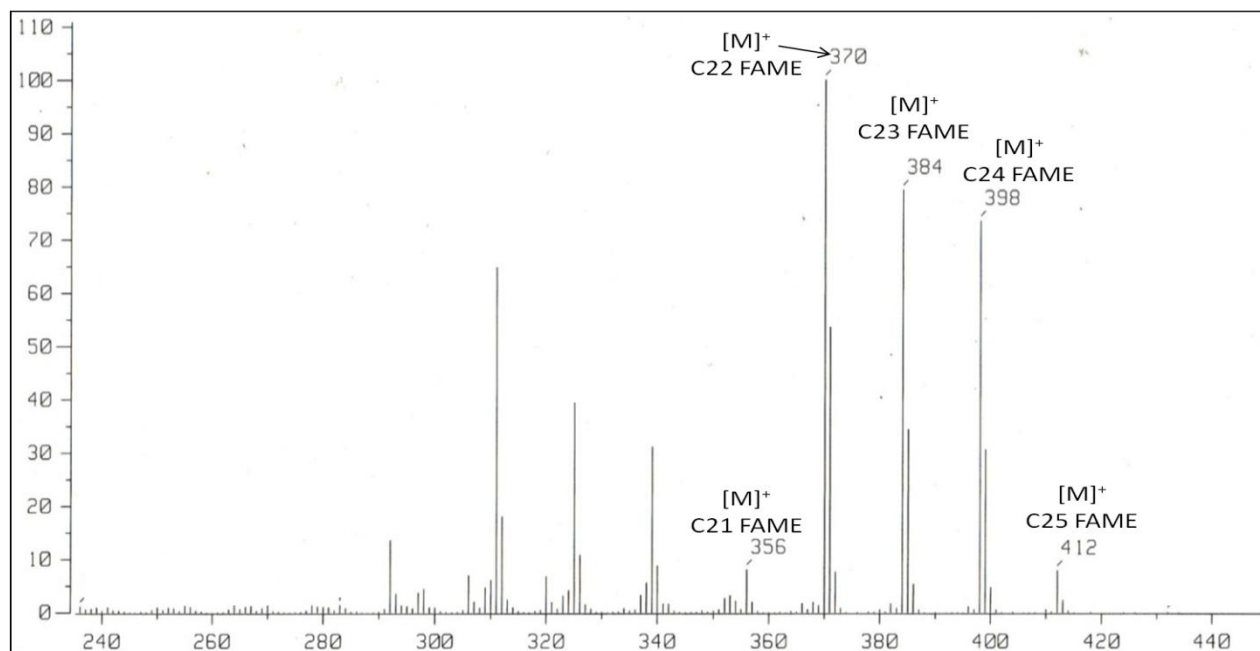


Fig. 2.55. EI-MS of FAMEs after hydrolysis of MEC-1

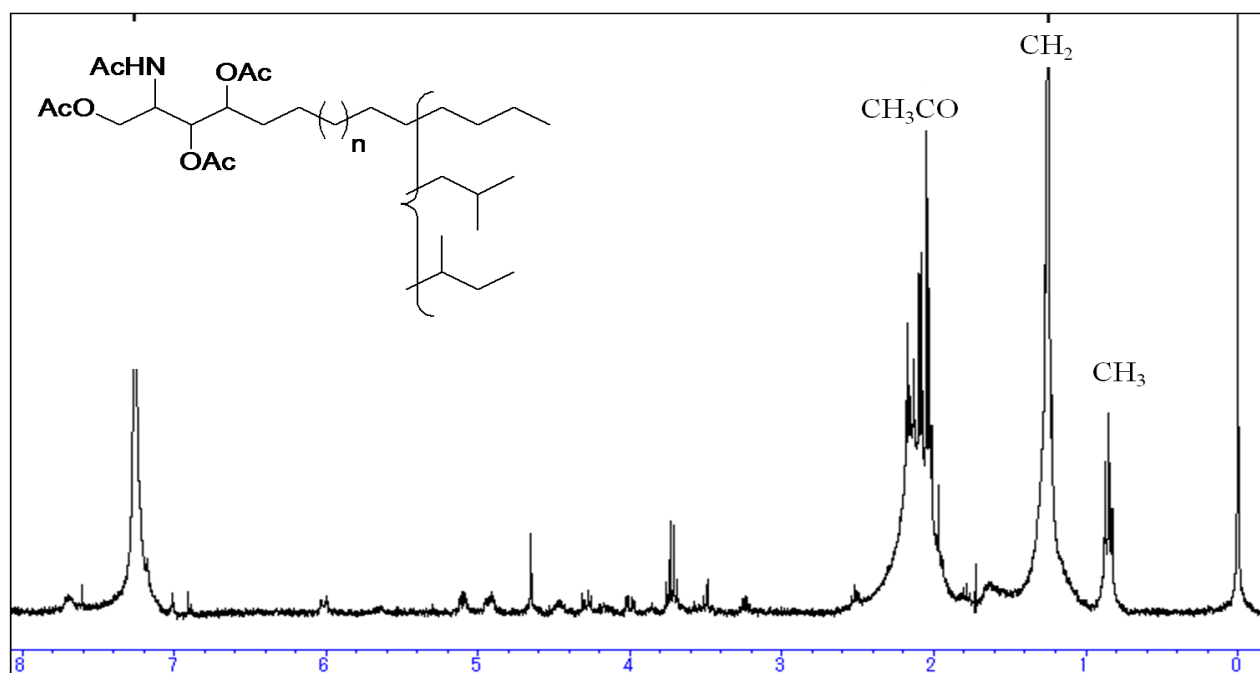


Fig. 2.56. <sup>1</sup>H-NMR spectrum of LCB after hydrolysis of MEC-1 (400 MHz, CD<sub>3</sub>OD)

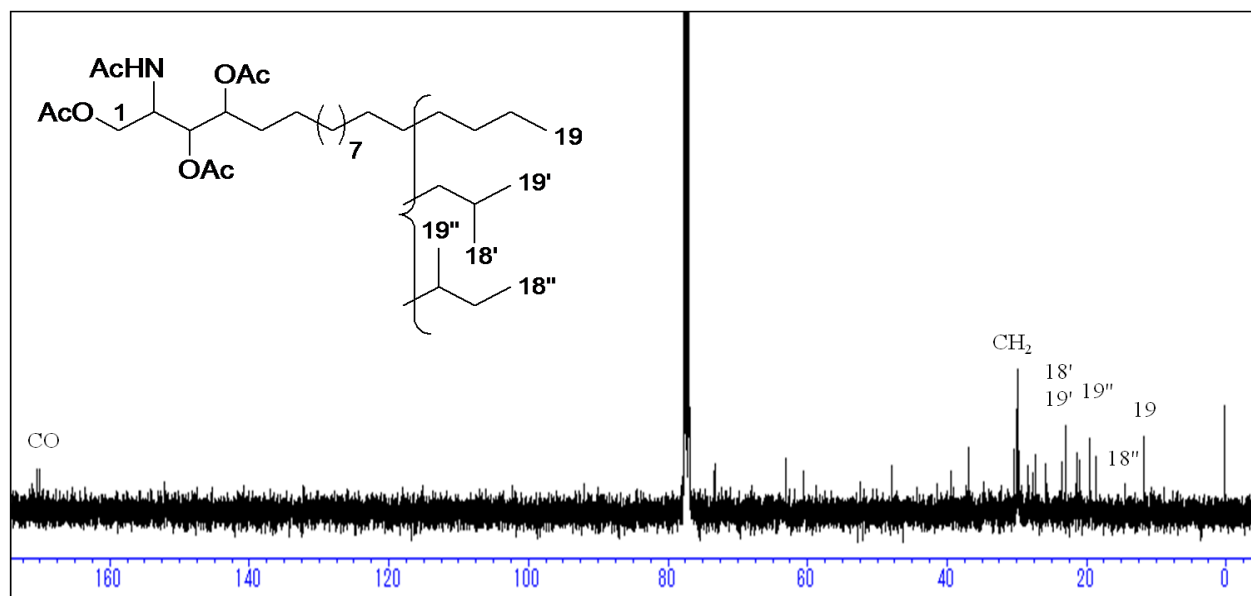


Fig. 2.57.  $^{13}\text{C}$ -NMR spectrum of LCB after hydrolysis of MEC-1 (400 MHz,  $\text{CD}_3\text{OD}$ )

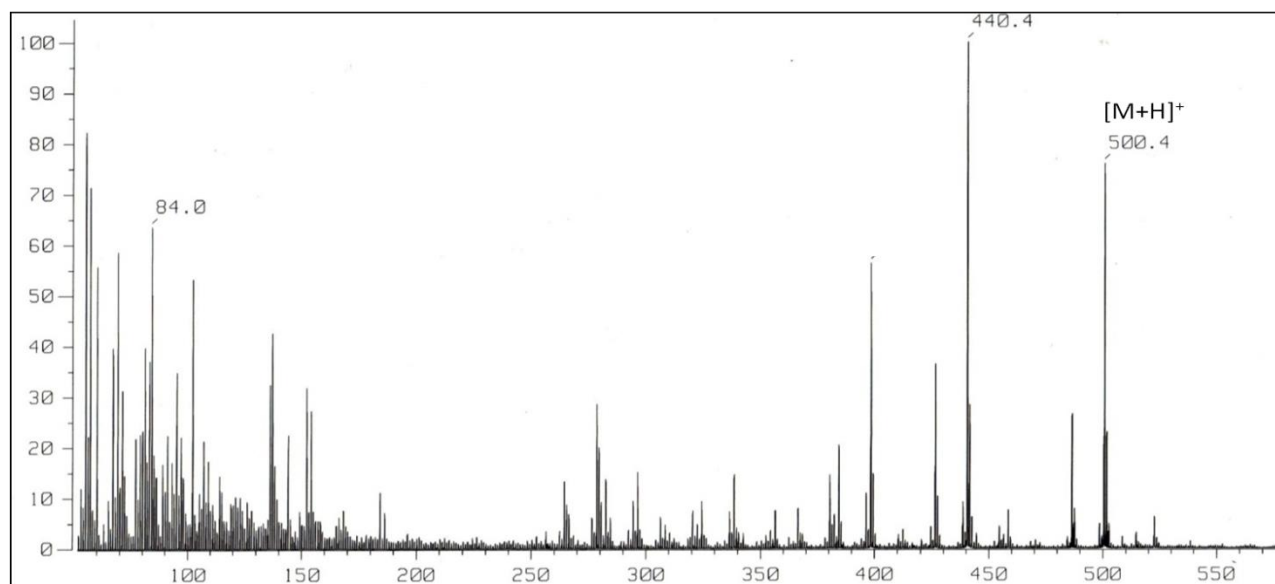


Fig. 2.58. FAB-MS (positive ion mode) of LCB after hydrolysis of MEC-1

$^{13}\text{C}$ -NMR (100 MHz) and  $^1\text{H}$ -NMR (400 MHz) data for MEC-1 in  $\text{C}_5\text{D}_5\text{N}$  are listed in **Table 2.7**.

Table 2.7:  $^{13}\text{C}$ -NMR (100 MHz) and  $^1\text{H}$ -NMR (400 MHz) spectroscopic data of MEC-1 ( $\text{C}_5\text{D}_5\text{N}$ ,  $\delta$  in ppm,  $J$  in Hz).

| <i>MEC-1</i>     |                         |  |
|------------------|-------------------------|--|
| <i>No.</i>       | $\delta_{\text{C}}$     | $\delta_{\text{H}}$ ( <i>No.</i> , <i>M</i> , <i>J</i> <sub>Hz</sub> ) |
| NH               |                         | 8.58 (1H, d, $J=8.9$ Hz)   |
| 1a               | 62.0 (CH <sub>2</sub> ) | 4.43 (1H, dd, $J=10.8, 5.2$ Hz)  |
| 1b               |                         | 4.49 (1H, dd, $J=10.8, 4.6$ Hz)  |
| 2                | 52.9 (CH)               | 5.12 (1H, m)   |
| 3                | 76.7 (CH)               | 4.35 (1H, m)   |
| 4                | 73.0 (CH)               | 4.27 (1H, m)   |
| 1'               | 175.2 (C)               |  |
| 2'               | 72.4 (CH)               | 4.61 (1H, m)   |
| -CH <sub>3</sub> | 14.2 (CH <sub>3</sub> ) | 0.88 (m)   |
|                  | 11.5 (CH <sub>3</sub> ) |  |
|                  | 19.3 (CH <sub>3</sub> ) |  |
|                  | 22.4 (CH <sub>3</sub> ) |  |

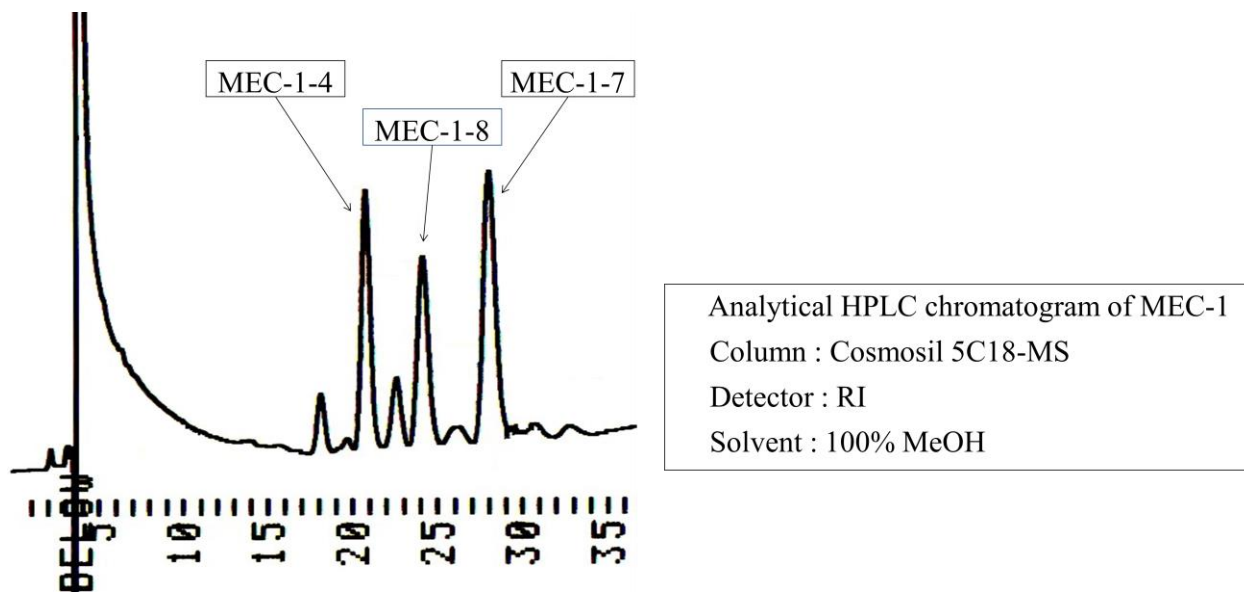
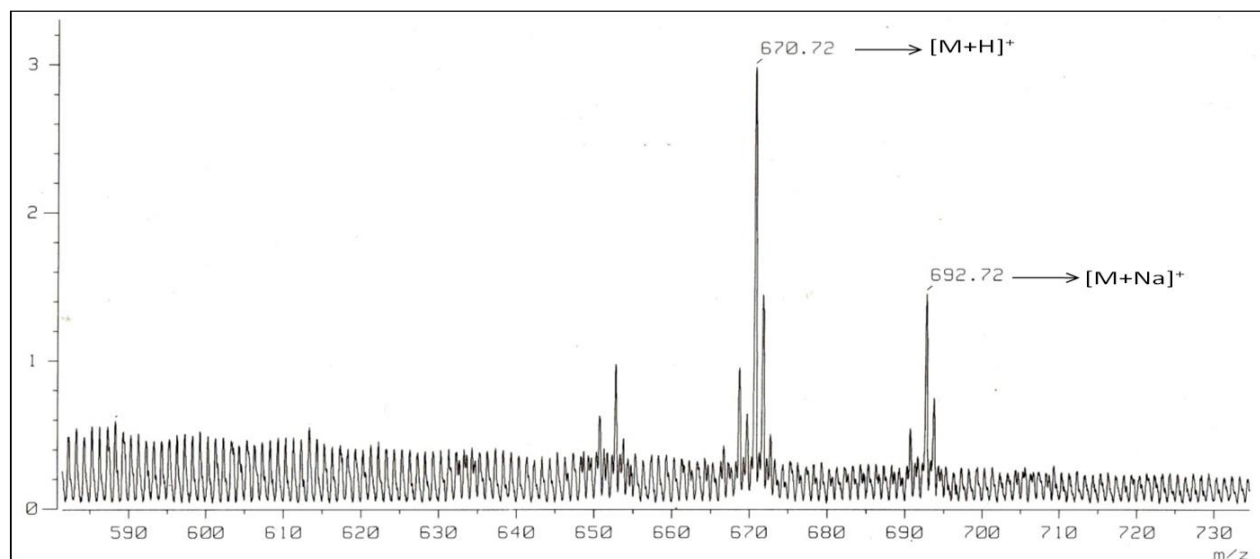
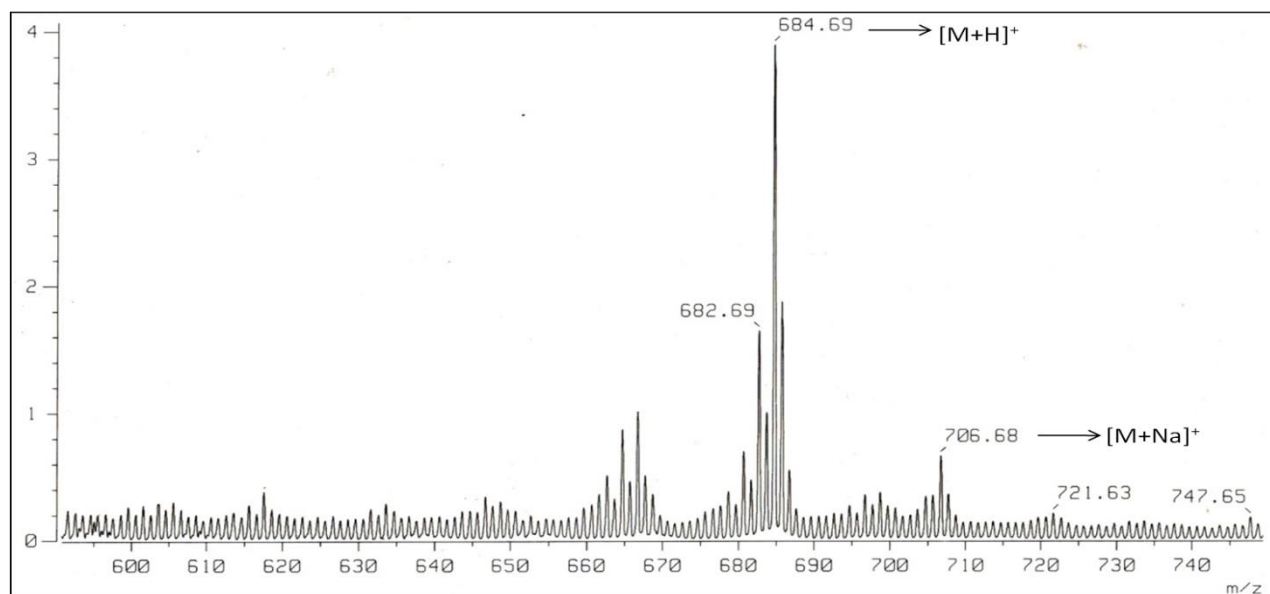


Fig. 2.59. Analytical HPLC chromatogram of MEC-1



**Fig. 2.60.** FAB-MS (positive ion mode) of MEC-1-4



**Fig. 2.61.** FAB-MS (positive ion mode) of MEC-1-7



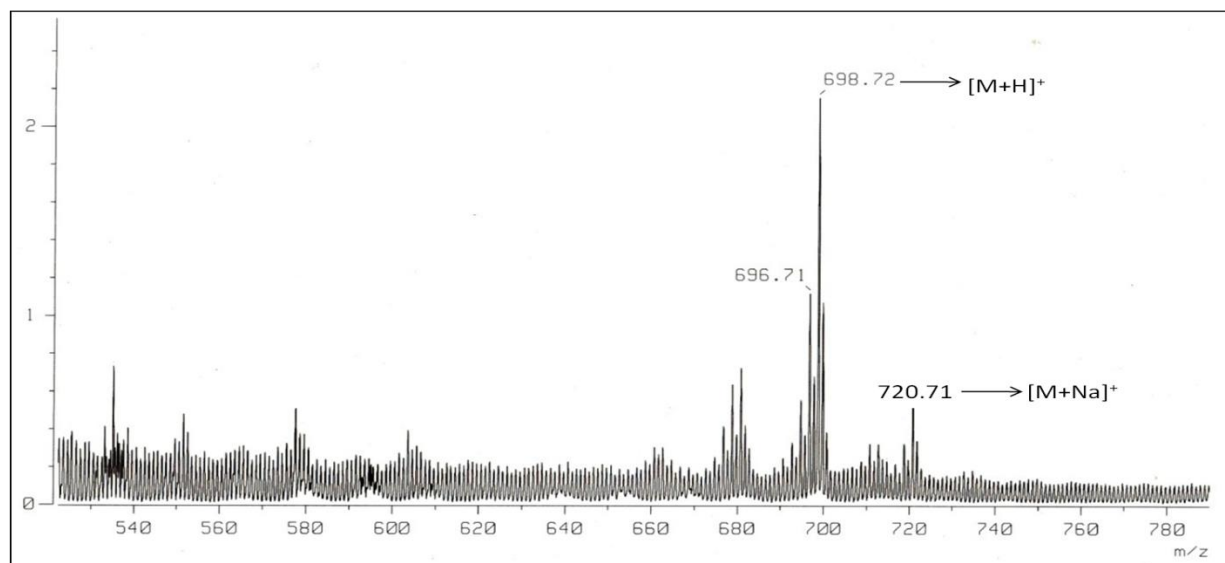


Fig. 2.62. FAB-MS (positive ion mode) of MEC-1-8

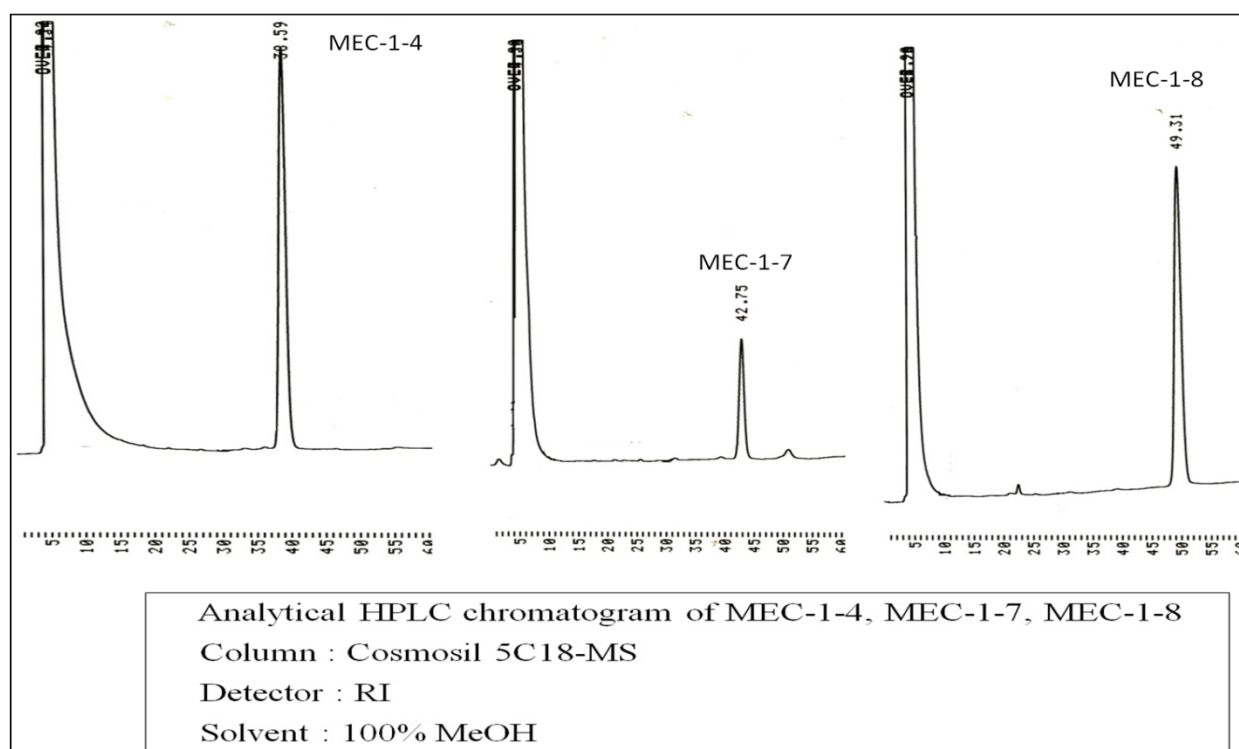


Fig. 2.63. Analytical HPLC chromatogram of MEC-1-4, MEC-1-7 and MEC-1-8.

## Discussion

MEC-1 exhibited a strong hydroxy ( $3300\text{ cm}^{-1}$ ), C-H ( $2900\text{ cm}^{-1}$ ) and amide absorption ( $1623$ ,  $1545\text{ cm}^{-1}$ ) in the IR spectrum.

The  $^1\text{H-NMR}$  spectrum in  $\text{C}_5\text{D}_5\text{N}$  showed resonances of an amide proton doublet at  $\delta_{\text{H}}$  8.58 (1H, d,  $J=8.9\text{ Hz}$ ), protons of a long methylene chain centered at  $\delta_{\text{H}}$  1.25, and overlapped methyls at  $\delta_{\text{H}}$  0.85 indicating sphingolipid skeleton. The characteristic resonance of 2-amino-1,3,4,2'-tetrol of the hydrocarbon chain was observed at  $\delta_{\text{H}}$  5.12 (1H, m, H-2), 4.61 (1H, m, H-2'), 4.49 (1H, dd,  $J=10.8, 5.2\text{ Hz}$ , H-1b), 4.43 (1H, dd,  $J=10.8, 4.6\text{ Hz}$ , H-1a), 4.35 (1H, m, H-3), 4.27 (1H, m, H-4) in the  $^1\text{H-NMR}$  spectrum and at  $\delta_{\text{C}}$  52.9 (C-2), 72.4 (C-2'), 62.0 (C-1), 76.7 (C-3), 73.0 (C-4) in the  $^{13}\text{C-NMR}$  spectrum. In addition to amide carbonyl at  $\delta_{\text{C}}$  175.2 (C-1'). A series of molecular ion peaks due to  $[\text{M}+\text{Na}]^+$  were observed in the positive ion FAB-MS spectrum at  $m/z$ : 678, 692, 706, 720, 734. Therefore, MEC-1 is presumed to be a molecular species of a phytosphingosine-type ceramide possessing 2- hydroxy fatty acid groups. Furthermore, MEC-1 is suggested to have normal, iso, *ante*- iso type terminal methyls,<sup>73)</sup> since the carbon signals for the terminal methyl groups were observed at  $\delta_{\text{C}}$  14.2 (normal type), 22.4 (iso type), 11.3 and 19.1 (*ante*- iso type) in the  $^{13}\text{C-NMR}$  spectrum (Fig. 2.51, Table 2.7). The structure of MEC-1 was characterized by comparison of its  $^{13}\text{C-NMR}$  spectral data with that of known ceramides.<sup>73-75)</sup> The absolute stereo chemistry of the ceramide molecular species is suggested to be (2*S*, 3*S*, 4*R*, 2'*R*), since the aforementioned  $^1\text{H-NMR}$  (H-2, H-3, H-4, H-2') and  $^{13}\text{C-NMR}$  signals (C-1, C-2, C-3, C-4, C-2') were in good agreement with those of phytosphingosine-type ceramide molecular species possessing (2*S*, 3*S*, 4*R*, 2'*R*) configurations.<sup>77,78)</sup> Based on the results of MEC-1 methanolysis with methanolic hydrochloric acid followed by  $^1\text{H-NMR}$ ,  $^{13}\text{C-NMR}$ , and FAB-MS analysis, the length and branching pattern of the long chain bases and fatty acids could be determined. The *n*-hexane layer afforded a mixture of fatty acid methyl esters (FAMES), which were subjected to  $^1\text{H-NMR}$ ,  $^{13}\text{C-NMR}$ , and EI-MS analysis. EI-MS analysis of the FAMES mixture showed the presence of five components at  $m/z$ : 356, 370, 384, 398 and 412  $[\text{M}]^+$ , which were characterized as FAM-1, FAM-2, FAM-3, FAM-4, and FAM-5 indicating C-21, C-22, C-23, C-24 and C-25 fatty acid methyl esters, respectively.

Furthermore, FAMES mixture was thought to possess normal and iso type terminal methyl groups, since the carbon signals for the terminal methyl groups in the  $^{13}\text{C}$ -NMR spectrum were observed at  $\delta_{\text{C}} = 14.2$  (normal) and  $\delta_{\text{C}} = 22.4$  (iso). On the other hand, the methanol layer provided long chain base, which reacted with acetic anhydride to afford the corresponding acetate followed by analysis of its to  $^1\text{H}$ -NMR,  $^{13}\text{C}$ -NMR, and FAB-MS. The FAB-MS analysis of the LCB indicated a  $\text{C}_{19}$  long chain base identified by the corresponding molecular ion peak at  $m/z$  500  $[\text{M}+\text{H}]^+$  and the  $^{13}\text{C}$ -NMR spectrum indicated that the LCB exhibit normal, iso and ante-iso terminal methyl groups (Fig. 2.57, Table 2.7).

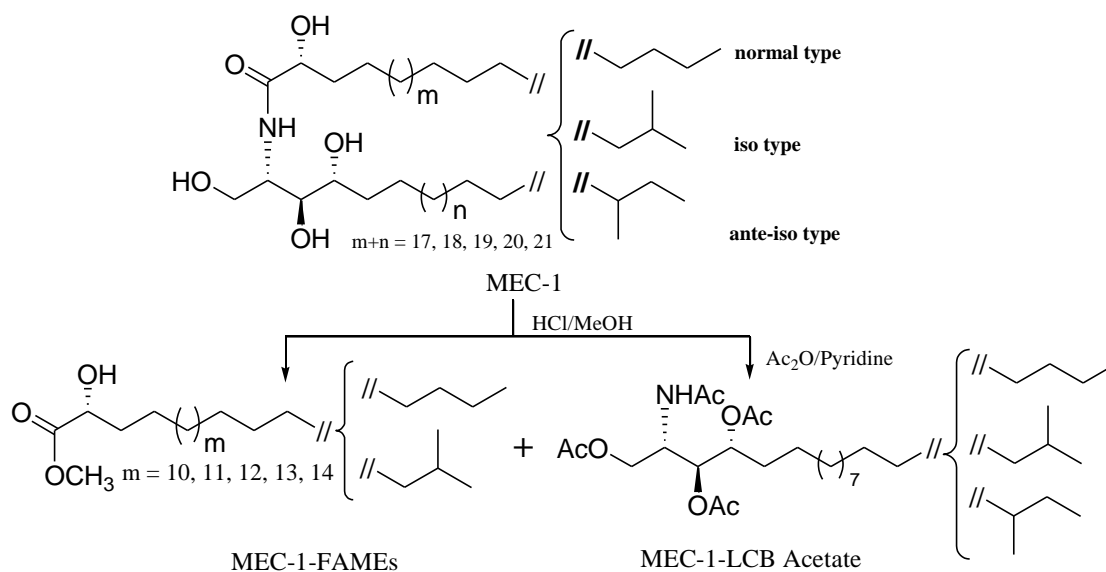


**Fig. 2.64. Structure of MEC-1.**

Based on the considerable interest and importance of determining the molecular species composition of sphingolipids, isolation and structure elucidation of the ceramide components in the molecular species MEC-1 was conducted. By means of reversed phase HPLC, MEC-1 was separated into eight peaks and they were recovered to give eight fractions range from MEC-1-1 to MEC-1-8. Three of these eight fractions, MEC-1-4 (**15**), MEC-1-7 (**16**) and MEC-1-8 (**17**) revealed the single molecular ion peak  $[\text{M}+\text{Na}]^+$  in the positive ion FAB-MS spectrum. Based on the molecular mass of MEC-1-4 (**15**)  $m/z$  692  $[\text{M}+\text{Na}]^+$ , MEC-1-7 (**16**)  $m/z$  706  $[\text{M}+\text{Na}]^+$ , MEC-1-8 (**17**)  $m/z$  720  $[\text{M}+\text{Na}]^+$ , the structures of MEC-1-4, MEC-1-7 and MEC-1-8 were determined as shown in Fig. 2.65.

## Conclusion

From the above data and discussion, the structure of MEC-1 was found to be a molecular species of phytoceramides. Further purification of MEC-1 led to isolation of MEC-1-4 (**15**), MEC-1-7 (**16**) and MEC-1-8 (**17**) as shown in Fig. 2.65.

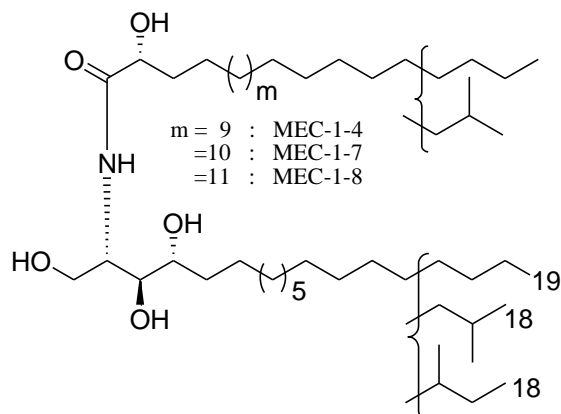


Fig. 2.65. Structure of MEC-1-4 (**15**), MEC-1-7 (**16**) and MEC-1-8 (**17**).

### 2.2.2. Compound 18

Compound **18** was isolated as a white solid from the major fraction M-2 of the marine sponge *Mycale euptectellioides*.

### Spectroscopic analysis

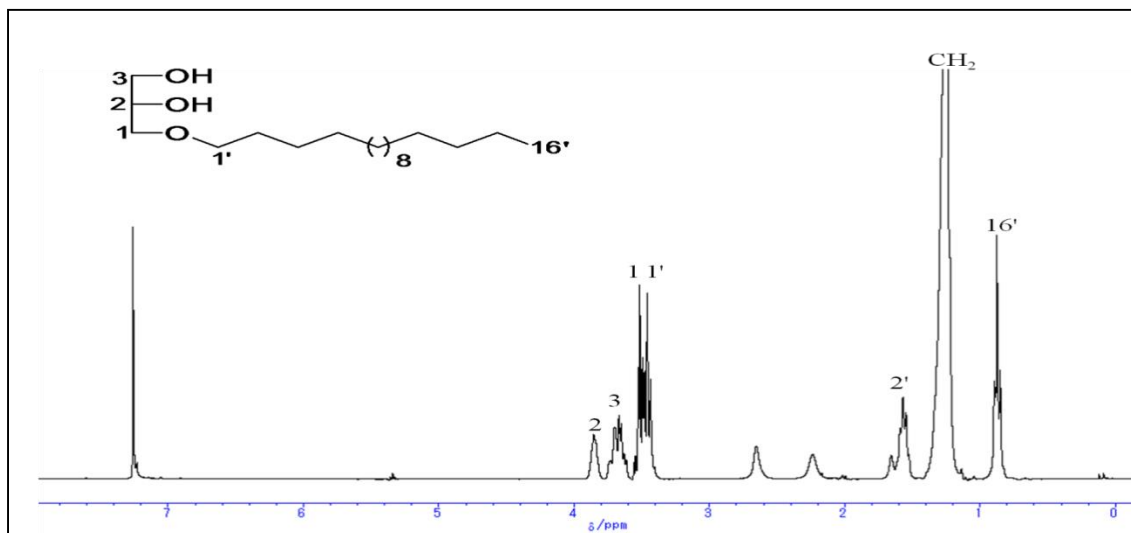


Fig. 2.66.  $^1\text{H-NMR}$  spectrum of compound **18** (400 MHz,  $\text{CDCl}_3$ ).

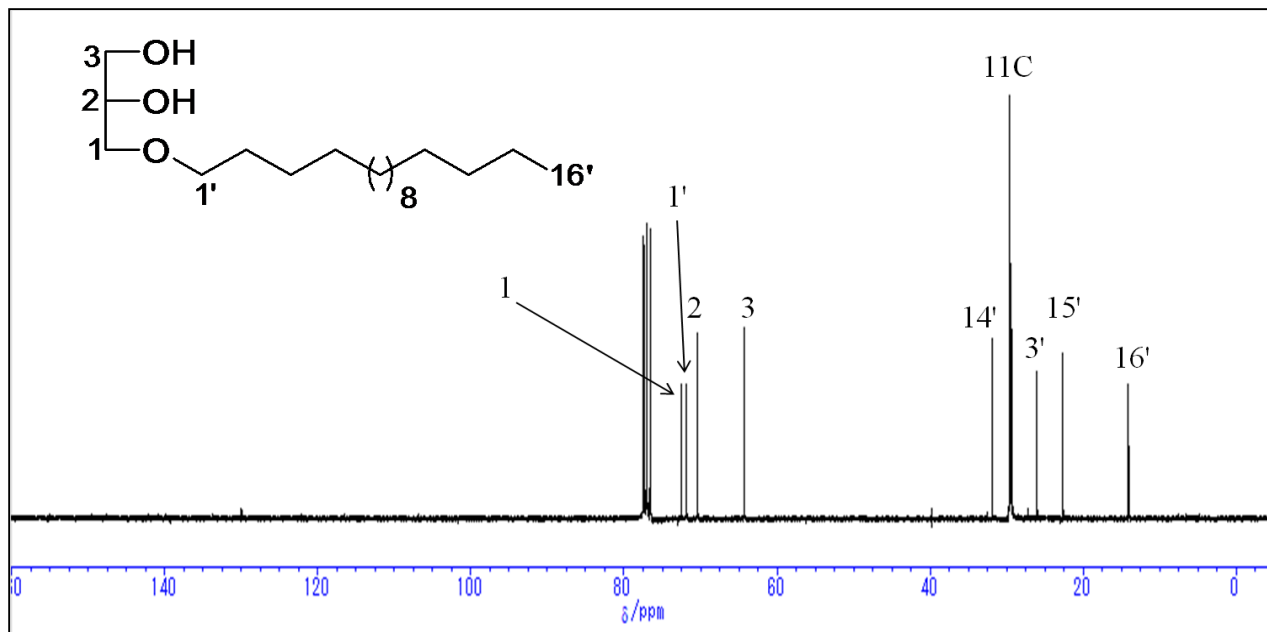


Fig. 2.67.  $^{13}\text{C}$ -NMR spectrum of compound **18** (100 MHz,  $\text{CDCl}_3$ ).

$^{13}\text{C}$ -NMR (100 MHz) and  $^1\text{H}$ -NMR (300 MHz) data for compound **18** in  $\text{CDCl}_3$  are listed in Table 2.8.

Table 2.8:  $^{13}\text{C}$  -NMR (100 MHz) and  $^1\text{H}$ -NMR (400 MHz) spectroscopic data of compound **18** ( $\text{CDCl}_3$ ,  $\delta$  in ppm,  $J$  in Hz).

| No.    | $\delta_c$                     | $\delta_H$ (No., $M$ , $J_{Hz}$ ) |
|--------|--------------------------------|-----------------------------------|
| 1      | 72.5 ( $\text{CH}_2$ )         | 3.52 (2H, m)                      |
| 2      | 70.4 (CH)                      | 3.86 (1H, m)                      |
| 3      | 64.3 ( $\text{CH}_2$ )         | 3.67 (2H, m)                      |
| 1'     | 71.8 ( $\text{CH}_2$ )         | 3.46 (2H, m)                      |
| 2'     |                                | 1.57 (2H, m)                      |
| 3'-15' | 22.6 (15', $\text{CH}_2$ )     | 1.25 (26H)                        |
|        | 26.0 (3', $\text{CH}_2$ )      |                                   |
|        | 29.3- 29.6 (11 $\text{CH}_2$ ) |                                   |
|        | 31.9 (14', $\text{CH}_2$ )     |                                   |
| 16'    | 14.1 ( $\text{CH}_3$ )         | 0.87 (3H, t, $J=5.78$ Hz)         |

## Discussion

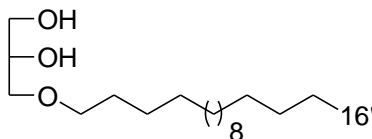
Compound **18** was obtained as a white solid from M-2 fraction of the marine sponge *Mycale euplectellioides*. The structure elucidation of compound **18** began with the analysis of its  $^1\text{H}$ -NMR,  $^{13}\text{C}$ -NMR spectrum and DEPT experiment exhibited the structure of a glycerol ether

derivatives. Three oxymethylenes were at  $\delta_C$  64.30 (t, C<sub>3</sub>), 71.85 (t, C<sub>1</sub>) and 72.51 (t, C<sub>1</sub>), one oxymethine was at  $\delta_C$  70.40 (d, C<sub>2</sub>). The methyl group was confirmed at  $\delta_C$  14.10 (q, C<sub>16</sub>) /  $\delta_H$  0.88 (3H, t,  $J=5.78$  Hz, 16'), and the left signals were methylene carbons.

The molecular formula of compound **18** was deduced as C<sub>19</sub>H<sub>40</sub>O<sub>3</sub> based on the NMR spectra and further confirmed by the mass spectra with the appearance of the molecular ion peak at  $m/z$ , 317 [M+H]<sup>+</sup> in the positive FAB-MS spectra. The NMR data of compound **18** was compared with a reference data and found to be matched.<sup>91,92)</sup>

### Conclusion

From the above data and discussion the structure of compound **18** was assigned as chimyl alcohol.

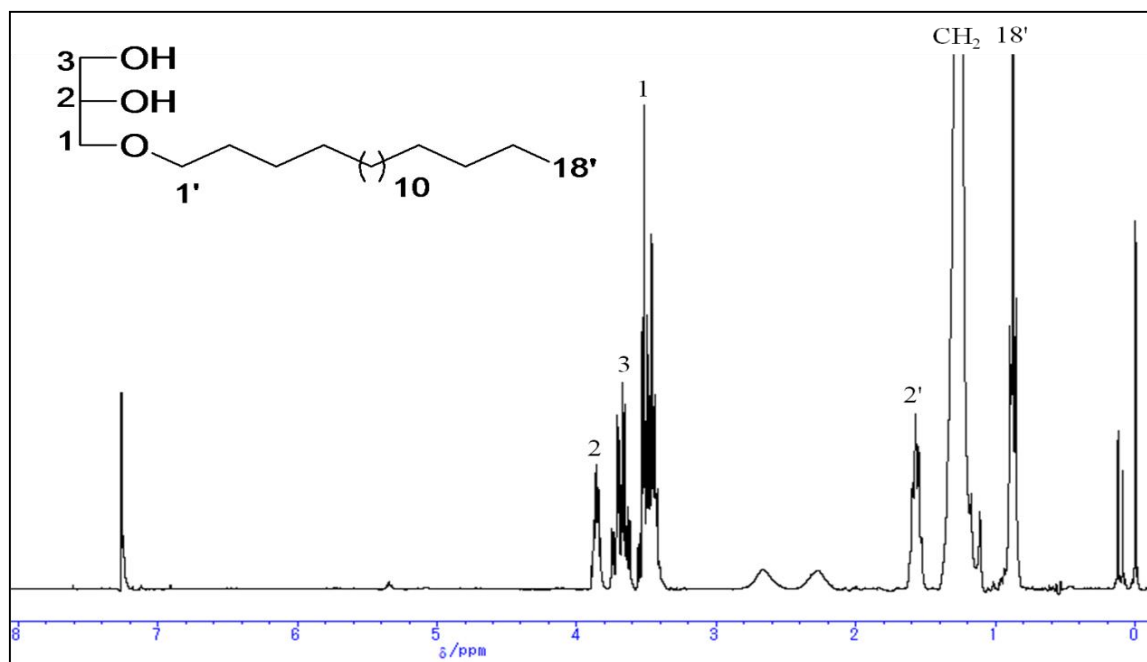
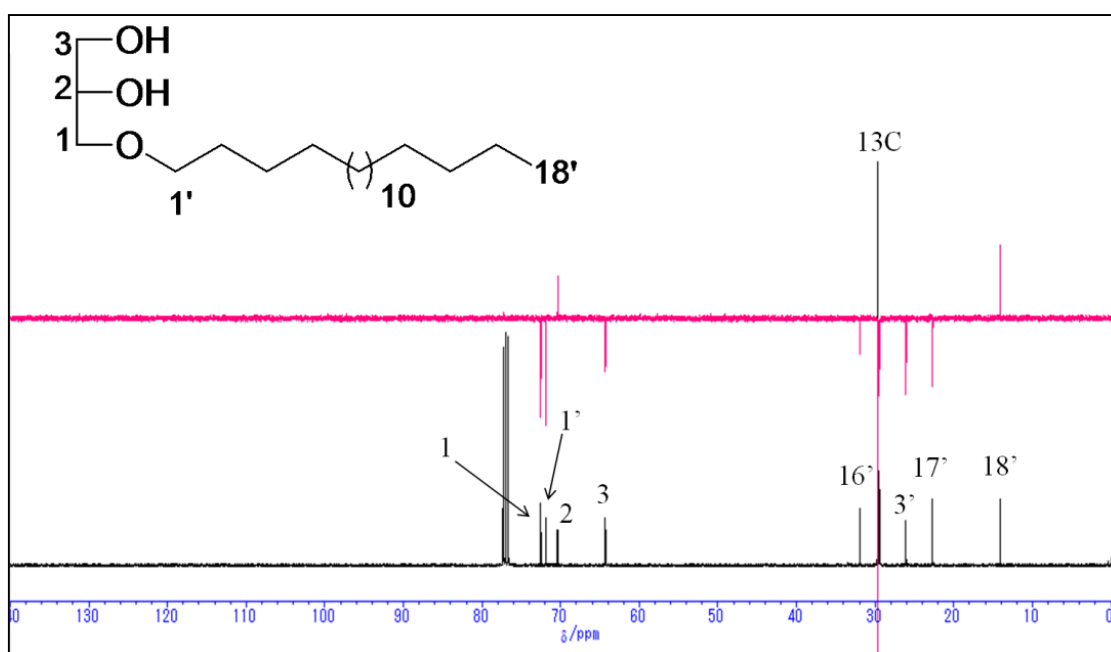


**Fig. 2.68. Structure of chimyl alcohol (18).**

### 2.2.3. Compound 19

Compound **19** was isolated as a white solid from the major fraction M-2 of the marine sponge *Mycale euplectellioides*.

## Spectroscopic analysis

Fig. 2.69. <sup>1</sup>H-NMR spectrum of compound 19 (400 MHz, CDCl<sub>3</sub>).Fig. 2.70. <sup>13</sup>C-NMR spectrum of compound 19 (100 MHz, CDCl<sub>3</sub>).

<sup>13</sup>C-NMR (100 MHz) and <sup>1</sup>H-NMR (400 MHz) data for compound 19 in CDCl<sub>3</sub> are listed in Table 2.9.

**Table 2.9:**  $^{13}\text{C}$ -NMR (100 MHz) and  $^1\text{H}$ -NMR (400 MHz) spectroscopic data of compound **19** ( $\text{CDCl}_3$ ,  $\delta$  in ppm,  $J$  in Hz).

| No.    | $\delta_{\text{C}}$            | $\delta_{\text{H}}$ (No., M, $J_{\text{Hz}}$ ) |
|--------|--------------------------------|--|
| 1      | 72.4 ( $\text{CH}_2$ )         | 3.52 (2H, m)                                   |
| 2      | 70.4 (CH)                      | 3.85 (1H, m)                                   |
| 3      | 64.2 ( $\text{CH}_2$ )         | 3.67 (2H, m)                                   |
| 1'     | 71.8 ( $\text{CH}_2$ )         | 3.46 (2H, m)                                   |
| 2'     |                                | 1.57 (2H, m)                                   |
| 2'-17' | 22.6 (17', $\text{CH}_2$ )     | 1.25 (30H)                                     |
|        | 26.0 (3', $\text{CH}_2$ )      |  |
|        | 29.3- 29.6 (13 $\text{CH}_2$ ) |  |
|        | 31.9 (16', $\text{CH}_2$ )     |  |
| 18'    | 14.1 ( $\text{CH}_3$ )         | 0.87 (3H, t, $J=6.85$ Hz)                      |

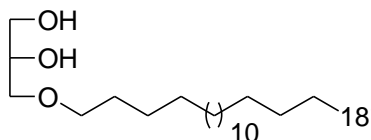
### Discussion

Compound **19** was obtained as a white solid from M-2 fraction of the marine sponge *Mycale euplectellioides*. The structure elucidation of compound **19** began with the analysis of its  $^1\text{H}$ -NMR,  $^{13}\text{C}$ -NMR spectrum and DEPT experiment exhibited the structure of a glycerol ether derivatives. Three oxymethylenes were at  $\delta_{\text{C}}$  64.26 (t,  $\text{C}_3$ ), 71.85 (t,  $\text{C}_{1'}$ ) and 72.48 (t,  $\text{C}_1$ ), one oxymethine was at  $\delta_{\text{C}}$  70.52 (d,  $\text{C}_2$ ). The methyl group was confirmed at  $\delta_{\text{C}}$  14.11 (q,  $\text{C}_{18'}$ ) /  $\delta_{\text{H}}$  0.88 (3H, t,  $J=6.85$  Hz,  $18'$ ), and the left signals were methylene carbons.

The molecular formula of compound **19** was deduced as  $\text{C}_{21}\text{H}_{44}\text{O}_3$  based on the NMR spectra and further confirmed by the mass spectra with The appearance of the molecular ion peak at  $m/z$ , 345 $[\text{M}+\text{H}]^+$  in the positive FAB-MS spectra. The NMR data of **19** was compared with that of batilol, and found to be matched.<sup>91,92)</sup>

### Conclusion

From the above data and discussion, the structure of compound **19** was assigned as batyl alcohol.

**Fig. 2.71.** Structure of batyl alcohol (**19**).



### 2.2.4. Compound 20

Compound **20** was isolated as colorless needles from the major fraction M-3 of the marine sponge *Mycale euplectellioides*.

#### Spectroscopic analysis

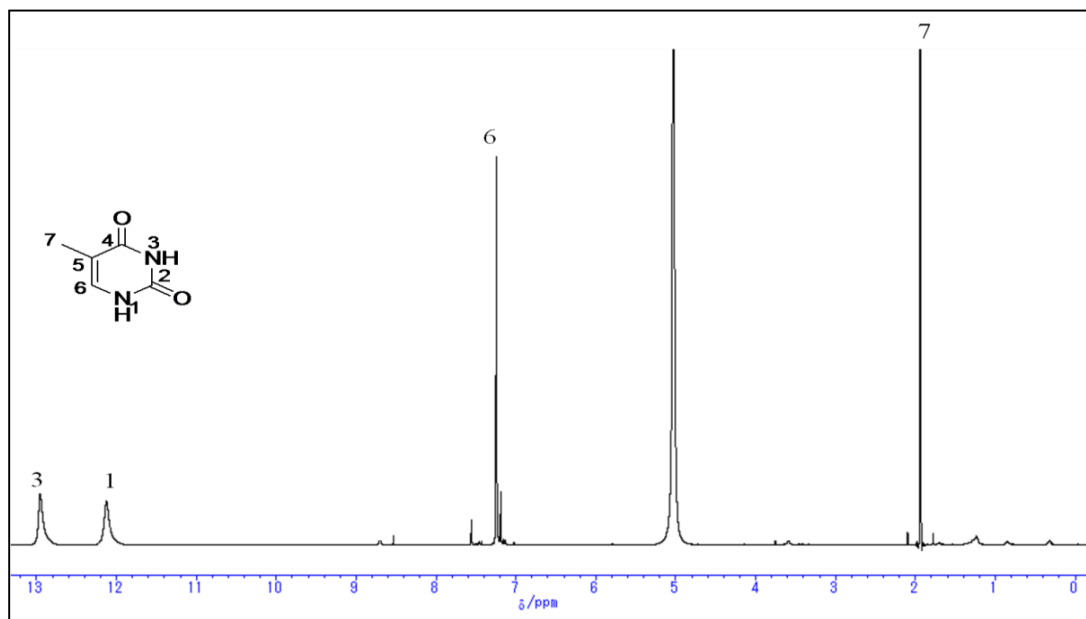


Fig. 2.72. <sup>1</sup>H-NMR Spectrum of compound 20 (400 MHz, C<sub>5</sub>D<sub>5</sub>N).

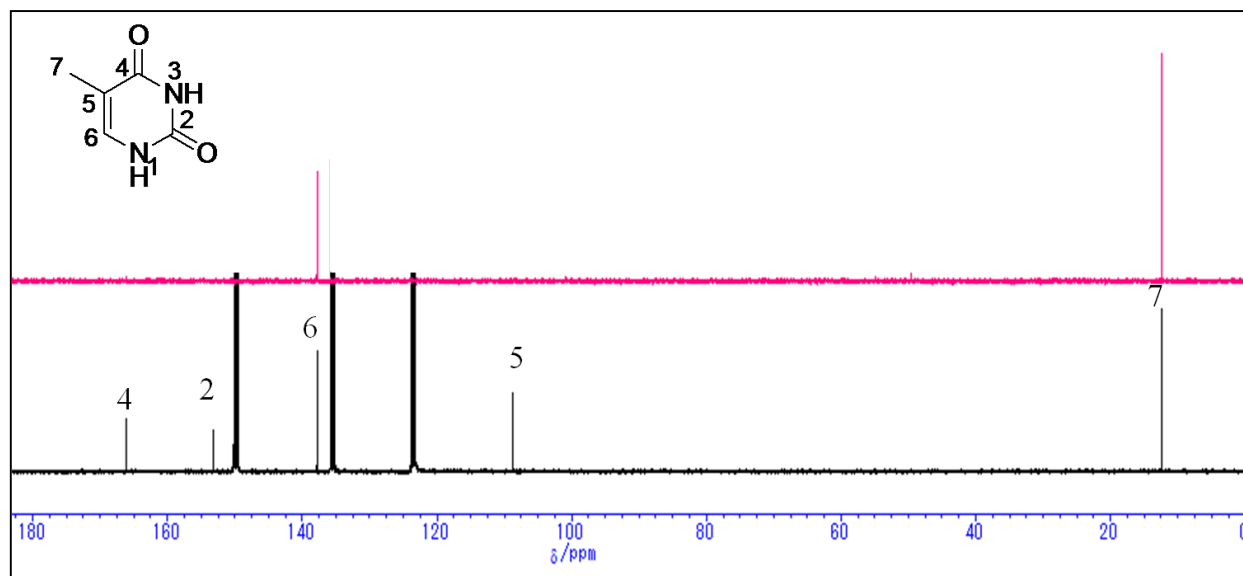


Fig. 2.73. <sup>13</sup>C-NMR Spectrum of compound 20 (100 MHz, C<sub>5</sub>D<sub>5</sub>N).

$^{13}\text{C}$ -NMR (100 MHz) and  $^1\text{H}$ -NMR (400 MHz) data for compound **20** in pyridine-  $d_5$  are listed in **Table 2.10**.

**Table 2.10:**  $^{13}\text{C}$ -NMR (100 MHz) and  $^1\text{H}$ -NMR (400 MHz) spectroscopic data of compound **20** ( $\text{C}_5\text{D}_5\text{N}$ ,  $\delta$  in ppm,  $J$  in Hz).

| No. | $\delta_{\text{C}}$    | $\delta_{\text{H}}$ (No., M, $J_{\text{Hz}}$ ) |
|-----|------------------------|--|
| 1   |                        | 12.12 (1H, brs)                                |
| 2   | 153.2 (C)              |  |
| 3   |                        | 12.95 (1H, brs)                                |
| 4   | 166.1 (C)              |  |
| 5   | 108.7 (C)              |  |
| 6   | 137.8 (CH)             | 7.25 (1H,s)                                    |
| 7   | 12.4 ( $\text{CH}_3$ ) | 1.94 (3H, s)                                   |

## Discussion

Compound **20** was obtained as colorless needles From M-3 fraction of the marine sponge *Mycale euplectellioides*. The structure elucidation of compound **20** began with the analysis of its  $^1\text{H}$ -NMR,  $^{13}\text{C}$ -NMR spectrum and DEPT experiment exhibited the structure of thymine.  $^{13}\text{C}$  NMR spectrum and DEPT experiment showed five carbon signals, which could be attributable to two imides carbonyl [ $\delta_{\text{C}}= 166.17$  ppm. ( $\text{C}_4$ ),  $\delta_{\text{C}}= 153.23$  ppm. ( $\text{C}_2$ )], one quaternary [ $\delta_{\text{C}}= 108.79$  ppm. ( $\text{C}_5$ )], one methine [ $\delta_{\text{C}}= 137.80$  ppm. ( $\text{C}_6$ )], and one methyl [ $\delta_{\text{C}}= 12.46$  ppm. ( $\text{C}_7$ )] carbons. The  $^1\text{H}$ -NMR displayed two exchangeable imido protons at  $\delta_{\text{H}}= 12.95$  (1H, brs, NH-3) and  $\delta_{\text{H}}= 12.12$  (1H, brs, NH-1); one methine proton at  $\delta_{\text{H}}= 7.25$  (1H, s, H-6); one methyl proton at  $\delta_{\text{H}}= 1.94$  (3H, s, H-7).

The molecular formula of compound **20** was deduced as  $\text{C}_5\text{H}_6\text{N}_2\text{O}_2$  based on the NMR spectra and further confirmed by the mass spectra with the appearance of the molecular ion peak at  $m/z$ , 127  $[\text{M}+\text{H}]^+$  in the positive FAB-MS spectra. The structure was identified as 5-methyl uracil by comparison of its NMR data with those in the related literature.<sup>93)</sup>

## Conclusion

From the above data and discussion, the structure of compound **20** was assigned as thymine.

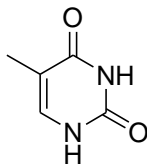


Fig. 2.74. Structure of thymine (**20**).

### 2.2.5. Compound **21**

Compound **21** was isolated as colorless needles from M-3 fraction of the marine sponge *Mycale euplectellioides*.

#### Spectroscopic analysis

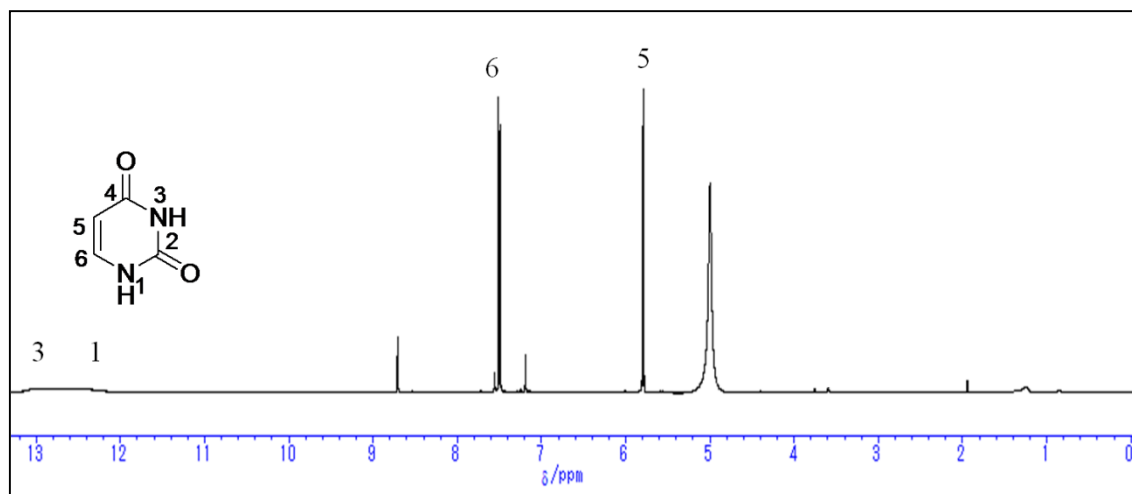


Fig. 2.75. <sup>1</sup>H-NMR Spectrum of compound **21** (400 MHz, C<sub>5</sub>D<sub>5</sub>N).

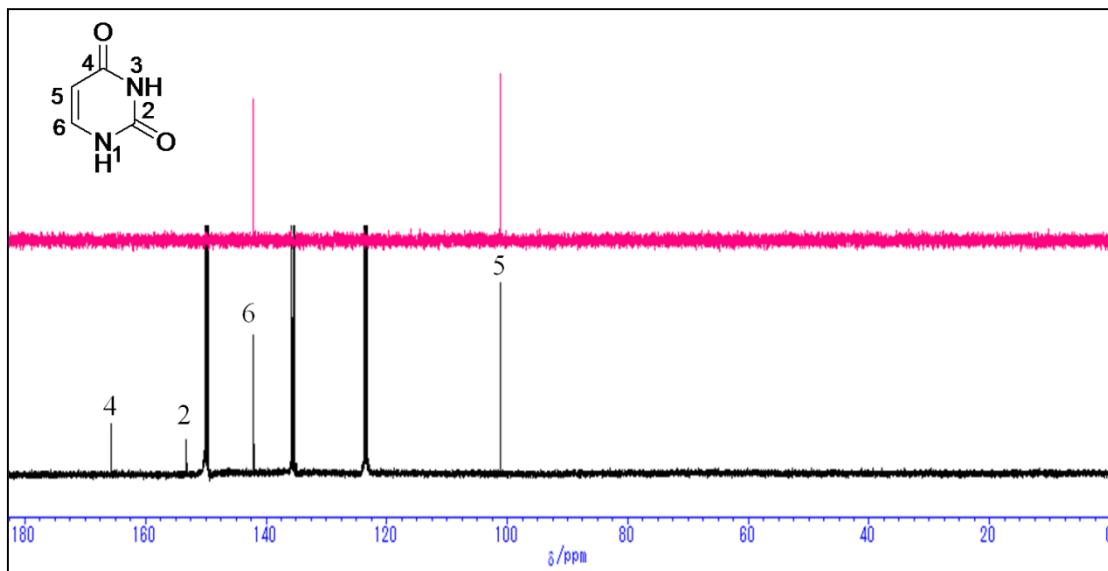


Fig. 2.76.  $^{13}\text{C}$ -NMR Spectrum of compound **21** (100 MHz,  $\text{C}_5\text{D}_5\text{N}$ ).

$^{13}\text{C}$ -NMR (100 MHz) and  $^1\text{H}$ -NMR (400 MHz) data for compound **21** in pyridine- $d_5$  are listed in Table 2.11.

Table 2.11:  $^{13}\text{C}$ -NMR (100 MHz) and  $^1\text{H}$ -NMR (400 MHz) and spectroscopic data of compound **21** ( $\text{C}_5\text{D}_5\text{N}$ ,  $\delta$  in ppm,  $J$  in Hz).

| No. | $\delta_{\text{C}}$ | $\delta_{\text{H}}$ (No., $M$ , $J_{\text{Hz}}$ ) |
|-----|---------------------|---|
| 1   |                     | 12.13 (1H, brs)                                   |
| 2   | 153.1 (C)           |   |
| 3   |                     | 12.96 (1H, brs)                                   |
| 4   | 165.7 (C)           |   |
| 5   | 101.1 (CH)          | 5.79 (1H, d, $J=7.50$ Hz)                         |
| 6   | 142.0 (CH)          | 7.50 (1H, d, $J=7.68$ Hz)                         |

## Discussion

Compound **21** was obtained as colorless needles from the major fraction M-3 of the marine sponge *Mycale euplectellioides*. The structure elucidation of compound **21** began with the analysis of its  $^1\text{H}$ -NMR,  $^{13}\text{C}$ -NMR spectrum and DEPT experiment exhibited the structure of uracil.  $^{13}\text{C}$ -NMR spectrum and DEPT experiment showed four carbon signals, which could be attributable to two imide carbonyl [ $\delta_{\text{C}}= 165.72$  ppm. ( $\text{C}_4$ ),  $\delta_{\text{C}}= 153.19$  ppm. ( $\text{C}_2$ )], and two methine [ $\delta_{\text{C}}= 142.05$  ppm. ( $\text{C}_6$ ),  $\delta_{\text{C}}= 101.19$  ppm. ( $\text{C}_5$ )] carbons. The  $^1\text{H}$ -NMR displayed two

exchangeable imido protons at  $\delta_{\text{H}}= 12.96$  (1H, brs, NH-3) and  $\delta_{\text{H}}= 12.13$  (1H, brs, NH-1); two methine protons coupled together at  $\delta_{\text{H}}= 7.50$  (1H, d,  $J=7.68$  Hz, H-6) and  $\delta_{\text{H}}= 5.79$  (1H, d,  $J=7.50$  Hz, H-5).

The molecular formula of compound **21** was deduced as  $\text{C}_4\text{H}_4\text{N}_2\text{O}_2$  based on the NMR spectra and further confirmed by the mass spectra with the appearance of the molecular ion peak at  $m/z$ , 113  $[\text{M}+\text{H}]^+$  in the positive FAB-MS spectra. The structure was identified as uracil by comparison of its NMR data with those in the related literature.<sup>93)</sup>

### Conclusion:-

From the above data and discussion, the structure of compound **21** was assigned as uracil.

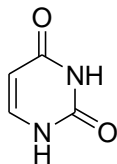


Fig. 2.77. Structure of uracil (21).

### 2.2.6. Compound 22

Compound **22** was isolated as colorless solid from M-3 fraction of the marine sponge *Mycale euplectellioides*.

### Spectroscopic analysis

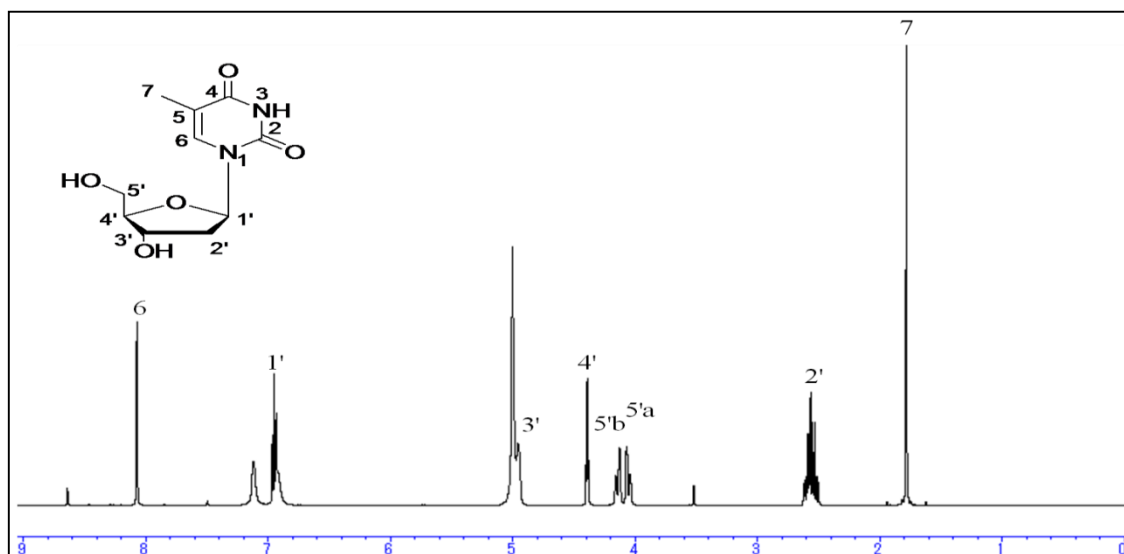


Fig. 2.78.  $^1\text{H-NMR}$  Spectrum of compound **22** (400 MHz,  $\text{C}_5\text{D}_5\text{N}$ ).

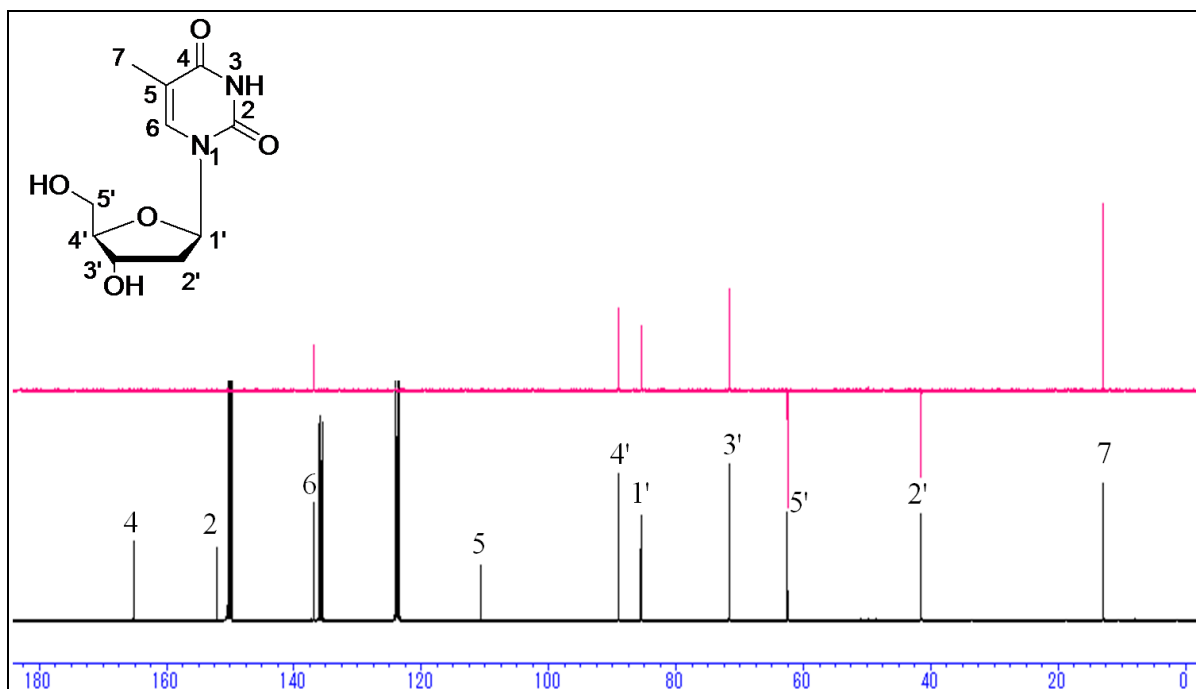


Fig. 2.79.  $^{13}\text{C}$ -NMR Spectrum of compound **22** (100 MHz,  $\text{C}_5\text{D}_5\text{N}$ ).

$^{13}\text{C}$ -NMR (100 MHz) and  $^1\text{H}$ -NMR (400 MHz) data for compound **22** in pyridine- $d_5$  are listed in Table 2.12.

Table 2.12:  $^{13}\text{C}$ -NMR (100 MHz) and  $^1\text{H}$ -NMR (400 MHz) spectroscopic data of compound **22** ( $\text{C}_5\text{D}_5\text{N}$ ,  $\delta$  in ppm,  $J$  in Hz).

| No. | $\delta_{\text{C}}$    | $\delta_{\text{H}}$ (No., $M$ , $J_{\text{Hz}}$ )  |
|-----|------------------------|--|
| 1   |                        |  |
| 2   | 152.1 (C)              |  |
| 3   |                        |  |
| 4   | 165.2 (C)              |  |
| 5   | 110.6 (C)              |  |
| 6   | 136.8 (CH)             | 8.07 (1H, s)   |
| 1'  | 85.5 (CH)              | 6.94 (1H, t, $J=6.32$ Hz)  |
| 2'  | 41.5 ( $\text{CH}_2$ ) | 2.56 (2H, m)   |
| 3'  | 71.6 (CH)              | 4.95 (1H, brs)   |
| 4'  | 89.0 (CH)              | 4.38 (1H, q, $J=2.92$ Hz)  |
| 5'  | 62.5 ( $\text{CH}_2$ ) | 4.05 (1H, dd, $J=12.2$ Hz, $J=2.76$ , H5'a)<br>4.13 (1H, dd, $J=12.2$ Hz, $J=2.36$ , H5'b) |
| CH3 | 12.9 ( $\text{CH}_3$ ) | 1.78 (3H, s)   |

## Discussion

Compound **22** was obtained as a colorless solid from the major fraction M-3 of the marine sponge *Mycale euplectellioides*. The structure elucidation of compound **22** began with the analysis of its  $^1\text{H-NMR}$ ,  $^{13}\text{C-NMR}$  spectrum and DEPT experiment exhibited the structure of 2'-deoxy thymidine. The  $^1\text{H-NMR}$  spectrum showed two signals characteristic for the thymine moiety, an aromatic 1H singlet at  $\delta$  8.07 (H-6), and an up-field singlet of a methyl group at  $\delta$  1.78, probably linked to an  $sp^2$  carbon in an  $\alpha, \beta$ -unsaturated system. Furthermore, the spectrum exhibited a triplet at  $\delta$  6.94 (H-1), signals of two oxygenated methine protons at  $\delta$  4.95 and 3.38 ppm, two proton doublet of doublet each and one multiplet of two methylene groups at  $\delta$  4.05, 4.13 and 2.56 respectively, of which the first one is oxygenated. The  $^{13}\text{C-NMR}$  spectrum and DEPT experiment exhibited 10 carbon signals, which could be attributable to five of which are similar as in thymine as follow, two imides carbonyl [ $\delta_{\text{C}}= 165.20$  ppm. (C<sub>4</sub>),  $\delta_{\text{C}}= 152.15$  ppm. (C<sub>2</sub>)], one quaternary [ $\delta_{\text{C}}= 110.66$  ppm. (C<sub>5</sub>)], one methine [ $\delta_{\text{C}}= 136.89$  ppm. (C<sub>6</sub>)], and one methyl [ $\delta_{\text{C}}= 12.94$  ppm. (C<sub>7</sub>)] carbons. In addition to, five carbon signals, three oxygenated methines [ $\delta_{\text{C}}= 85.53$  ppm. (C<sub>1'</sub>),  $\delta_{\text{C}}= 71.66$  ppm. (C<sub>3'</sub>),  $\delta_{\text{C}}= 89.05$  ppm. (C<sub>4'</sub>)] and two methylene carbons [ $\delta_{\text{C}}= 41.57$  ppm. (C<sub>2'</sub>),  $\delta_{\text{C}}= 62.52$  ppm. (C<sub>5'</sub>)] constituting the 2'-deoxy ribose moiety.

The molecular formula of compound **22** was deduced as  $\text{C}_{10}\text{H}_{14}\text{N}_2\text{O}_5$  based on the NMR spectra and further confirmed by the mass spectra with the appearance of the molecular ion peak at  $m/z$ , 243  $[\text{M}+\text{H}]^+$  in the positive FAB-MS spectra. The structure was identified as 2'-deoxy thymidine by comparison of its NMR data with those in the related literature.<sup>93)</sup>

## Conclusion

From the above data and discussion, the structure of compound (**22**) was assigned as 2'-deoxy thymidine.

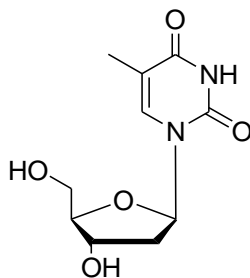


**Fig. 2.80. Structure of deoxy thymidine (22).**

### 2.2.7. Compound 23

Compound **23** was isolated as colorless solid from the major fraction M-3 of the marine animal *Mycale euplectellioides*.

#### Spectroscopic analysis

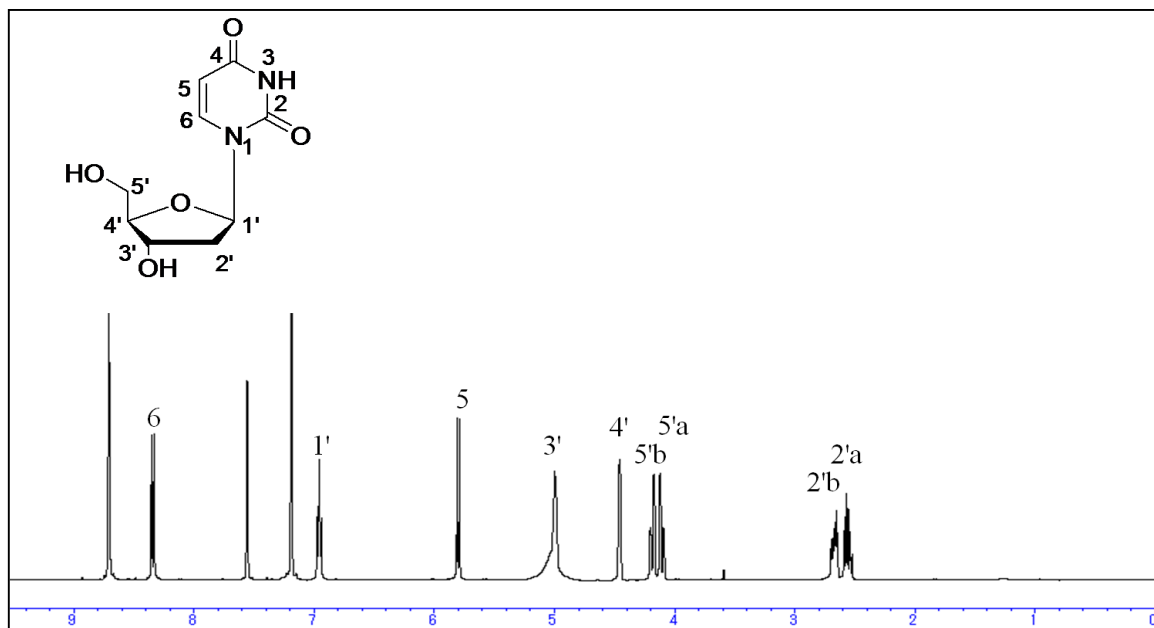


Fig. 2.81. <sup>1</sup>H-NMR spectrum of compound 23 (400 MHz, C<sub>5</sub>D<sub>5</sub>N).

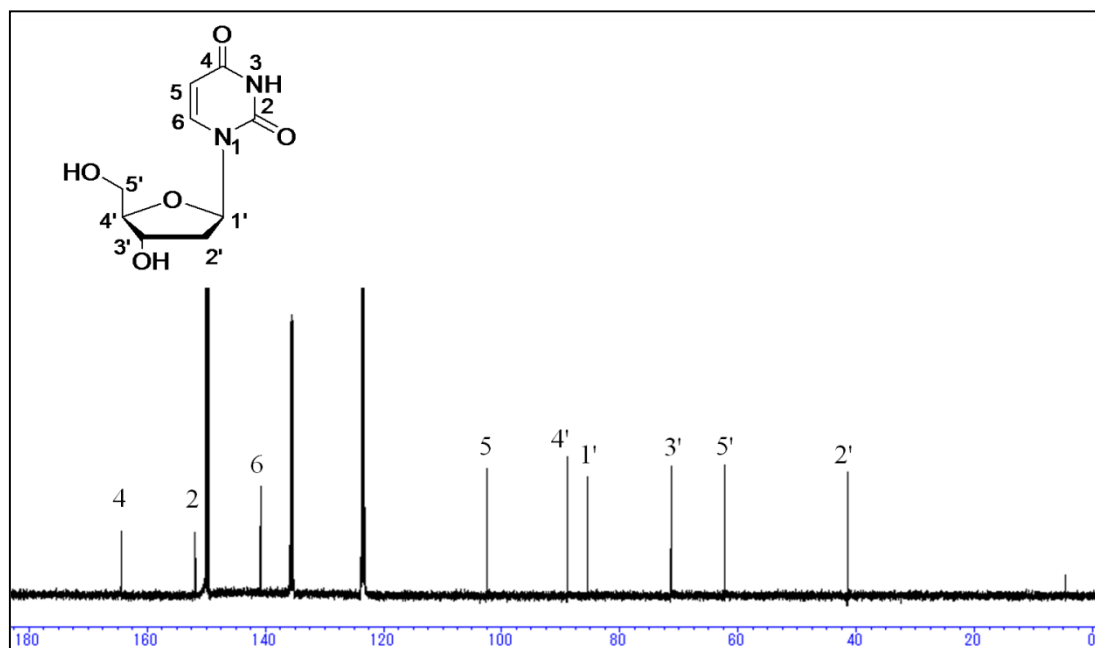


Fig. 2.82. <sup>13</sup>C-NMR Spectrum of compound 23 (100 MHz, C<sub>5</sub>D<sub>5</sub>N).



$^{13}\text{C}$ -NMR (100 MHz) and  $^1\text{H}$ -NMR (400 MHz) data for compound **23** in pyridine-  $d_5$  are listed in **Table 2.13**.

**Table 2.13:**  $^{13}\text{C}$ -NMR (100 MHz) and  $^1\text{H}$ -NMR (400 MHz) spectroscopic data of compound (**23**) ( $\text{C}_5\text{D}_5\text{N}$ ,  $\delta$  in ppm,  $J$  in Hz).

| No. | $\delta_{\text{C}}$    | $\delta_{\text{H}}$ (No., $M$ , $J_{\text{Hz}}$ )  |
|-----|------------------------|--|
| 1   |                        |  |
| 2   | 151.8 (C)              |  |
| 3   |                        |  |
| 4   | 164.4 (C)              |  |
| 5   | 102.4 (CH)             | 5.80 (1H, d, $J=8.2$ Hz )  |
| 6   | 140.8 (CH)             | 8.35 (1H, d, $J=8.3$ Hz )  |
| 1'  | 85.5 (CH)              | 6.96 (1H, t, $J=6.3$ Hz )  |
| 2'  | 41.5 ( $\text{CH}_2$ ) | 2.56 (1H, m, H2'a )<br>2.67 (1H, m, H2'b )   |
| 3'  | 71.3 (CH)              | 4.99 (1H, brs )  |
| 4'  | 88.9 (CH)              | 4.46 (1H, brs)   |
| 5'  | 62.2 ( $\text{CH}_2$ ) | 4.05 (1H, dd, $J=11.7$ Hz, $J=2.4$ , H5'a)<br>4.13 (1H, dd, $J=11.7$ Hz, $J=2.9$ , H5'b) |

## Discussion

Compound **23** was obtained as a colorless solid from M-3 fraction of the marine sponge *Mycale euplectellioides*. The structure elucidation of compound **23** began with the analysis of its  $^1\text{H}$ -NMR and  $^{13}\text{C}$ -NMR spectrum exhibited the structure of 2'-deoxy uridine. The  $^1\text{H}$ -NMR spectrum showed two signals characteristic for the uracil moiety, an aromatic 1H doublet at  $\delta$  5.80 (H-5) and an aromatic 1H doublet at  $\delta$  8.35 (H-6). Furthermore, the spectrum exhibited a triplet at  $\delta$  6.96 (H-1'), signals of two oxygenated methine protons at  $\delta$  4.99 and 4.46 ppm, two protons doublet of doublet at  $\delta$  4.10, 4.18 each and two protons multiplet at  $\delta$  2.56, 2.67 each of two methylene groups respectively, of which the first one is oxygenated. The  $^{13}\text{C}$ -NMR spectrum exhibited 9 carbon signals, which could be attributable to five of which are similar as in uracil as follow, two imides carbonyl [ $\delta_{\text{C}}= 164.43$  ppm. ( $\text{C}_4$ ),  $\delta_{\text{C}}= 151.85$  ppm. ( $\text{C}_2$ )], two methines [ $\delta_{\text{C}}= 102.46$  ppm. ( $\text{C}_5$ ),  $\delta_{\text{C}}= 140.82$  ppm. ( $\text{C}_6$ )] carbons. In addition to, five carbon signals, three oxygenated methines [ $\delta_{\text{C}}= 85.53$  ppm. ( $\text{C}_1$ ),  $\delta_{\text{C}}= 71.36$  ppm. ( $\text{C}_3$ ),  $\delta_{\text{C}}= 89.93$  ppm. ( $\text{C}_4$ )] and two methylene carbons [ $\delta_{\text{C}}= 41.50$  ppm. ( $\text{C}_2$ ),  $\delta_{\text{C}}= 62.21$  ppm. ( $\text{C}_5$ )] constituting the 2'-deoxy ribose moiety.

The structure of compound **23** was identified as 2'-deoxy uridine by comparison of its NMR data with those in the related literature.<sup>93)</sup>

### Conclusion

From the above data and discussion, the structure of compound **23** was assigned as 2'-deoxy uridine.

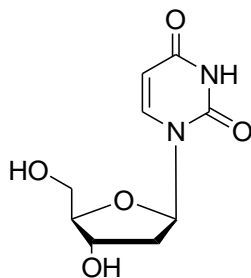
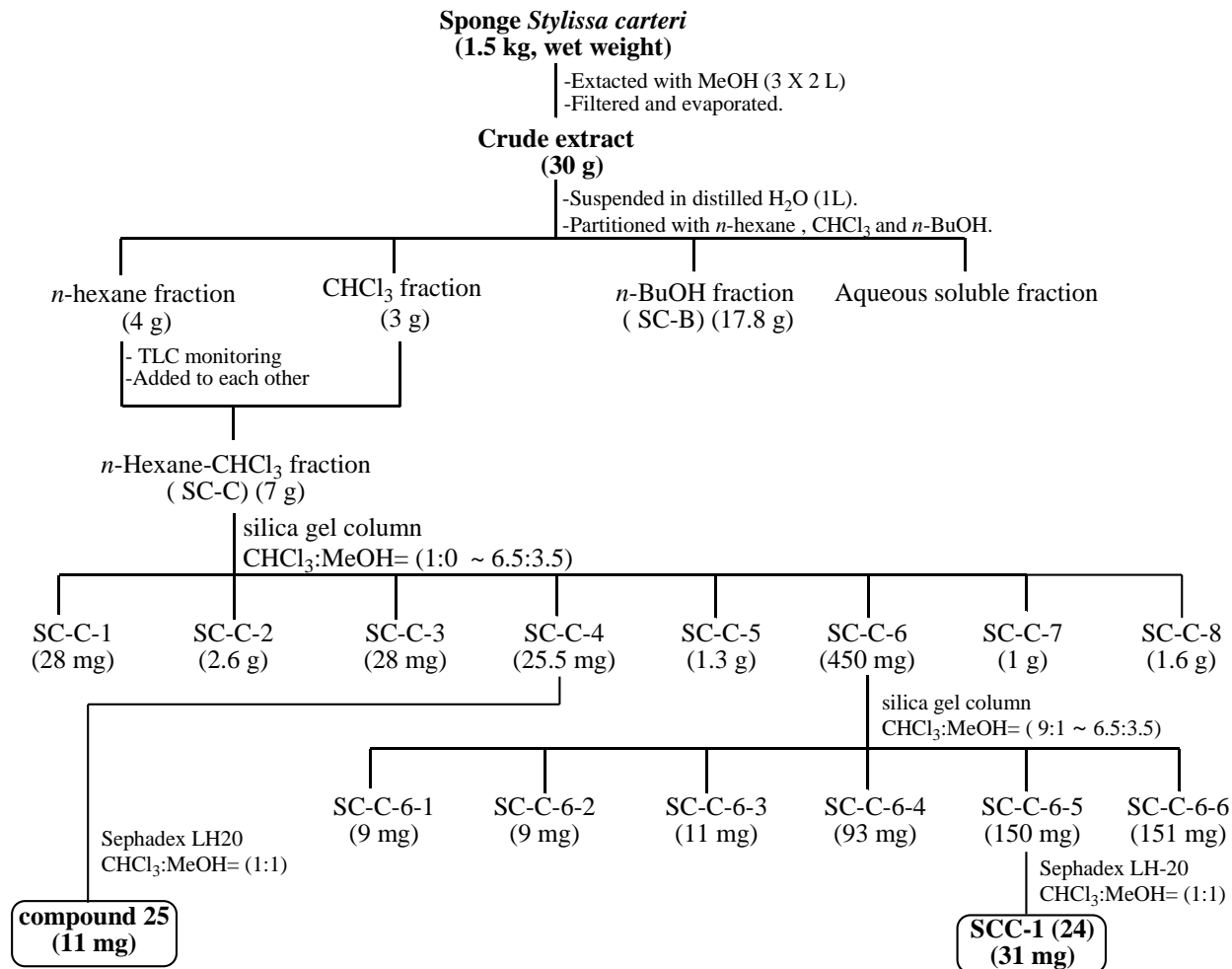


Fig. 2.83. Structure of deoxy uridine (**23**).

### 2.3. Secondary metabolites isolated from *Stylissa carteri*

In our quest to augment the efforts of providing chemical profiles of some Red Sea marine organisms. The methanolic extract of the Red Sea sponge *Stylissa carteri* was subjected to liquid liquid partition technique between different organic solvent including *n*-hexane, chloroform and *n*-butanol. According to TLC monitoring, the *n*-hexane soluble fraction and the chloroform soluble fraction were combined together. Chemical investigation of the *n*-hexane-chloroform fraction led to isolation of glycosphingogpids possessing  $\alpha$  galactosyl ceramide structure (**24**) along with the bromopyrrole alkaloid, 2-bromo aldisine (**25**). the galactosyl ceramide molecular species is being reported for the first time in this genus. The isolated compounds were clarified on the basis of chemical methods, spectroscopic techniques (IR, NMR experiments and mass spectrometry) in addition to, the comparison with appropriate literature data.

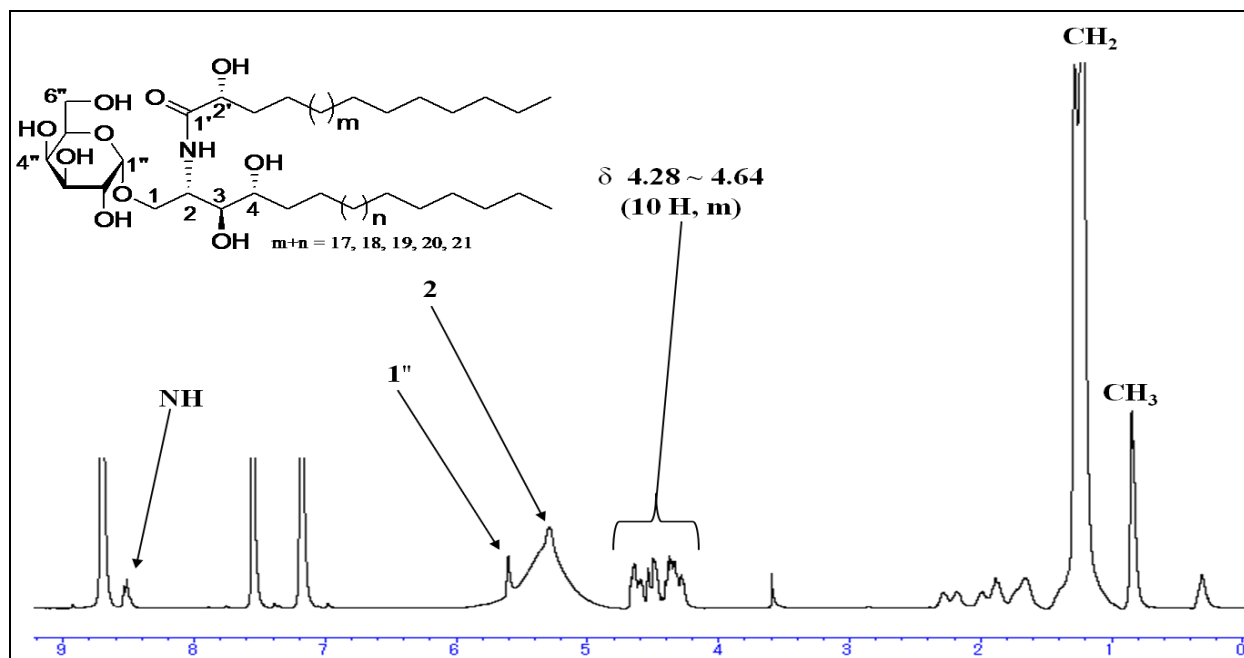
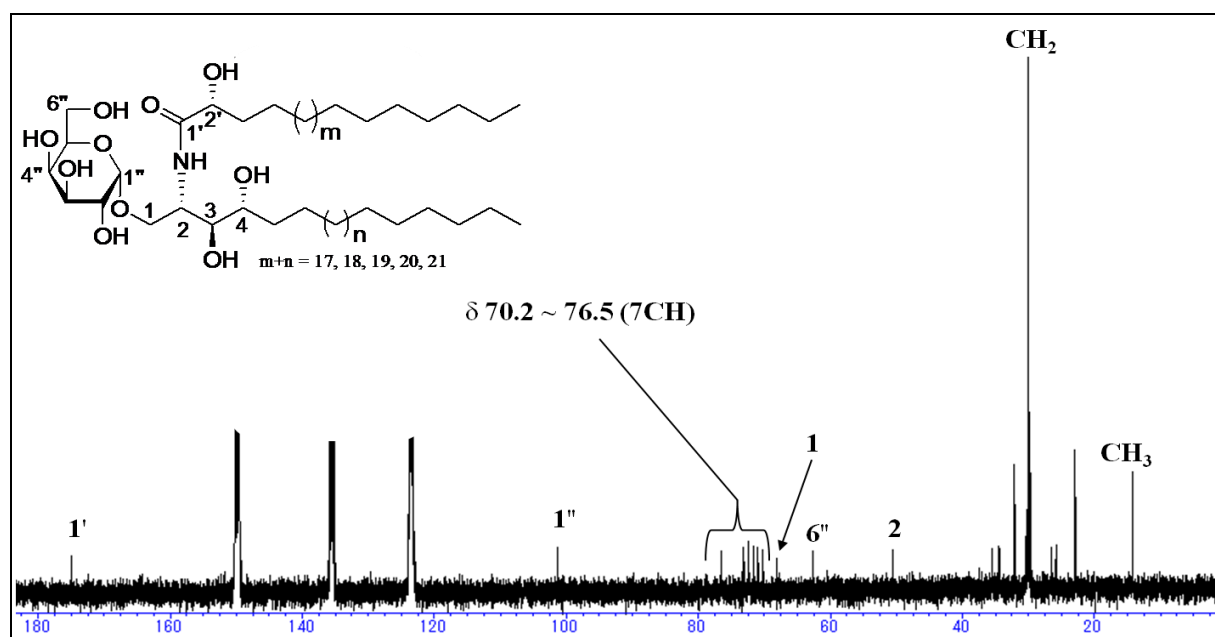


**Fig. 2.84. Extraction and isolation scheme from *Stylissa carteri***

### 2.3.1. Compound 24

SCC-1 (31.0 mg) was obtained as a white amorphous solid, showing a single spot on silica gel thin layer chromatography (TLC).

## Spectroscopic analysis

Fig. 2.85.  $^1\text{H-NMR}$  spectrum of SCC-1 (400 MHz,  $\text{C}_5\text{D}_5\text{N}$ )Fig. 2.86.  $^{13}\text{C-NMR}$  spectra of SCC-1 (400 MHz,  $\text{C}_5\text{D}_5\text{N}$ )

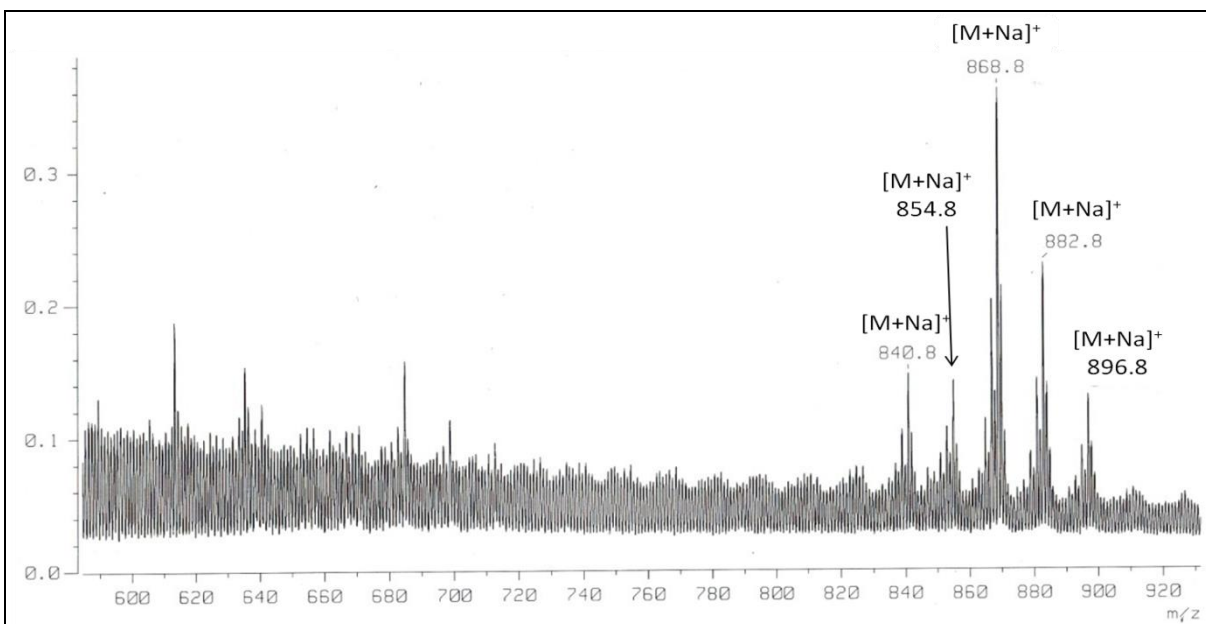


**Fig. 2.87. FAB-MS (positive ion mode) of SCC-1**

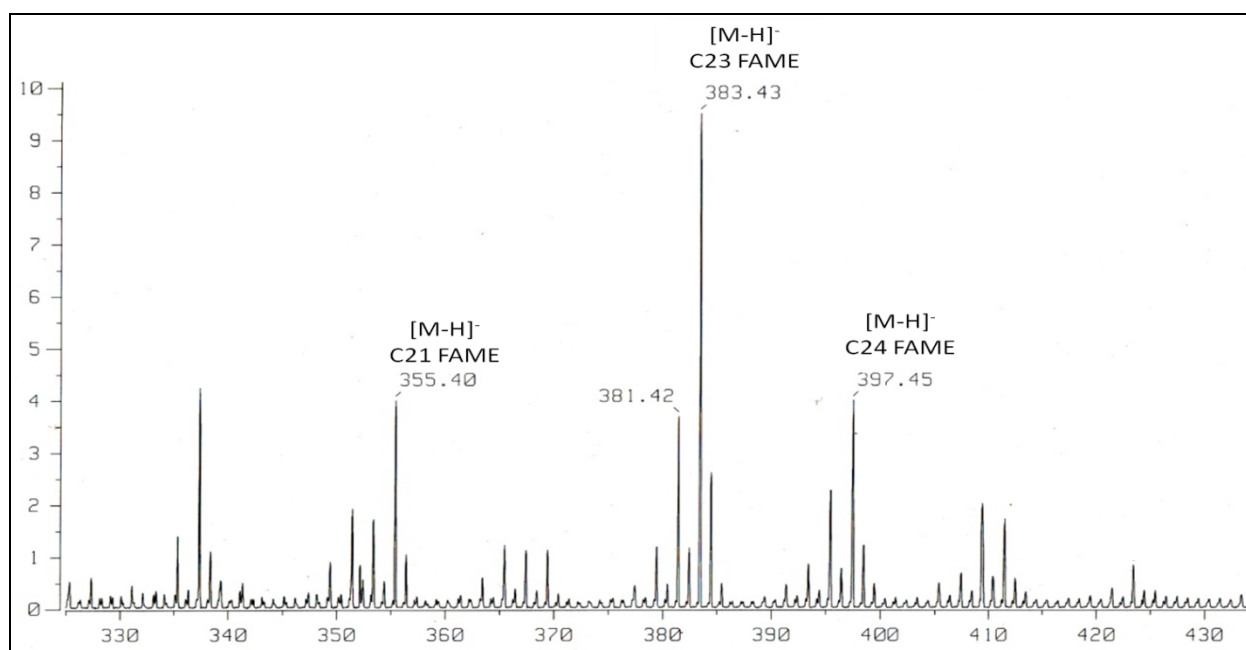


**Fig. 2.88. FAB-MS of FAMES after hydrolysis of SCC-1**

$^{13}\text{C}$ -NMR (100 MHz) and  $^1\text{H}$ -NMR (400 MHz) data for SCC-1 in  $\text{C}_5\text{D}_5\text{N}$  are listed in **Table 4.1**.

**Table 2.14:**  $^{13}\text{C}$ -NMR (100 MHz) and  $^1\text{H}$ -NMR (400 MHz) spectroscopic data of SCC-1 (24) ( $\text{C}_5\text{D}_5\text{N}$ ,  $\delta$  in ppm,  $J$  in Hz).

| No.              | SCC-1               |   |
|------------------|---------------------|---|
|                  | $\delta_{\text{C}}$ | $\delta_{\text{H}}$ (No., $M$ , $J_{\text{Hz}}$ ) |
| NH               |                     | 8.53 (1H, d, $J=9.2$ Hz)                          |
| 1a               | 68.2 (t)            | 4.32 (1H, m)                                      |
| 1b               |                     | 4.59 (1H, m)                                      |
| 2                | 50.4 (d)            | 5.29 (1H, m)                                      |
| 3                | 76.5 (d)            | 4.39 (1H, m)                                      |
| 4                | 72.3 (d)            | 4.28 (1H, m)                                      |
| 1'               | 175.0 (s)           |   |
| 2'               | 72.4 (d)            | 4.63 (1H, m)                                      |
| -CH <sub>3</sub> | 14.2 (q)            | 0.85 (m)  |
| 1''              | 101.2 (d)           | 5.61 (1H, d, $J=3.4$ Hz)                          |
| 2''              | 70.2 (d)            | 4.64 (1H, m)                                      |
| 3''              | 71.6 (d)            | 4.50 (1H, m)                                      |
| 4''              | 71.0 (d)            | 4.54 (1H, m)                                      |
| 5''              | 73.1 (d)            | 4.50 (1H, m)                                      |
| 6''              | 62.6 (d)            | 4.33 (2H, m)                                      |

## Discussion

SCC-1 was obtained as a white amorphous powder from the major subfraction SC-C-6. The  $^1\text{H}$ -NMR spectrum in  $\text{C}_5\text{D}_5\text{N}$  showed resonances of an amide proton doublet at  $\delta_{\text{H}}$  8.48 (1H, d,  $J=9.2$  Hz), protons of a long methylene chain centered at  $\delta_{\text{H}}$  1.25, and overlapped methyls at  $\delta_{\text{H}}$  0.85 indicating sphingolipid skeleton. The characteristic resonance of 2-amino-1,3,4,2'-tetrol of the hydrocarbon chain was observed at  $\delta_{\text{H}}$  5.29 (1H, m, H-2), 4.63 (1H, m, H-2'), 4.32 (1H, m, H-1b), 4.59 (1H, m, H-1a), 4.39 (1H, m, H-3), 4.28 (1H, m, H-4) in the  $^1\text{H}$ -NMR spectrum and at  $\delta_{\text{C}}$  50.4 (C-2), 72.4 (C-2'), 68.2 (C-1), 76.5 (C-3), 72.3 (C-4) in the  $^{13}\text{C}$ -NMR spectrum. Also, the  $^{13}\text{C}$ -NMR spectrum showed the presence of an anomeric carbon  $\delta_{\text{C}}$  101.2 along with the characteristic signals at  $\delta_{\text{C}}$  70.2, 71.6, 71.0, 73.1, 62.6 indicated the presence of a sugar moiety. In addition to amide carbonyl at  $\delta_{\text{C}}$  175.0 (C-1'), A series of molecular ion peaks due to  $[\text{M}+\text{Na}]^+$  were observed in the positive ion FAB-MS spectrum at  $m/z$ : 840.8, 854.8, 868.8, 882.8, 896.8. Therefore, SCC-1 is presumed to be a molecular species of a phytosphingosine-type

cerebroside possessing 2- hydroxy fatty acid groups.<sup>94,95)</sup> Furthermore, SCC-1 is suggested to have normal terminal methyls,<sup>73)</sup> since the carbon signals for the terminal methyl groups were observed at  $\delta_c$  14.2 (normal type), with the absence of the characteristic signals at 22.4 (iso type), 11.3 and 19.1 (*ante*- iso type) in the  $^{13}\text{C}$ -NMR spectrum (Fig.2.86, Table 2.14).<sup>96)</sup> The structure of SCC-1 was characterized by comparison of its  $^{13}\text{C}$ -NMR spectral data with that of known cerebroside.<sup>95)</sup> Acid hydrolysis of SCC-1 followed by analysis of the its methylated sugar against standard sugars (glucose and galactose) using HPLC indicated that the sugar moiety was galactose. The  $^1\text{H}$ -NMR signal at  $\delta_H$  5.61 (d,  $J = 3.4$  Hz) clearly pointed that the galactose had an  $\alpha$ -linkage.<sup>94)</sup> The relative stereo chemistry of the cerebroside molecular species is suggested to be (2*S*, 3*S*, 4*R*, 2'*R*), since the aforementioned  $^1\text{H}$ -NMR (H-2, H-3, H-4, H-2') and  $^{13}\text{C}$ -NMR signals (C-1, C-2, C-3, C-4, C-2') were in good agreement with those of phytosphingosine-type cerebroside molecular species possessing (2*S*, 3*S*, 4*R*, 2'*R*) configurations.<sup>97)</sup> Based on the results of SCC-1 methanolysis with methanolic hydrochloric acid followed by FAB-MS analysis, the length of the fatty acids could be determined. The *n*-hexane layer afforded a mixture of fatty acid methyl esters (FAMES), which were subjected to FAB-MS analysis. FAB-MS analysis of the FAMES mixture showed the presence of three components at  $m/z$ : 355, 383 and 397 in the negative mode, which were characterized as FAM-1, FAM-2 and FAM-3 indicating C-21, C-23 and C-24 fatty acid methyl esters, respectively. In order to determine the absolute configuration of the sugar moiety, SCC-1 was hydrolyzed by heating in 0.5 M HCl and neutralized with amberlite IRA400. After drying in vacuum, the residue was dissolved in pyridine and derivatized by heating with L-cysteine methyl ester in pyridine at 60 °C for 60 min, and then *o*-tolyl iso thiocyanate was added to the reaction mixture and further reacted at 60 °C for 60 min. Then, the reaction mixture was directly analyzed by standard C<sub>18</sub> HPLC and detected by a UV detector (at 250 nm). Direct HPLC analysis of the reaction mixture exhibited peaks at 18.6 min, which were coincided with derivatives of D-galactose, confirming the absolute configuration of the sugar moiety.<sup>98)</sup>

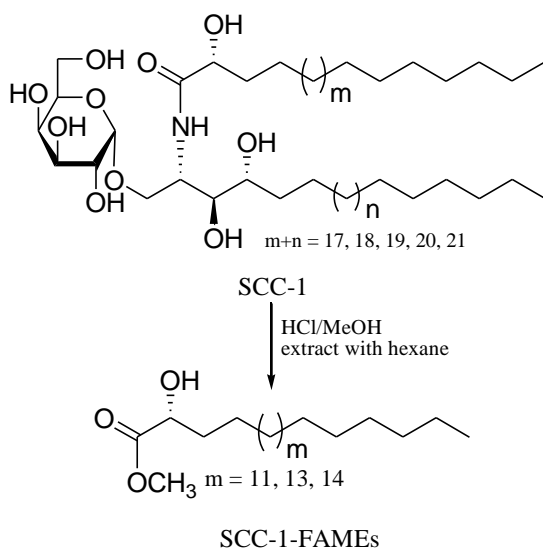


**Fig. 2.89. Structure of SCC-1 and FAMES.**

Isolation and structure elucidation of the cerebroside components in the molecular species SCC-1 still required in our future plan.

### Conclusion

From the above data and discussion, the structure of SCC-1 was found to be a molecular species of phytocerebroside as shown in Fig. 2.90.

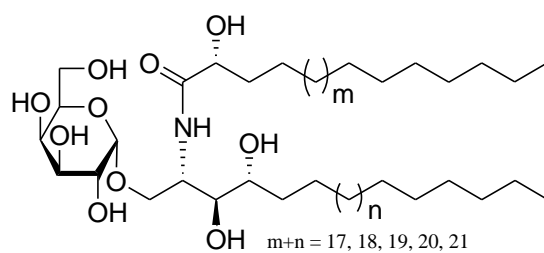


**Fig. 2.90. Structure of SCC-1 (24).**



### 2.3.2. Compound 25

Compound **25** was isolated as a white amorphous powder from the major fraction SC-C-4 of the marine sponge *Stylissa carteri*.

#### Spectroscopic analysis

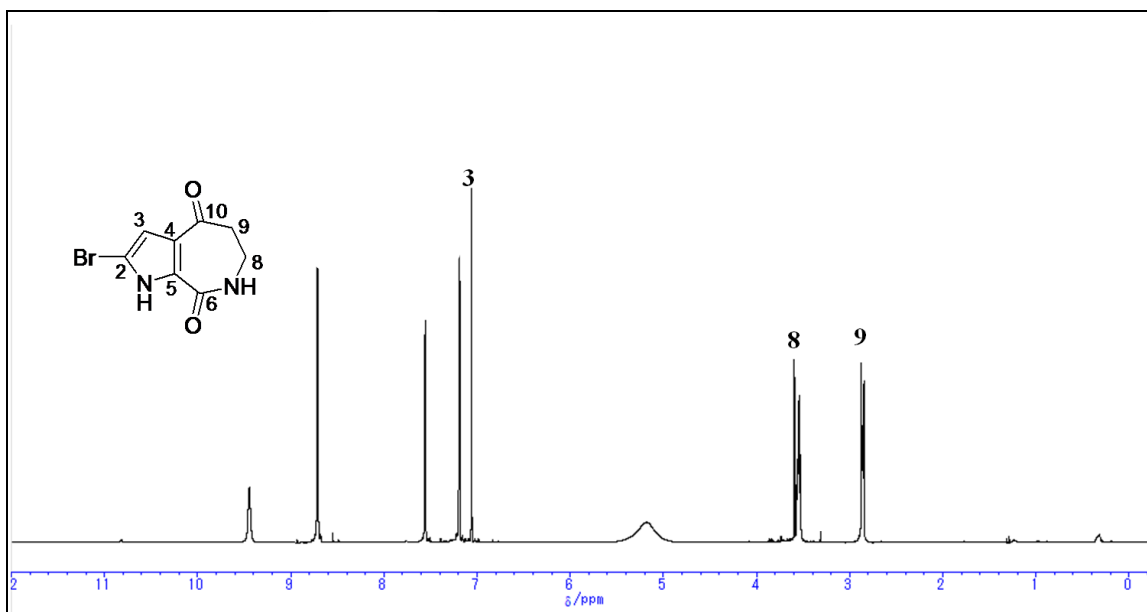


Fig. 2.91. <sup>1</sup>H-NMR spectrum of compound **25** (400 MHz, CDCl<sub>3</sub>).

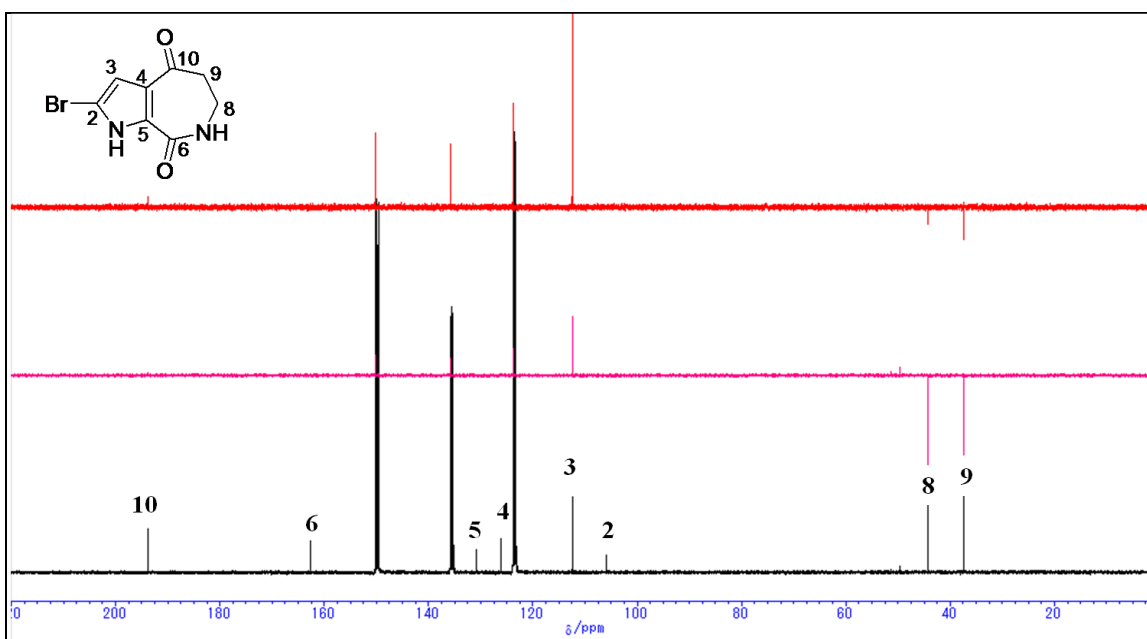


Fig. 2.92. <sup>13</sup>C-NMR spectrum of compound **25** (100 MHz, CDCl<sub>3</sub>).

**Table 2.15:**  $^{13}\text{C}$ -NMR (100 MHz) and  $^1\text{H}$ -NMR (400 MHz) spectroscopic data of compound **25** ( $\text{CDCl}_3$ ,  $\delta$  in ppm,  $J$  in Hz).

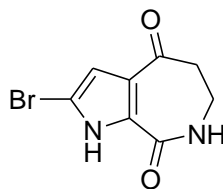
| No. | $\delta_{\text{C}}$    | $\delta_{\text{H}}$ (No., $M$ , $J_{\text{Hz}}$ ) |
|-----|------------------------|---|
| 1   |                        |   |
| 2   | 105.09 (C)             |   |
| 3   | 112.4 (CH)             | 7.08 (1H, s)                                      |
| 4   | 126.0 (C)              |   |
| 5   | 130.0 (C)              |   |
| 6   | 162.7 (C)              |   |
| 7   |                        |   |
| 8   | 44.2 ( $\text{CH}_2$ ) | 3.55 (1H, m)                                      |
| 9   | 37.3 ( $\text{CH}_2$ ) | 2.84 (1H, m)                                      |
| 10  | 193.7 (C)              |   |

### Discussion

Compound **25** was isolated as a white powder. Compound **25** showed  $[\text{M}+\text{H}]^+$  a molecular ion peaks at  $m/z$  243 and 245 in its FAB-MS spectra which indicated the presence of one bromine substituent in the molecule. The  $^1\text{H}$ -NMR spectrum of compound **25** (Fig. 2.91) exhibited two methylene proton signals at  $\delta_{\text{H}}$  2.84 ( $\text{H}_2$ -9) and at  $\delta_{\text{H}}$  3.55 ( $\text{H}_2$ -8) together with a methine proton in the aromatic region at  $\delta_{\text{H}}$  7.08 as found in a pyrrole ring. The  $^{13}\text{C}$ -NMR spectrum (Fig. 2.92) exhibited two methylenes were at  $\delta_{\text{C}}$  37.3 (t,  $\text{C}_9$ ) and 44.2 (t,  $\text{C}_8$ ), one methine was at  $\delta_{\text{C}}$  112.4 (d,  $\text{C}_3$ ), five quaternary carbons at 105.9 (s,  $\text{C}_2$ ), 126.0 (s,  $\text{C}_4$ ), 193.7 (s,  $\text{C}_{10}$ ), 162.7 (s,  $\text{C}_6$ ) and 130.0 (s,  $\text{C}_5$ ). Based on the FAB-MS,  $^1\text{H}$ -NMR and  $^{13}\text{C}$ -NMR data and in comparison with a reference data. Compound **25** was found to be matched with 2-bromoaldisine.<sup>99)</sup>

### Conclusion

From the above data and discussion the structure of compound **25** was assigned as 2-bromoaldisine.

**Fig. 2.93.** Structure of 2-bromoaldisine (**25**).

### 3. Biological activity

#### 3.1. Acetylcholine esterase inhibitory activity (AChEI-assay) of the marine sponge *Mycale euplectelloides*

Neuroprotection of MEC-1 was evaluated using Ellman's assay to investigate its ability to inhibit AChE enzyme which is responsible for the degradation and hydrolysis of the neurotransmitter; acetylcholine. The results showed that MEC-1 could inhibit AChE enzyme with  $IC_{50} = 20.9 \pm 2.4 \mu\text{M}$  (Table 3.1).

**Table 3.1. *In vitro* microplate assay for AChE activity of the marine sponge *M. euplectelloides***

| Compound    | AChE inhibition, $IC_{50}$ ( $\mu\text{M}$ ) |
|-------------|--|
| MEC-1       | 20.9   |
| Galantamine | 1.7  |

#### 3.2. Determination of potential inhibitory activity of MEC-1 against AChE by molecular docking

A powerful approach to anticipate the coupling of a substrate with its receptor is docking simulation, which is effectively executed in numerous applications. Nowadays, the coupling of computational, chemical, and biological technique was extensively grown in order to streamline drug design, discovery, and development.<sup>100</sup> Computer-based molecular docking simulation could save the effort, time, and resources required by traditional drug development methodology. In this study, the potential inhibitory activity of ceramides against AChE was determined by molecular simulation using glide docking.

AChE is a serine protease, catalyzes the hydrolysis of the neurotransmitter acetylcholine (ACh) in neuromuscular junctions and cholinergic brain synapses. Inhibiting the activities of cholinesterases increases the level of ACh in the brain, which affects the cognitive capacity positively. AChE has an overall ellipsoid shape containing a deep groove, usually called the gorge, which is about 20 Å deep. Although the hydrolysis process occurs in the base of the gorge, initial binding of ACh is thought to occur at its outer rim in a region called the peripheral site. At the bottom of the gorge, where the actual hydrolysis occurs, there are four main subsites, these

being the esteratic site, the oxyanion hole, the anionic subsite and the acyl pocket. The esteratic site contains the catalytic machinery of the enzyme, which is dependent on a catalytic triad of Ser200–His440–Glu327. Catalytic triad enhances the nucleophilicity of the catalytic serine to attack on the substrate while Glu stabilizes the histidinium cation of the transition state. The oxyanion hole consists of Gly118, Gly119 and Ala201, which stabilize the tetrahedral intermediate of Ach. The anionic subsite (hydrophobic subsite) is largely comprised of aromatic residues that contain Trp84, Phe330 and Glu199, which are believed to bind to quaternary ammonium ligands by p-cation interactions. Trp84 is an important residue for binding ACh. Mutation of Trp84 by an aliphatic residue results in a severe decrease in reactivity toward Ach. The acyl pocket consists of Phe288 and Phe290, which are assumed to play a role in limiting the dimension of substrates which are able to enter the active site.<sup>101)</sup>

Our docking study was shown that AChE can accommodate ceramides clearly within aromatic gorge giving it the opportunity to interact with peripheral anionic and quaternary ammonium binding site (Fig.3.1). Ceramides structure is more or less similar to some aliphatic bis-quaternary ammonium containing inhibitors like decamethonium. The skeleton simplicity of ceramides gave them the ability to penetrate till catalytic triad of AChE compared to donepezil (Fig.3.2). The orientation of Phe 330 can control the access to the bottom of gorge and there are three major conformations, open, close, and intermediate were identified. The closed conformation was identified for enzyme complex with huperzine A, and intermediate was recognized for tacrine. While Phe 330 was adopting an open access position for gorge-spanning ligands such as donepezil and decamethonium.<sup>102)</sup> Due to the size and shape of ceramides, a gorge spanning binding mode was selected for molecular docking simulation. Therefore, a known X-rays AchE-E2020 (donepezil) complex was nominated as template for our docking study.

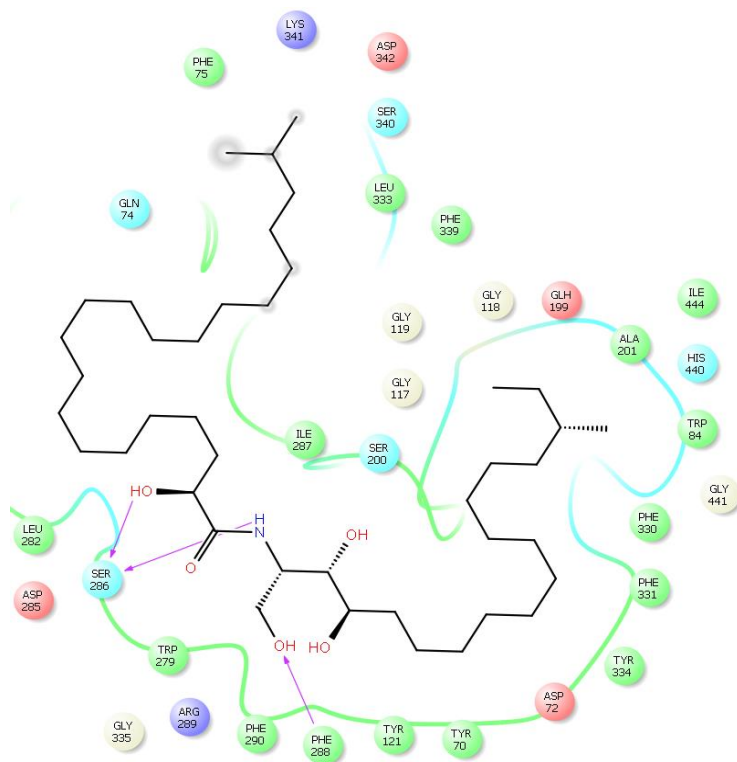


**Fig.3.1. Glide XP docked structure of ceramide with active site of AChE highlighting the hydrophobic interaction of ceramide with PAS and deeply penetration to esterating site.**

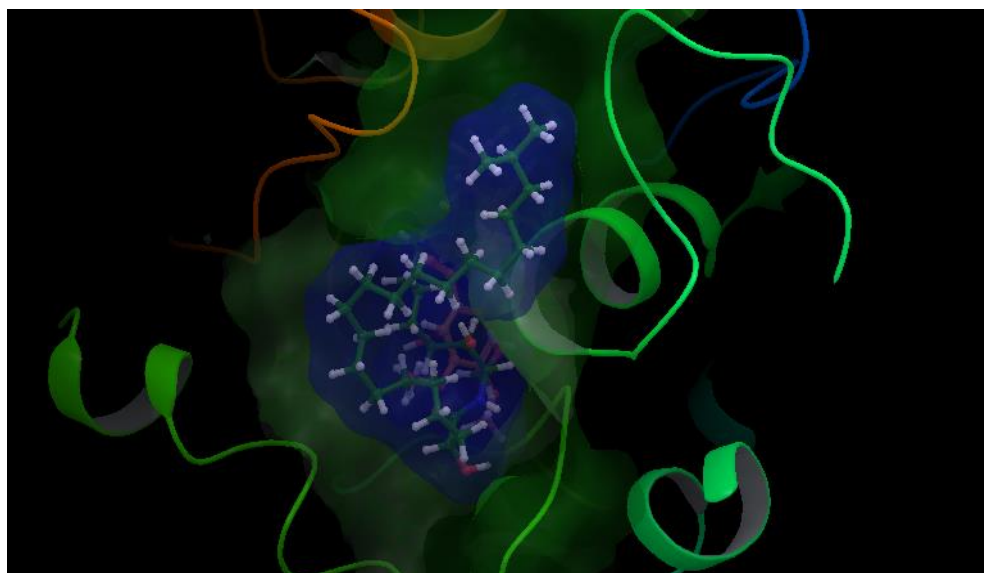


**Fig.3.2. Superimposition of ceramides (green colour) and donepezil (red colour) with AChE (PDBID:1EVE) generated by glide docking**

The potential inhibitory activity of ceramides towards AChE was carried out on *TcAChE*, obtained from the electric eel *Torpedo californica*. The structure similarity of *TcAChE* to mammalian AChE makes it the most popular enzyme applied for *in vitro* and molecular docking study and consequently it was used in our study.<sup>101)</sup> *TcAChE*-coupled donepezil was utilized for protein preparation and glide preparation, then our target compounds were prepared *via* ligand preparation before glide docking. Although normal, iso, and *ante*-iso forms of MEC-1 phytoceramides are difficult to be separated at this stage, the molecular docking study of all were performed. The docking protocol was repeated several times and the best docking pose with lowest energy was selected. The results of each docking protocol were identical to other repeating protocols; meaning that the high reproducibility of glide docking methodology.

Ceramides interact with AChE *via* hydrogen bonding, hydrophobic contacts, and hydrophilic-hydrophobic interactions. Hydroxyl proton of sphingosine moiety can form hydrogen bond (2.51 Å) with amide group of Phe288 and hydroxyl proton of fatty acid moiety and amide proton of sphingosine form hydrogen bond (1.95 Å) and (2.2 Å), respectively with amide group of Ser286 (Fig.3.3). These hydrogen bonds might participate in stabilization of ceramides-*TcAChE* complex. Ceramides can occupy aromatic gorge of AChE forming multiple-binding sites. They interact with PAS residues Tyr70, Tyr121, Trp279, and Tyr334 and oxyanion hole residue Phe330 *via* hydrophobic contacts. The binding to PAS residue seem to play a vital role in the tight binding and energetic stabilization of ceramides within AChE. The carboxylate group of Asp72 and Gln74 also form hydrophilic-hydrophobic interaction with methylene group of fatty acid and sphingosine moieties. These interaction forces help the tight contact of ceramides to AChE. Extra precision glide docking of ceramides to AChE showed reasonable G score or docking score of (-9.688) and glide Emodel of (-70.083 kcal mol<sup>-1</sup>) compared to donepezil that gave docking score of (-10.404) and glide Emodel of (-63.869 kcal mol<sup>-1</sup>). Under identical docking methodology, decamethonium showed glide score of (-9.349) and glide Emodel of (-23.409 kcal mol<sup>-1</sup>). Moreover, the suggested docking study was compared to juliflorine, a potent natural PAS inhibitor of AChE which showed docking score of (-9.015) and glide Emodel of (-71.588).<sup>103)</sup> Under our docking experimental condition normal ceramides showed better binding comparing to iso and *ante*-iso ceramides. Additionally, the length of methylene chain of both fatty acid and sphingosine moieties could affect molecular docking score. This result is agreed with the previous publications,<sup>104-106)</sup> which claimed that the

ceramides' structure could strangely affect their biological activities. C6-dehydroceramide, unsaturated sphingosine base, could induce A $\beta$ -aggregation while the dihydroceramides, like our studied molecules, lacked this role. Our docking study confirmed that by comparing the docking score of saturated and unsaturated molecules and found that unsaturated molecules showed weak docking score, (-5593). The low value of docking score might attribute to 4-5 *trans* double bond which restricts the rotation of long chain and makes the molecules more rigid to be fit into receptor.

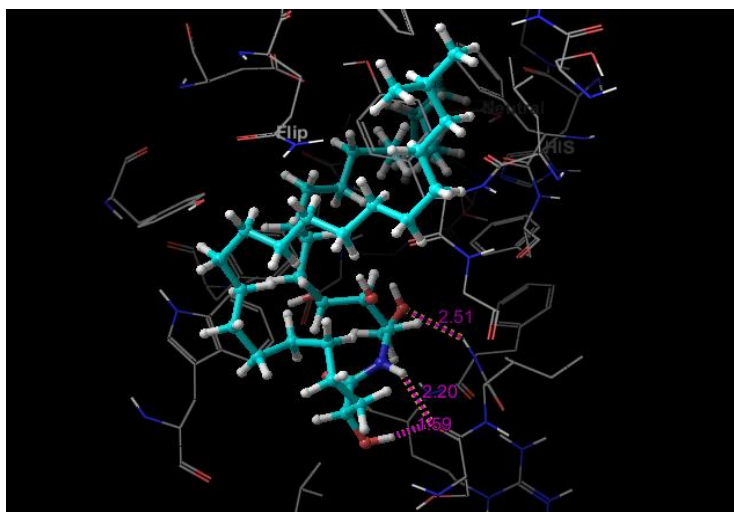


**Fig.3.3. Hydrogen bond interaction between ceramide and AChE (PDBID: 1EVE)**

A major observation is that all ceramides are potentially able to bind inside catalytic triad gorge, however whole molecule is not capable of interacting with amino acids residue of enzyme (fig.3.35). This observation might be attributed to the size problem, which reduces the inhibitory activity compared to other AChEI. Our target compounds lack the reactivity with Trp 84 at gorge bottom as in case of donepezil. Moreover, ceramides lack quaternary ammonium group, which plays a key role in binding of AChEI like donepezil, tacrine, and huperzine A to enzyme. Moreover, we utilized MEC-1, which contains mixture of ceramides; some of them showed good biological activity and other showed weak activity. Although the docking study showed good docking score of ceramides compared to known AChEIs, the *in vitro* assay showed moderate to weak activity. We attributed the moderate biological activity to the difficulty of pure ceramide

separation. In future, our main goal is the separation of each ceramide in the MEC-1 mixture and prepares a complete biological and computational study.

From the docking results, we can deduce that ceramides are powerfully interact with amino acids residues of PAS and penetrate inside catalytic gorge, but are not interact with triad machinery amino acids. Thus, ceramides are considered a non-competitive inhibitor of AChE. It was reported that AChE may actively participate in the processing, maturation and deposition of  $\beta$ -amyloid peptide; this novel non-cholinergic function relating to its PAS.<sup>102,107</sup> As our targets are binding to PAS, they could be considered promising lead compounds for development of potent anti-Alzheimer agent. After confirmation that PAS at the rim of the cavity play a vital role in enzymatic activity and the ability of ceramides to interact with amino acids residue at PAS, the structure modification of ceramide by the addition of quaternary ammonium group to interact with catalytic triad and Trp84 at the base of gorge is an important step to develop a potent dual acting anti-Alzheimer candidate.

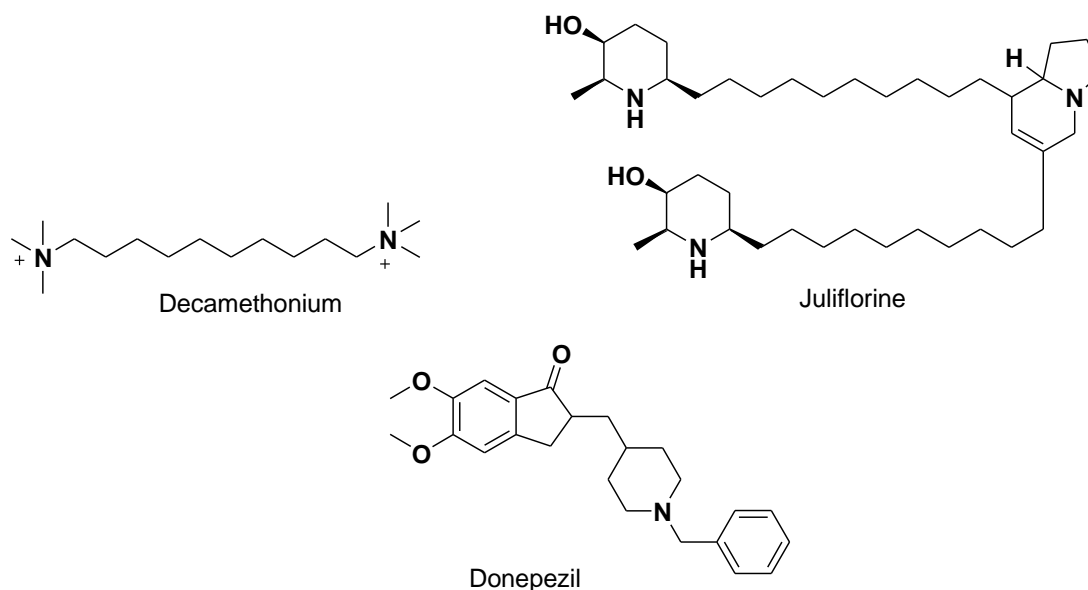


**Fig.3.4. Compounds with AChE inhibitory activity**



## 4. Experimental section

### 4.1. General experimental procedures

The used equipments include Portable ultraviolet lamp (254/365 nm), (Model UV GL-25, U.S.A.), IR spectra were measured on JASCO FT/IR-410 spectrophotometers, atomizer for spraying, capillary tubes for spotting, Glass tanks, test tubes and beakers, Glass columns for separation by column chromatography, Rotatory evaporator (Buchi, G. Switzerland). the chromatographic materials include TLC which was performed on precoated plates with Si-gel F254 (layer thickness 0.2 mm, Merck Ltd, Japan) as stationary phase, normal phase Si-gel F254 with a particle size of 0.0045 – 0.075 mm or 230-400 mesh (Wako pure industries Ltd Company) was used as stationary phase, Sephadex LH-20 (Sigma - Aldrich, Germany), reversed Phase silica gel (C18), Semi-preparative HPLC was performed on a Cosmosil 5C<sub>18</sub> – MS–II (4.6 ID x150 mm) at a flow rate of 0.5 mL/min, and Cosmosil- cholester column (250 x 4.6 mm) at a flow rate of 1 mL/min. Both columns were equipped with a TOSOH RI-8020 detector and a JASCO BIP-I HPLC pump. Analytical HPLC was performed on a Cosmosil 5C<sub>18</sub> – AR–II (4.6 ID x150 mm) at a flow rate of 0.8 mL/min and was equipped with a UV detector (250 nm). Organic solvents used for extraction, open columns and TLC were *n*-hexane, chloroform, ethyl acetate, and methanol and produced by Nacalai tesque Co., Ltd., Japan. All solvents were reagent grade and were subjected to distillation before use for chromatographic purposes. (60% v/v) H<sub>2</sub>SO<sub>4</sub> in methanol was prepared and used as a spray reagent. <sup>1</sup>H-NMR chemical shifts are expressed as  $\delta$  values and coupling constants expressed in Hz. The reference solvent Pyridine-*d*<sub>5</sub>, had characteristic peaks at  $\delta_{\text{H}}$  7.19, 7.55 and 8.71,  $\delta_{\text{H}}$  7.26 for CDCl<sub>3</sub> and  $\delta_{\text{H}}$  3.30, 4.80 for CD<sub>3</sub>OD. <sup>13</sup>C-NMR chemical shifts are expressed in  $\delta$  values referring to the solvent peak  $\delta_{\text{C}}$  123.5, 135.5 and 149.9 for Pyridine-*d*<sub>5</sub>, 77 for CDCl<sub>3</sub> and 49.0 for CD<sub>3</sub>OD. <sup>1</sup>H and <sup>13</sup>C-NMR spectra were recorded with a Unity plus 400 spectrometer (Varian Inc., U.S.A.) operating at 400 MHz for <sup>1</sup>H, and 100 MHz for <sup>13</sup>C. Positive ion FAB-MS spectra were recorded on JMS -700 spectrometer (JEOL Ltd., Japan), using *m*-nitrobenzyl alcohol or Magic bullet as a matrix. EI mass spectra were JMS -700 spectrometer (JEOL Ltd., Japan).

## **4.2. Marine organism materials**

Biological samples involved in this study were all marine organisms including one seagrass and two sponges. They were collected off the Red Sea in Egypt.

### **4.2.1. *Thalassodendron ciliatum*, Collection and Identification**

The sea grass *T. ciliatum* (coll. no. SAA-41) was collected from Sharm el Sheikh at the Egyptian Red Sea, air-dried and stored at low temperature (- 24°C) until processed. The plant was identified by Dr Tarek Temraz, Marine Science Department, Faculty of Science, Suez Canal University, Ismailia, Egypt. A voucher specimen was deposited in the herbarium section of Pharmacognosy Department, Faculty of Pharmacy, Suez Canal University, Ismailia, Egypt under registration number SAA-41.

### **4.2.2. *Mycale euplectellioides*, Collection and Identification**

The sponge *Mycale euplectellioides* was collected from Sharm El Sheikh at the Egyptian Red Sea, air-dried and stored at low temperature (-24 °C) until processed. Voucher specimens were deposited at the Zoological Museum of the University of Amsterdam under registration numbers ZMAPOR18964 and in the herbarium section of Pharmacognosy Department, Faculty of Pharmacy, Suez Canal University, Ismailia, Egypt under registration number SAA-7.

### **4.2.2. *Stylissacarteri*, Collection and Identification**

The sponge *Stylissa carteri* was collected from Sharm El Sheikh at the Egyptian Red Sea, air-dried and stored at low temperature (-24 °C) until processed. The sponge was identified by Dr Tarek Temraz, Marine Science Department, Faculty of Science, Suez Canal University, Ismailia, Egypt. Voucher specimens were deposited at the herbarium section of Pharmacognosy Department, Faculty of Pharmacy, Suez Canal University, Ismailia, Egypt under registration number SAA-46.

### 4.3. Marine organism, Extraction and isolation

#### 4.3.1. *Thalassodendron ciliatum*, Extraction and isolation

*T. ciliatum* was dried (250 g dry weight), grounded and repeatedly extracted with a mixture of CH<sub>2</sub>Cl<sub>2</sub>:MeOH (1:1) (3 x 2 L) at room temperature. The combined extracts were concentrated under vacuum to yield a dark green residue TC (30 g). The residue was chromatographed over silica gel column using CHCl<sub>3</sub>:MeOH:H<sub>2</sub>O (100:0:0 ~ 60:40:10) gradient elution to give 11 sub-fractions (TC-1 ~ TC-11) based on TLC analysis. Fraction TC-6 (0.64 g), was subjected to SiO<sub>2</sub> column elution with a gradient of increasing MeOH in CHCl<sub>3</sub> to afford 6 fractions (TC-6-1 ~ TC-6-6). Fraction TC-6-4 (114 mg) was chromatographed over Sephadex LH-20 column and eluted with CHCl<sub>3</sub>:MeOH(1:1) to yield 4 fractions (TC-6-4-1 ~ TC-6-4-4). Fraction TC-6-4-3 (56 mg) was successively rechromatographed over silica gel column using CHCl<sub>3</sub>:MeOH (9.5:0.5) isocratic elution to give a pure phytoceramide molecular species TCC-1 (28 mg). TCC-1 (23 mg) was finally purified on semi-preparative HPLC (Cosmosil 5C<sub>18</sub>, 100% MeOH) to afford TCC-1-1 (**1**, 0.3 mg), TCC-1-2 (**2**, 0.9 mg), TCC-1-3 (**3**, 0.6 mg), TCC-1-4 (**4**, 0.8 mg), TCC-1-5 (**5**, 2.1 mg), TCC-1-6 (**6**, 6.4 mg), TCC-1-7 (**7**, 2.4 mg), TCC-1-8 (**8**, 1.3 mg) and TCC-1-9 (**9**, 1.0 mg) as pure phytoceramides. Fraction TC-4 (1.4 g), was further chromatographed over SiO<sub>2</sub> column using CHCl<sub>3</sub>:MeOH (100:0 ~ 80:20) gradient elution to afford 10 fractions (TC-4-1 ~ TC-4-10). Fraction TC-4-5 (320 mg) was chromatographed over Sephadex LH-20 column and eluted with CHCl<sub>3</sub>:MeOH (1:1) followed by silica gel column using *n*-hexane: EtOAc (70:30 ~ 50:50) to yield 6 fractions (TC-4-5-1 ~ TC-4-5-6). Fraction TC-4-5-3 (65 mg) was chromatographed over silica gel column using *n*-hexane: EtOAc (70:30) isocratic elution followed by semi-preparative reversed-phase HPLC (cholester, 100% MeOH) to give compounds **10** (2.5 mg) and **11** (2.2 mg). Fraction TC-7 (0.64 g), was subjected to silica gel column using CHCl<sub>3</sub>:MeOH (100:0 ~ 90:10) gradient elution to afford 7 fractions (TC-7-1 ~ TC-7-7). Compound **12** (7.7 mg) and **13** (13.5 mg) were isolated after Sephadex LH-20 column chromatographic elution with CHCl<sub>3</sub>:MeOH (1:1) followed by semi-preparative reversed-phase HPLC (cholester, 90% MeOH) from fraction TC-7-5 (66 mg). Fraction TC-9 (1.43 g), was subjected to SiO<sub>2</sub> column elution using CHCl<sub>3</sub>:MeOH (90:10) isocratic elution to afford 4 fractions (TC-9-1 ~ TC-9-4). Fraction TC-9-3 (243 mg) was successively chromatographed over Sephadex LH-20 column using CHCl<sub>3</sub>:MeOH (1:1), followed by reversed-phase silica gel column and eluted with MeOH:H<sub>2</sub>O (1:1) to give compound **14** (14.5 mg).

**TCC-1:** White amorphous powder. IR (KBr)  $\text{cm}^{-1}$ : 3300 (hydroxyl), 2900 (C-H) 1624, 1545 (amide). Positive ion FAB-MS  $m/z$ : 678, 692, 706, 720, 734  $[\text{M}+\text{Na}]^+$  series.  $^1\text{H}$ - and  $^{13}\text{C}$ -NMR: See Table 2.1.

**Methanolysis of TCC-1:** Hydrolysis was achieved by heating TCC-1 (5 mg) with 5% HCl in MeOH (0.5 mL) at 70 °C for 8 h in a sealed small-volume vial. The reaction mixture was extracted with *n*-hexane, and the hexane layer was evaporated under vacuum till dryness to give a mixture of FAMES for  $^1\text{H}$ ,  $^{13}\text{C}$ - NMR and mass analysis.

**EI mass analysis of FAMES from TCC-1:** The FAM mixture from TCC-1 showed four molecular ion peak series at 370, 384, 398, 412  $[\text{M}]^+$  indicating C22, C23, C24, C25 fatty acid methyl esters respectively.

**Isolation of ceramides from TCC-1:** The ceramide molecular species TCC-1 showed nine peaks in the reversed phase HPLC [column, Cosmosil 5C<sub>18</sub> (4.6 mm X 150 mm); solvent, MeOH; flow rate, 0.5 ml/min; RI detector]. By these conditions, 23 mg of TCC-1 was separated to give nine compounds: TCC-1-1 (0.3 mg), TCC-1-2 (0.9 mg), TCC-1-3 (0.6 mg), TCC-1-4 (0.8 mg), TCC-1-5 (2.1 mg), TCC-1-6 (6.4 mg), TCC-1-7 (2.4 mg), TCC-1-8 (1.3 mg) and TCC-1-9 (1.0 mg)

**TCC-1-1 (1):** Amorphous powder, positive-ion FAB-MS:  $m/z$  656  $[\text{M}+\text{H}]^+$ , 678  $[\text{M}+\text{Na}]^+$ .

**TCC-1-2 (2):** Amorphous powder, positive-ion FAB-MS:  $m/z$  656  $[\text{M}+\text{H}]^+$ , 678  $[\text{M}+\text{Na}]^+$ .

**TCC-1-3 (3):** Amorphous powder, positive-ion FAB-MS:  $m/z$  670  $[\text{M}+\text{H}]^+$ , 692  $[\text{M}+\text{Na}]^+$ .

**TCC-1-4 (4):** Amorphous powder, positive-ion FAB-MS:  $m/z$  670  $[\text{M}+\text{H}]^+$ , 692  $[\text{M}+\text{Na}]^+$ .

**TCC-1-5 (5):** Amorphous powder, positive-ion FAB-MS:  $m/z$  684  $[\text{M}+\text{H}]^+$ , 706  $[\text{M}+\text{Na}]^+$ ,  $[\alpha]_{\text{D}}^{26.5} = +8.4$  ( $c=0.2$ , pyridine).

**TCC-1-6 (6):** Amorphous powder, positive-ion FAB-MS:  $m/z$  684  $[\text{M}+\text{H}]^+$ , 706  $[\text{M}+\text{Na}]^+$ ,  $[\alpha]_{\text{D}}^{26.5} = +7.2$  ( $c=0.6$ , pyridine).

**TCC-1-7 (7):** Amorphous powder, positive-ion FAB-MS:  $m/z$  698  $[\text{M}+\text{H}]^+$ , 720  $[\text{M}+\text{Na}]^+$ ,  $[\alpha]_{\text{D}}^{26.5} = +26.3$  ( $c=0.2$ , pyridine).

**TCC-1-8 (8):** Amorphous powder, positive-ion FAB-MS:  $m/z$  698  $[\text{M}+\text{H}]^+$ , 720  $[\text{M}+\text{Na}]^+$ .

**TCC-1-9 (9):** Amorphous powder, positive-ion FAB-MS:  $m/z$  712  $[\text{M}+\text{H}]^+$ , 734  $[\text{M}+\text{Na}]^+$ .

#### 4.3.2. *Mycale euplectellioides*, Extraction and isolation

All experimental protocols of the present study were approved by Research Ethics Committee at the Faculty of Pharmacy, Suez Canal University, Ismailia, Egypt (approval no. PG-NR3-16-1). A sample (500 g, wet weight) of *Mycale euplectellioides* was defrosted and repeatedly extracted with methanol (3 × 2 L). The combined extracts were concentrated under vacuum to afford a crude extract (4.5 g). The crude extract was subjected to silica gel column chromatography using CHCl<sub>3</sub>:MeOH:H<sub>2</sub>O (1:0:0 ~ 6.5:3.5:0.5) giving seven fractions; M-1 ~ M-7. The fraction eluted with 97% CHCl<sub>3</sub>: MeOH, M-2 (500 mg) was chromatographed over silica gel column using *n*-hexane: EtOAc (10:90 ~ 0:100) to give 12 sub-fractions (M-2-1 ~ M-2-12). Fraction M-2-3 (10 mg) was chromatographed on silica gel column using *n*-hexane:EtOAc (10:90 ~ 0:100) followed by reversed phase silica gel column chromatography using MeOH (100%) isocratic elution to afford (**18**) [chimyl alcohol, 4 mg] and (**19**) [batyl alcohol, 2 mg]. Fraction M-2-12 (262 mg) was further chromatographed on Sephadex LH-20 column twice using CHCl<sub>3</sub>: MeOH (1:1) followed by silica gel column chromatography using CHCl<sub>3</sub>: MeOH (98:2) isocratic elution to afford **MEC-1** (17.7 mg, white amorphous powder). MEC-1 (6 mg) was finally purified on semi-preparative HPLC (Develosil C30-UG, 100% MeOH) to afford (**15**) [MEC-1-4, 1.2 mg], (**16**) [MEC-1-7, 0.4 mg], and (**17**) [MEC-1-8, 1.4 mg] as pure phytoceramides. Fraction M-3 (105 mg) was subjected to silica gel column chromatography using CHCl<sub>3</sub>: MeOH: H<sub>2</sub>O (1:0:0 ~ 6.5:3.5:0.5) to give six sub-fractions (M-3-1 ~ M-3-6). Fraction M-3-4 (10 mg) was chromatographed on Sephadex LH-20 column using CHCl<sub>3</sub>: MeOH (1:1) to give (**20**) [thymine, 4 mg] and (**21**) [uracil, 3 mg], while Fraction M-3-5 (12 mg) was purified on Sephadex LH-20 column using CHCl<sub>3</sub>: MeOH (1:1) to yield (**22**) [thymidine, 5 mg] and (**23**) [uridine, 3 mg].

**MEC-1:** White amorphous powder. IR (KBr) cm<sup>-1</sup>: 3300 (hydroxyl), 1624, 1545 (amide). Positive ion FAB-MS *m/z*: 678, 692, 706, 720, 734 [M+Na]<sup>+</sup> series. <sup>1</sup>H and <sup>13</sup>C-NMR: See Table 2.7.

**Methanolysis of MEC-1:** MEC-1 (5 mg) was heated with 5% HCl in MeOH (0.5 mL) at 70 °C for 8 h in a sealed small-volume vial. The reaction mixture was extracted with *n*-hexane, and the hexane layer was evaporated under vacuum till dryness to give a mixture of FAM for <sup>1</sup>H, <sup>13</sup>C-NMR and mass analysis. The methanolic was neutralized with Ag<sub>2</sub>CO<sub>3</sub> to give the LCB which further evaporated and reacted with acetic anhydride/ pyridine (1:1) (0.2 mL) at 70 °C for 8 h in

a sealed small-volume vial followed by evaporation under vacuum till dryness to afford LCB acetate for further  $^1\text{H}$ ,  $^{13}\text{C}$ - NMR and mass analysis.

**EI mass analysis of FAM from MEC-1:** the FAM mixture from MEC-1 showed five molecular ion peak series at 356, 370, 384, 398, 412  $[\text{M}]^+$  indicating  $\text{C}_{21}$ ,  $\text{C}_{22}$ ,  $\text{C}_{23}$ ,  $\text{C}_{24}$ ,  $\text{C}_{25}$  fatty acid methyl esters.

**FAB mass analysis of LCB from MEC-1:** The positive ion FAB-MS analysis of LCB from MEC-1 showed a molecular ion peak at 500  $[\text{M}+\text{H}]^+$  and 522  $[\text{M}+\text{Na}]^+$  indicating that MEC-1 exhibit  $\text{C}_{19}$  LCB.

**Isolation of ceramides from MEC-1:** The ceramide molecular species MEC-1 showed eight peaks in the reversed phase HPLC [column, develosil  $5\text{C}_{18}$  (4.6 mm X 150 mm); solvent, MeOH; flow rate, ml/min]. By these conditions, 6 mg of MEC-1 was separated to give three compounds: MEC-1-4 (1.2 mg,  $t_R=12.06$  min), MEC-1-7 (0.4 mg,  $t_R=14.02$  min) and MEC-1-8 (1.4 mg,  $t_R=16.48$  min).

**MEC-1-4 (15):** Amorphous powder, positive-ion FAB-MS:  $m/z$  692  $[\text{M}+\text{Na}]^+$ , 670  $[\text{M}+\text{H}]^+$ .

**MEC-1-7 (16):** Amorphous powder, positive-ion FAB-MS:  $m/z$  706  $[\text{M}+\text{Na}]^+$ , 684  $[\text{M}+\text{H}]^+$ .

**MEC-1-8 (17):** Amorphous powder, positive-ion FAB-MS:  $m/z$  720  $[\text{M}+\text{Na}]^+$ , 698  $[\text{M}+\text{H}]^+$ .

#### 4.3.3. *Stylissa carteri*: Extraction and isolation

A sample (1.5 Kg, wet weight) of *Stylissa carteri* was repeatedly extracted with methanol (3  $\times$  2 L). The combined extracts were concentrated under vacuum to afford a crude extract (30 g). The crude extract was suspended in  $\text{H}_2\text{O}$  (1L) and extracted with *n*-Hexane,  $\text{CHCl}_3$ , *n*-BuOH successively. These fractions concentrated under reduced pressure to afford *n*-Hexane soluble fraction (4 g),  $\text{CHCl}_3$  soluble fraction (3 g), *n*-BuOH soluble fraction SC-B (17.8 g) and aqueous soluble fraction. According to TLC monitoring, the *n*-Hexane soluble fraction and the  $\text{CHCl}_3$  soluble fraction were combined together to afford fraction SC-C (7 g) as shown in fig.4.10. Fraction SC-C (7 g) was chromatographed on silica gel column using  $\text{CHCl}_3$ : MeOH (1:0 ~ 6.5:3.5) afford eight sub-fractions (SC-C-1 ~ SC-C-8). Fraction SC-C-4 (25.5 mg) was further chromatographed on Sephadex LH-20 column twice using  $\text{CHCl}_3$ : MeOH (1:1) isocratic elution to afford compound **25** (11 mg, white amorphous powder). Fraction SC-C-6 (450 mg) was chromatographed on silica gel column using  $\text{CHCl}_3$ : MeOH (9:1 ~ 6.5:3.5) followed by

Sephadex LH-20 column using CHCl<sub>3</sub>: MeOH (1:1) isocratic elution to afford compound **24** (SCC-1, 11 mg, white amorphous powder).

**SCC-1:** White amorphous powder. Positive ion FAB-MS  $m/z$ : 840.8, 854.8, 868.8, 882.8, 896.8 [M+Na]<sup>+</sup> series. <sup>1</sup>H and <sup>13</sup>C-NMR: See Table 2.14.

**Methanolysis of SCC-1:** SCC-1 (2 mg) was heated with 5% HCl in MeOH (0.5 mL) at 70 °C for 8 h in a sealed small-volume vial. The reaction mixture was extracted with *n*-hexane, and the hexane layer was evaporated under vacuum until dryness to give a mixture of FAM for mass analysis.

**FAB-MS analysis of FAM from SCC-1:** the FAM mixture from SCC-1 showed three molecular ion peak series at 355, 383 and 397 [M-H]<sup>-</sup> indicating C<sub>21</sub>, C<sub>23</sub> and C<sub>24</sub> fatty acid methyl esters.

**Identification of the sugar moiety:** SCC-1 (5 mg) was heated with 5% HCl/MeOH (0.5 mL) at 70 °C for 8 h in a sealed small-volume vial. The reaction mixture was extracted with CHCl<sub>3</sub> to remove the release fatty acid. The methanolic was neutralized with Ag<sub>2</sub>CO<sub>3</sub> to give the methylated sugar followed by HPLC analysis (Cosmosil-sugar-D, 4.6 ID X 250 mm, 1 mL/min, RI detector, 95% acetonitril) against standard glucose and galactose. Galactose showed retention time at 4.76 min, which was identical to our sample retention time while glucose retention time was 4.62 min.

**Determination of the sugar moiety configuration:** SCC-1 (**24**) (2 mg, was hydrolyzed by heating in 0.5 M HCl (0.1 ml) and neutralized with Amberlite IRA400. After drying in vacuo, the residue was dissolved in pyridine (0.1 ml) containing L-cysteine methyl ester hydrochloride (0.5 mg) and heated at 60 °C for 1 h. A 0.1 ml solution of *o*-tolylisothiocyanate (0.5 mg) in pyridine was added to the mixture, which was heated at 60 °C for 1 h. The reaction mixture was directly analyzed by reversed-phase HPLC<sup>97</sup>(Cosmosil-5C<sub>18</sub>-AR-II, 4.6ID X 250 mm, 0.8 mL/min, UV detector (250 nm, 25% acetonitril in 50 mM H<sub>3</sub>PO<sub>4</sub>). The peak at 18.6 min was coincided with derivatives of D-galactose. Same derivatization procedures were done for 5 mg of standards, D-glucose ( $t_R$ =19.7 min), L-glucose ( $t_R$ = 19.5 min), D-galactose ( $t_R$ =18.6 min) and L-galactose ( $t_R$ =19.3 min).

## 4.4. Biological activity

### 4.4.1. Acetylcholine esterase (AChE) inhibitory assay:

AChEI activity was measured using Ellman's method.<sup>109)</sup> AChE hydrolyzes the substrate Acetylthiocholine iodide (ACTI) into acetate and thiocholine. In a neutral and alkaline medium; thiocholine reacts with 5,5-dithiobis-2-nitrobenzoic acid (DTNB) to give yellow colored 2-nitro-5-thiobenzoate, which can be detected spectrophotometrically at 405 nm. Briefly, in a 96-well plate, 25  $\mu$ L of 15 mM ACTI, 125  $\mu$ L of 3 mM DTNB in buffer B (50 mM TrisHCl, pH = 8, 0.1 M NaCl, 0.02 M MgCl<sub>2</sub>.6 H<sub>2</sub>O), 50  $\mu$ L of buffer A (50 mM Tris-HCl, PH 8, 0.1% BSA) and 25  $\mu$ L of tested sample (dissolved in 25% DMSO) were mixed, and the absorbance was measured using a microplate reader (Biotek, Winooski, VT, USA) at 412 nm every 16 s ten times. Then, 25  $\mu$ L of (0.25 U/mL in buffer A) AChE (from *Electrophorus electricus* (electric eel)) was added and the absorbance was measured ten times every 16 s. A solution of 25% DMSO was used as a negative control. Absorbance was plotted against time and enzyme activity was calculated from the slope of the line so obtained and expressed as a percentage compared to an assay using a buffer without any inhibitor. To avoid any increase in the absorbance due to spontaneous hydrolysis of the substrate, the absorbance before addition of the enzyme was subtracted from the absorbance after adding the enzyme.

### 4.4.2. Molecular modeling studies for Acetylcholine esterase (AChE) inhibitory assay for the isolated compounds 15, 16 and 17:

#### 4.4.2.A. Protein preparation for docking study

In the present study, the X-ray crystal structure of AChE in complex with donepezil (PDB ID: 1EVE) was obtained from Protein Data Bank and further prepared by protein preparation wizards, which is accessible in Glide, Schrodinger 10.1. After ensuring chemical accuracy, the preparation component adds hydrogen and neutralizes side chains that are neither close to the binding cavity nor involve in the formation of salt bridges. The OPLS-2005 force field was used for this purpose and then the active site of the protein was defined. In the next step, water molecules were removed and H atoms were added to the crystal structure, most likely positions of hydroxyl and thiol hydrogen atoms, protonation states and tautomers of the His residue and Chi 'flip' assignment for Asn, Gln and His residues were selected by the protein assignment script provided by Schrodinger. Minimization was performed to relieve steric clashes using the



---

OPLS2005 force field until the average root mean square deviation (RMSD) of the non-hydrogen atoms reached a maximum value of 0.3 Å.<sup>110-112)</sup>

#### 4.4.2.B. Ligand preparation

All the compounds were constructed using the fragment library of Maestro 10.1 and prepared by using the LigPrep 2.1, which can produce a number of structures from each input structure with various ionization states, tautomers, stereochemistries and ring conformations. The OPLS-2005 force field was used for optimization, which produces the low energy conformer of the ligand.<sup>112, 113)</sup>

#### 4.4.2.C. Molecular Docking

To test the docking parameters all compounds were docked into the binding site of AChE protein (PDB ID: 1EVE) using Grid-Based Ligand Docking With Energetics (Glide) software from Schrodinger. To soften the potential for non-polar parts of the receptor, we scaled van der Waal radii of receptor atoms by 0.8 with a partial atomic charge of 0.15. A grid box with coordinates  $X = 2.87$ ,  $Y = 64.62$  and  $Z = 67.93$  was generated at the centroid of the active site. The ligands were docked with the active site using the 'extra precision' glide docking (Glide XP) which docks ligands flexibly. Glide generates conformations internally and passes these through a series of filters. The particular methodology of XP docking has been explained elsewhere. The final best docked structure was chosen using a Glide score function. The lowest-energy docked complex was found in the majority of similar docking conformations. Finally, the lowest-energy docked complex was selected for further study.<sup>110-112)</sup>

## 5. Acknowledgement

I am most indebted to my supervisor, Prof. Koji Yamada, for providing invaluable insights, timely encouragement, and guidance balanced by the freedom to pursue my research ideas. I have always admired his thorough understanding of the fundamental concepts, clarity in the implementation of an idea, approach towards the design of an experiment, and troubleshooting skills. He also taught me how to organize and express thoughts during the preparation of paper manuscripts. It is impossible for me to finish the PhD study without the help of Prof. Koji Yamada. He has been a great mentor and I am fortunate to be a member of his research group. Really, the past three years (2013-2016) were invaluable in my scientific life and I will exploit what I learned to the rest of my life.

Besides my advisor, I would like to thank the rest of my thesis committee: Prof. Takashi Tanaka, Prof. Masakazu Tanaka, and Prof. Osamu Onomura, for their insightful comments and encouragement, but also for the hard question which incited me to widen my research from various perspectives.

My sincere thanks also goes to Prof. Ahmed I. Youssef, Prof. Abdel Satar Arafa, Dr. Amira Mera, and Dr. Mohamed Saleh Elgawish, who performed the biological activities and the molecular docking study. Without their precious support it would not be possible to conduct this research.

My gratitude is also extended to the Faculty of Pharmaceutical Sciences particularly Natural Products Chemistry, and SC-NMR Laboratory, Nagasaki University for all the facilities provided. I thank also Mr. K. Inada, Mr. N. Yamaguchi, and Mr. N. Tsuda (Nagasaki University) for NMR and MS measurements.

I would like to thank my lab members-past and present for their daily support, encouragement, and friendship; they also provided a great work environment and making the lab a fun place to me.

I would like to thank my friends, Mohamed Omar, Mahmoud Elmaghraby, Tariq Numir, prof. Yasser El hadad and Dr. Abdelmotagaly for their daily support while writing this dissertation and companionship during tough times.

Most importantly I would like to thank my family who has always supported and believed in me; in particular, my wife Asmaa Said for giving me the best support, advice, and strength, also she cares about my child Omar, which is an extremely demanding and rewarding

job, although she was completing her PhD too. My most heartfelt thanks goes to my parents for being a powerful source of inspiration and energy, my sisters for providing love and prayer to me. It is to them that I dedicate this thesis work.

I would like to thank my Egyptian Professors (Hashim Abdelhalim Hassanin, Safwat Abdelmaksoud Ahmed and Amany Kamal Ibrahim) for their continuous support and valuable scientific advices.

First and foremost, I thank Allah for His help and guidance; he gives me everything, peace, love, family, friends, health and good life.

---

**6. References**

- 1) Cordell G. *Phytochemistry*, **55**, 463-480 (2000).
- 2) Young, R. *Pure Appl. Chem.*, **71**, 1655-1661 (1999).
- 3) Wilson R., Danishefsky S. J. *J. Org. Chem.*, **71**, 8329-8351 (2006).
- 4) Newman, D. *J. Med. Chem.*, **51**, 2589-2599 (2008).
- 5) Sunazuka T., Hirose T., Omura S. *Acc. Chem. Res.*, **41**, 302-314 (2008).
- 6) Cragg G., Grothaus P., Newman D. *Chem. Rev.*, **109**, 3012-3043 (2009).
- 7) Faulkner D. J. *Chemistry in Britain*, **31**, 680-684 (1995).
- 8) Nontji A. *Proceedings 9th international coral reef symposium*, Indonesia, **1**, pp.17 (2000).
- 9) kijjoa A., Wong P. *Mar. drugs*, **2**, 73-82 (2004).
- 10) Frommann S., Jas G. *Business Briefing: Future Drug Discovery*, **2002**, 84-90 (2002).
- 11) Cragg G., Newman D. *Expert Opin. Investig. Drugs*, **9**, 2783-2797 (2000).
- 12) Ebada S. S., Lin W. H., Proksch P. *Mar. Drugs*, **8**, 313-346 (2010).
- 13) Molinski T. F., Dalisay D. S., Lievens S. L., Saludes J. P. *Nat. Rev. Drug Disc.*, **8**, 69-85 (2009).
- 14) Neeman I., Fishelson L., Kashmann Y. *Mar. Biol.*, **30**, 293-296 (1975).
- 15) Lindquist N., Hay M. E., Fenical W. *Ecol. Monogr.*, **62**, 547-568 (1992).
- 16) Proksch P., Ebel R., Ecological significance of alkaloids from marine invertebrates alkaloids, biochemistry, ecology and medicinal application, Edited by Margaret F. Roberts and Michael Wink, *Plenum Publishing*, 379-394 (1998).
- 17) Ebel R., Brenzinger M., Kunze A., Gross H. J., Proksch P. *J. Chem. Ecol.*, **23**, 1451-1457 (1997).
- 18) Fenical W. *Chem. Rev.*, **93**, 1673-1683 (1993).
- 19) Riguera R. *J. Mar. Biotechnol.*, **5**, 187-193 (1997).
- 20) Jirge S., Chaudhari Y. *IJRAP*, **1**, 55-62 (2010).
- 21) Faulkner D. J., Attaway D. H., Zaborsky O. R. *Mar. Biotechnol.*, **1**, 459-474 (1993).
- 22) Perry N. B., Blunt J. W., Munro M. H. G., Thompson A. M. *J. Org. Chem.*, **55**, 223-227 (1990).
- 23) Sunil S., Kaur M., Minneman K. P. *Mar. Drugs*, **8**, 2619-2638 (2010).
- 24) Cutignano A., Bifulco G., Bruno I., Casapullo A., Gomez-Paloma L., Riccio R. *Tetrahedron*, **56**, 3743-3748 (2000).

- 25) Sipkema D., Franssen M., Osinga R., Tramper J., Wijffels R. *Mar. Biotechnol.*, **7**, 142-162 (2005).
- 26) Minale L., Riccio R., Sodano G. *Tetrahedron Lett.*, **15**, 3401-3404 (1974).
- 27) Rinehart K. L., Shield L. S., Cohen-Parsons M., Attaway D. H., Zaborsky O.R. *Mar. Biotechnol.*, **1**, 309-342 (1993).
- 28) Takagi M., Motohashi K., Khan S. T., Hashimoto J., Shin-ya K. *J. Antibiot.*, **63**, 401-403 (2010).
- 29) Rao K. V., Donia M. S., Peng J., Garcia-Palomero E., Alonso D., Martinez A., Medina M., Franzblau S. G., Tekwani B. L., Khan S. I., Wahyuono S., Willett K. L., Hamann M. T. *J. Nat. Prod.*, **69**, 1034-1040 (2006).
- 30) Suarez-Jimenez GM., Burgos-Hernandez A., Ezquerra-Brauer JM. *Mar. Drugs*, **10**, 963-986 (2012).
- 31) Li YX., Himaya S. W. A., Kim SK. *Molecules*, **18**, 7886-7909 (2013).
- 32) Simmons T.L., Andrianasolo E., McPhail K. *Mol. Cancer Ther.*, **4**, 333-342 (2005).
- 33) Feling R. H., Buchanan G. O., Mincer T. J., Kauffman C. A., Jensen P. R., Fenical W. *Angew. Chem. Int. Ed.*, **42**, 355-357 (2003).
- 34) Jensen P. R., Williams P. G., Oh D.C., Zeigler L., Fenical W. *Appl. Environ. Microbiol.*, **73**, 1146-1152 (2007).
- 35) Chauhan D., Catley L., Li G. *Cancer Cell*, **8**, 407-19 (2005).
- 36) Fenical W., Jensen P. R., Palladino M. A., Lam K. S., Lloyd G. K., Potts B. C. *Bioorg. Med. Chem.*, **17**, 2175-2180 (2009).
- 37) Mathieu V., Wauthoz N., Lefranc F. *Molecules*, **18**, 3543-3561 (2013).
- 38) Sakai E., Kato H., Rotinsulu H., Losung F., Mangindaan R. E. P., De Voogd N. J., Yokosawa H., Tsukamoto S. *J. Nat. Med.*, **18**, 215-219 (2014).
- 39) FDA approves new treatment option for late-stage breast cancer, (2010) <http://www.fda.gov/NewsEvents/Newsroom/PressAnnouncements/ucm233863.htm>
- 40) Towle M. J., Salvato K. A., Budrow J., Wels B. F., Kuznetsov G., Aalfs K. K., Welsh S., Zheng W., Seletsky B. M., Palme M. H., Habgood G. J., Singer L. A., Dipietro L.V., Wang Y., Chen J. J., Quincy D. A., Davis A., Yoshimatsu K., Kishi Y., Yu M.J., Littlefield B. A. *Cancer Res.*, **61**, 1013-21 (2001).
- 41) De Silva E. D., Scheuer P. J. *Tetrahedron Lett.*, **21**, 1611-1614 (1980).

- 42) Soriente A., De Rosa M. M., Scettri A. *Curr. Med. Chem.*, **6**, 415-431 (1999).
- 43) Posadas I., Terencio M. C., De Rosa S., Paya M. *Life Sci.*, **67**, 3007-3014 (2000).
- 44) Costantino V., Fattorusso E., Mangoni A., Di Rosa M., Ianaro A. *J. Am. Chem. Soc.*, **119**, 12465-12470 (1997).
- 45) Burgoyne D.L., Andersen R.J., Allen T.M. *J. Org. Chem.*, **57**, 525-528 (1992).
- 46) Takei M., Burgoyne D.L., Andersen R.J. *J. Pharm. Sci.*, **83**, 1234-1235 (1994).
- 47) Kasserra C. E., Harris P., Stenton G. R., Abraham W., Langlands J. M. *Pulm. Pharmacol. Ther.*, **17**, 309-318 (2004).
- 48) Burkholder P. R., Ruetzler K. *Nature*, **222**, 983-984 (1969).
- 49) Sipkema D., Franssen M., Osinga R., Tramper J., Wijffels R. *Mar. Biotechnol.*, **7**, 142-162 (2005).
- 50) Dunbar D. C., Rimoldi J. M., Clark A. M., Kelly M., Hamann M. T. *Tetrahedron*, **56**, 8795-8798 (2000).
- 51) Tanaka N., Momose R., Takahashi Y., Kubota T., Takahashi-Nakaguchi A., Gono T., Fromont J., Kobayashi J. *Tetrahedron Lett.*, **54**, 4038-4040 (2013).
- 52) El-Gendy M. M., Shaaban M., Shaaban K. A., El-Bondkly A. M., Laatsch H. *J. Antibiot.*, **61**, 149-157 (2008).
- 53) Lakshmi V., Mishra S. K., Srivastava S., Chaturvedi A., Srivastava M. N., Shukla P. K. *J. Mycol. Med.*, **20**, 31-35 (2010).
- 54) Gao X., Lu Y., Xing Y., Ma Y., Lu J., Bao W. *Microbiol. Res.*, **167**, 616-622 (2012).
- 55) McArthur K. A., Mitchell S. S., Tsueng G., Rheingold A., White D. J., Grodberg J. J. *Nat. Prod.*, **71**, 1732-1737 (2008).
- 56) Rao K. V., Santersiero B. D., Mesecar A. D., Schinazi R. F., Tekwani B. L., Hamann M. T. *J. Nat. Prod.*, **66**, 823-828 (2003).
- 57) Ang K. H., Holmes M. J., Higa T., Hamann M. T., Kara U. K. *Antimicrob. Agents Chemothe.*, **44**, 1645-1649 (2000).
- 58) Ueoka R., Nakao Y., Kawatsu S., Yaegashi J., Matsumoto Y., Matsunaga S. *J. Org. Chem.*, **74**, 4203-4207 (2009).
- 59) Vinothkumar S., Parameswaran P. S. *Biotechnol. Adv.*, **31**, 1826-1845 (2013).
- 60) Regalado E. L., Tasdemir D., Kaiser M., Cachet N., Amade P., Thomas O. P. *J. Nat. Prod.*, **73**, 1404-1410 (2010).

- 61) Deepika T. L., Kannabiran K., Khanna V. G., Rajakumar G., Jayaseelan C., Santhoshkumar T., Rahuman A. A. *Parasitol. Res.* **111**, 1151-1163 (2012).
- 62) Donia M., Hamann M. T. *Lancet Infect Dis.* **3**, 338-348 (2003).
- 63) Kobayashi J., Ohizumi Y., Nakamura H., Hirata Y. *Experientia*, **42**, 1176-1177 (1986).
- 64) Assmann M., Köck M. Z. *Naturforsch., C: Biosci.*, **57**, 153-156 (2002).
- 65) Vicente J., Vera B., Rodríguez A. D., Rodríguez-Escudero I., Raptis R. G. *Tetrahedron Lett.*, **50**, 4571-4574 (2009).
- 66) Sato S., Iwata F., Yamada S., Kawahara H., Katayama M. *Bioorg. Med. Chem. Lett.*, **21**, 7099-7101 (2011).
- 67) Ahmed S. A., Khalifa S. I., Hamann M. T. *J. Nat. Prod.*, **71**, 513-515 (2008).
- 68) Mark S., Butler B. R., Matthew A. C. *Nat. Prod. Rep.*, **31**, 1612-1661 (2014).
- 69) Blunt J. W., Copp B. R., Keyzers R. A., Munro M. H., Prinsep M. R. *Nat. Prod. Rep.*, **32**, 116-211 (2015).
- 70) Choi D. Y., Choi H. *Arch. Pharm. Res.*, **38**, 139-170 (2015).
- 71) Pejin B., Mojovic M., Savic A. G. *Nat. Prod. Rep.*, **28**, 2237-2244 (2014).
- 72) Ibrahim A. K., Youssef A. I., Arafa A., Foad R., Radwan M. M., Ross S., Hassanean H. A., Ahmed S. A. *Nat. Prod. Res.*, **27**, 1625-1632 (2013).
- 73) Yamada K., Matsubara R., Kaneko M., Miyamoto T., Higuchi R. *Chem. Pharm. Bull.*, **49**, 447-452 (2001).
- 74) Ahmed S. A., Khalifa S. I., Hamann M. T. *J. Nat. Prod.*, **71**, 513-515 (2008).
- 75) Loukaci A., Bultel-Poncé V., Longeon A., Guyot M. *J. Nat. Prod.*, **63**, 799-802 (2000).
- 76) Krishna N., Muralidhar P., Kumar M., Rao D., Rao C. *J. Nat. Prod.*, **67**, 1423-1425 (2004).
- 77) Chen X., Wu Y., Chen D. *Tetrahedron Lett.*, **43**, 3529-3532 (2002).
- 78) Azuma H., Takao R., Niuro H., Shikata K., Tamagaki S., Tachibana T., Ogino K. *J. Org. Chem.*, **68**, 2790-2797 (2003).
- 79) Sandjo L. P., Hannewald P., Yemloul M., Kirsch G., Ngadjui B. T. *Helv. Chim. Acta.*, **91**, 1326-1335 (2008).
- 80) Kolter T., Sandhoff K. *Angew. Chem., Int. ED.*, **38**, 1532-1568 (1999).
- 81) Pruett S. T., Bushnev A., Hagedorn K., Adiga M., Haynes C. A., Sullards M. C., Liotta D. C., Merrill. A. H. *J. Lipid Res.*, **49**, 1621-1639 (2008).
- 82) Sun Y., Xu Y., Liu K., Hua H., Zhu H., Pei Y. *J. Nat. Prod.*, **69**, 1488-1491 (2006).

- 83) Roh E. M., Jin Q., Jin H. G., Shin J. E., Choi E. J., Moon Y. H., Woo E. R. *Arch. Pharm. Res.*, **33**, 1347-1353 (2010).
- 84) Kalinowski H. A., Berger S., Braum S. *<sup>13</sup>C-NMR Spektroskopie*(George ThiemeVerlaged.) Stuttgart, New York, Vol.2, p. 393 (1984).
- 85) Bai H., Li S., Yin F., Hu L. *J. Nat. Prod.*, **68**, 1159-1163 (2005).
- 86) Silverstein R. M., Bassler, G. C., Morrill T. C. *Spectrometric Identification of Organic Compounds*, Singapore, 221 (1991).
- 87) Rai N. P., Adhikari B. B., Paudel A., Masuda K., Mckelvey R. D., Manandhar M. D. *J. Nepal Chem. Soc.*, **21**, 1-7 (2006).
- 88) Hufford C. D and Oguntimein B. O. *J. Nat. Prod.*, **45**, 337-342 (1982).
- 89) Guang-Min Y., Yu D., Jian-Ping Z., Hong-Bing W., Yu-Bo W., Bing-Yang D., Pauline C., Guo-Wei Q. *J. Nat. Prod.* **68**, 392-396 (2005).
- 90) Nkengfack A.E., Van Heerden F. R., Fuendjiep V., Fomum Z. T. *Fitoterapia*, **72**, 834-836 (2001).
- 91) Oujano, L., Cruz, F., Navarrete, I., Gdmez, P., Rios, T. *Lipids*, **29**, 731-734 (1994).
- 92) Chao C., Huang H., Wu Y., Lu C., Chang-Feng Dal C., Sheu J. *Chem. Pharm. Bull.*, **55**, 1720-1723 (2007).
- 93) Guo-qiang, L., Zhi-wei, D., Jun, L., Zheng, F., Wen-han, L. *J. Chinese Pharm. Sci.*, **13**, 81-86 (2004).
- 94) Natori T., Morita M., Akimoto K., Koezuka Y. *Tetrahedron*. **50**, 2771-2784 (1994).
- 95) Natori T.,Koczuka Y.,Higa T., *Tetrahedron Lett.* **34**, 5591-5592 (1993).
- 96) Maruta T., Saito T., Inagaki M., Shibata O., Higushi R. *Chem. Pharm. Bull.* **53**, 1255-1258 (2005).
- 97) Kawatake S., Nakamura K., Inagaki M., Higushi R. *Chem. Pharm. Bull.* **50**, 1091-1096 (2002).
- 98) Tanaka T., Nakashima T., Ueda T., Tomil K., Kouno I., *Chem. Pharm. Bull.* **55**, 899-901 (2007).
- 99) Schmitz FJ., Gunasekera SP., Lakshimi V, Tillekeratne LMV. *J. Nat. Prod.* **48**, 47-53 (1985).
- 100) Dik-Lung M., Chana D. S., Leung C., *Chem. Sci.*, **2**, 1656-1665 (2011).
- 101) Houghton P. J., Ren Y., Ren Y., Howes M. *Nat. Prod. Rep.*, **23**, 181-199 (2006).



- 102) Bartolini M., Bertucci C., Cavrini V., Andrisano V. *Biochem. Pharmacol.*, **65**, 407-416 (2003)
- 103) Choudhary M. I., Nawaz S. A., Zaheer-ul-Haq, Azim M. K., Ghayur M. N., Lodhi M. A., Jalil S., Khalid A., Ahmed A., Rode B. M., Rahman A., Gilani A. U., Ahmad V. U. *Biochem. Biophys. Res. Commun.*, **332**, 1171-1177 (2005).
- 104) Puglielli L., Ellis B. C., Saunders A. J., Kovacs D. M. *J. Biol. Chem.*, **278**, 19777-19783 (2003).
- 105) Bielawska A., Crane H. M., Liotta D., Obeid L. M., Hannun Y. A. *J. Biol. Chem.*, **268**, 26226-26232 (1993).
- 106) Irie F., Hirabayashi Y. *J. Neurosci. Res.*, **54**, 475-485 (1998).
- 107) De Ferrari G.V., Canales M. A., Shin I., Weiner L., Silman M. I., Inestrosa N.C. *Biochemistry*, **40**, 10447-10457 (2001).
- 108) Hayden, F. G. *Philos. Trans. R. Soc. Lond., B, Biol. Sci.*, 356, 1877-1884 (2001).
- 109) Ellman G., Lourtney D., Andres V., Gmelin G. A. *Biochem. Pharm.*, **7**, 88-95 (1961).
- 110) Halgren T. A., Murphy R. B., Friesner R. A., Beard H. S., Frye L. L., Pollard W. T., Banks J. L. *J. Med. Chem.*, **47**, 1750-1759 (2004).
- 111) Friesner R. A., Banks J. L., Murphy R. B., Halgren T. A., Klicic J. J., Mainz D. T., Repasky M. P., Knoll E. H., Shelley M., Perry J. K., Shaw D. E., Francis P., Shenkin P. S. *J. Med. Chem.*, **47**, 1739-1749 (2004).
- 112) Tripathi S. K., Singh S. K. *Mol. BioSyst.*, **10**, 2189-2201 (2014).
- 113) LigPrep 2.5, Schrödinger, LLC, New York, 2011.